

Zeitschrift: IABSE congress report = Rapport du congrès AIPC = IVBH
Kongressbericht

Band: 13 (1988)

Rubrik: VI. Long span structures

Nutzungsbedingungen

Die ETH-Bibliothek ist die Anbieterin der digitalisierten Zeitschriften auf E-Periodica. Sie besitzt keine Urheberrechte an den Zeitschriften und ist nicht verantwortlich für deren Inhalte. Die Rechte liegen in der Regel bei den Herausgebern beziehungsweise den externen Rechteinhabern. Das Veröffentlichen von Bildern in Print- und Online-Publikationen sowie auf Social Media-Kanälen oder Webseiten ist nur mit vorheriger Genehmigung der Rechteinhaber erlaubt. [Mehr erfahren](#)

Conditions d'utilisation

L'ETH Library est le fournisseur des revues numérisées. Elle ne détient aucun droit d'auteur sur les revues et n'est pas responsable de leur contenu. En règle générale, les droits sont détenus par les éditeurs ou les détenteurs de droits externes. La reproduction d'images dans des publications imprimées ou en ligne ainsi que sur des canaux de médias sociaux ou des sites web n'est autorisée qu'avec l'accord préalable des détenteurs des droits. [En savoir plus](#)

Terms of use

The ETH Library is the provider of the digitised journals. It does not own any copyrights to the journals and is not responsible for their content. The rights usually lie with the publishers or the external rights holders. Publishing images in print and online publications, as well as on social media channels or websites, is only permitted with the prior consent of the rights holders. [Find out more](#)

Download PDF: 08.08.2025

ETH-Bibliothek Zürich, E-Periodica, <https://www.e-periodica.ch>

SEMINAR

VI

Long Span Structures

Structures à grandes portées

Weitgespannte Tragwerke

Chairman: Y. Fukumoto, Japan

Technical Adviser: B. Edlund, Sweden

Leere Seite
Blank page
Page vide

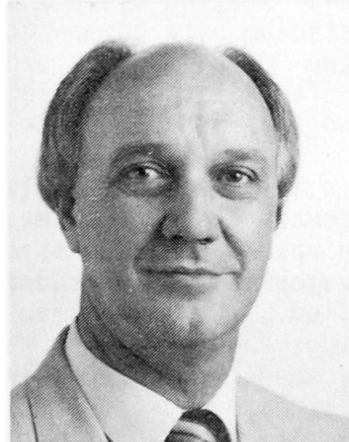
Centre Court Stadium Roof, Melbourne, Australia

Toiture du stade du court principal, Melbourne, Australie

Überdachung des Hauptspielplatz-Stadiums, Melbourne, Australien

Robert C. STRURROCK

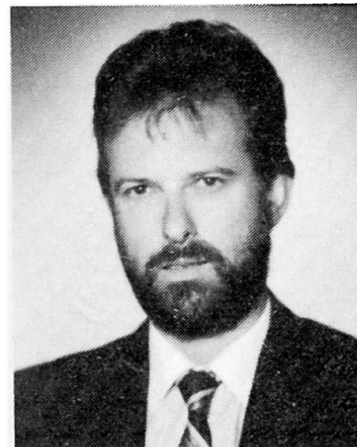
Assoc. & Princ.

Maunsell & Partners Pty. Ltd.
Melbourne, Australia

Bob Sturrock has over 30 years experience in structural engineering. He has worked worldwide on a variety of commercial, industrial, institutional and specialised structures. He is currently responsible for marketing and managing major construction projects with an emphasis on structural content.

Edwin J. ROGERS

Senior Struct. Eng.

Maunsell & Partners Pty. Ltd.
Melbourne, Australia

Edwin Rogers, born 1949, received his civil engineering degree at the University of Melbourne, Australia. He has over 15 years experience in the specialist areas of major bridge and industrial building design, with a close involvement in special structures.

SUMMARY

The centre court stadium of Australia's new National Tennis Centre seats 15,000 spectators and is required to double as a multi-function entertainment venue. For tennis use the stadium must be open, whilst for other uses it must be fully closed with an acoustically insulated roof. This paper describes the development and construction of the roof system, which comprises a cantilevered fixed roof and a unique retractable roof, which when retracted, leaves an opening 75 m x 60 m in the centre of the fixed roof.

RÉSUMÉ

Le stade du court principal du nouveau centre national australien de tennis dispose de 15000 places et doit doubler sa capacité lorsqu'il remplit sa fonction de centre de loisirs à buts multiples. D'une part le stade doit rester ouvert pour les joueurs de tennis, et d'autre part il doit être complètement couvert, avec un toit acoustiquement isolant pour les autres utilisateurs de ce centre. Ce document décrit le projet et la construction du système utilisé pour toiture, qui comprend un toit fixe à consoles et un unique toit ouvrant, qui lorsqu'il est ouvert, laisse une ouverture de 75 m x 60 m.

ZUSAMMENFASSUNG

Das Hauptspielplatz-Stadium des neuen nationalen Tenniszentrums ist mit Sitzplätzen für 15000 Zuschauer ausgestattet und dient mit doppelter Kapazität als ein multi-funktioneller Unterhaltungs-Treffpunkt. Für Tennisspiele muss das Stadium geöffnet sein, während es für die zweite Nutzung mit einem akustisch isolierten Dach völlig geschlossen sein muss. Dieser Beitrag beschreibt die Entwicklung und Konstruktion des Dach-Systems. Dieses besteht aus einem festen Ausleger-Dach und einem zurückziehbaren Dach, welches im eingezogenen Zustand eine Öffnung von 75 m x 60 m in der Mitte des festen Daches offen lässt.



1. INTRODUCTION

The National Tennis Centre provides world class tennis facilities aimed at maintaining the Australian Open Tennis Championships as one of the four Grand Slam events and for other major national and international tennis tournaments.

The facility includes the centre court stadium, which seats 15,000 spectators, plus two match court stadia seating 6,000 and 3,000 respectively, which are linked to the centre court stadium by a common concourse. Parking for 300 cars is provided beneath the two match courts and offices, player, umpire, ball staff, media and catering facilities are located beneath the centre court stadium. Thirteen outdoor and five indoor courts complete the centre.

The centre court stadium is also used as a multi-function entertainment venue for events such as rock concerts and circuses. The problem of providing for the different needs of an open air tennis stadium and a closed entertainment centre was solved by the development of an acoustically insulated roof covering the entire centre court stadium. The roof is in two sections: a fixed section covering the stadium seating; and a two-part retractable section covering the central area. When fully open the retractable roof halves are parked at the north and south ends of the stadium above the fixed roof, leaving an opening in the centre of the fixed roof 75m x 60m in size, oriented so as to minimise shadow effects on the court.

2. FIXED GRANDSTAND ROOF

2.1 Layout and Geometry

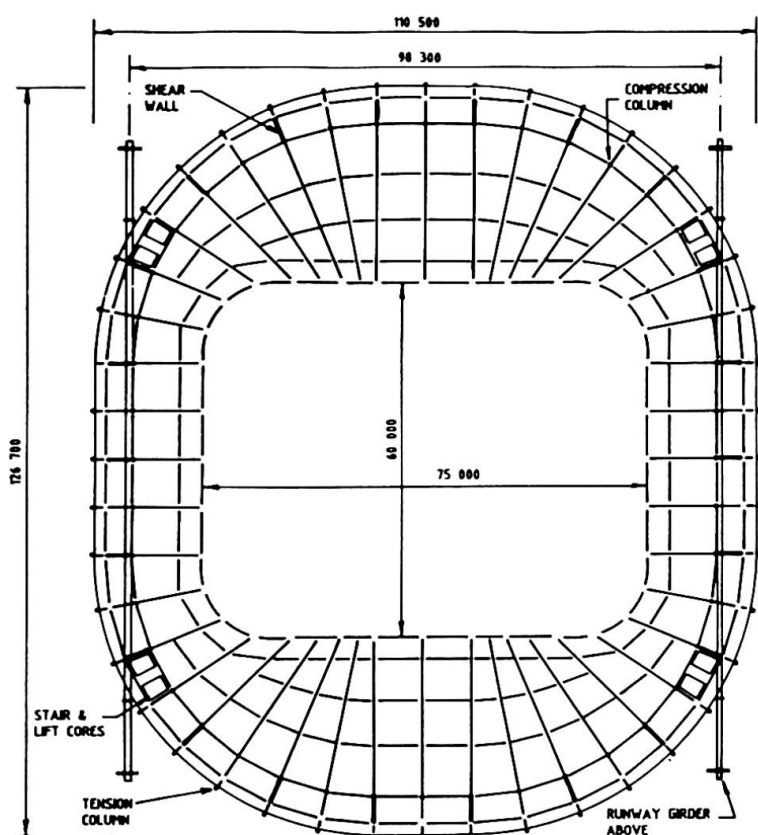


Fig. 1 Layout of Fixed Grandstand Roof

The fixed roof comprises 44 cantilevered radial trusses connected together by a series of circumferential trusses around the full perimeter of the stadium. Radial trusses vary in cantilever length from 11.35m along the East and West sides to 26.7m along the North and South sides, with a constant back span of 6.65m (Figure 1).

The geometry of the radial trusses was established by the requirement for all trusses to be at a constant level at three locations, these being the fascia around the roof opening, the fascia around the outside of the stadium and the roof line above the forward supporting column of the trusses. Because of the varying cantilever lengths this leads to radial trusses with varying grades from 1 in 40 (the minimum for drainage purposes) to 1 in 17 for the shorter cantilevers.

The radial trusses are supported vertically via the concrete raker beams which support the upper level seating. The front (compression) columns are located directly above the 600mm dia. concrete columns supporting the raker beams, whilst the rear (tension) columns are attached to the cantilever end of the raker beams. The tension column anchorage is adjustable to facilitate profile modifications during erection and at any stage during the life of the building. Radial trusses are connected to concrete shear walls located at every second raker beam to transfer horizontal loads to the substructure.

The radial trusses are supported upon 300mm diameter x 50mm elastomeric bearings at the front compression columns to accommodate thermal movements.

The radial trusses are connected together by 3 to 5 circumferential trusses at 8m centres maximum. These serve to brace the radial trusses, to distribute applied vertical loading and for the attachment of external perimeter fascia panels.

The total weight of structural steelwork in the fixed roof is 480 tonnes, excluding roof and ceiling purlins and catwalk grating.

2.2 Design

The fixed roof was analysed for static and dynamic vertical loading, thermal effects, wind pressures and support deformations. Taking advantage of symmetry effects, a single quadrant of the roof was modelled as a two dimensional grillage of horizontal beam elements with section properties specifically determined to simulate the deformation characteristics of the actual framework.

All cantilevered radial trusses were provided with spring supports to simulate the actual stiffnesses of the supports, and the separate effects of long term creep displacements at these supports were also included in the force envelopes for member design.

The determination of vertical wind loading for a roof containing a retractable section is complex and for this reason specialist assistance was sought to ascertain an appropriate upper bound pressure for design purposes. The critical case for uplift pressure occurs when the retractable roof is fully open and the wind approaches from the North or South across the stadium, striking the downwind cantilever. However, initial analyses proved that load cases incorporating wind effects were not the governing cases, so conservative wind pressures were adopted for design purposes to avoid the need for exhaustive model testing.

At the Southern end of the stadium the roof is designed to accommodate 35 tonnes of stage related entertainment equipment, such as speaker and lighting clusters. This loading is restricted to 1.1 tonnes at each of 32 specially provided hoisting points located at the nodal points of the radial trusses.

A separate study was made into the dynamic behaviour of the combined roof and concrete substructure to ascertain the susceptibility of the fixed roof to wind induced resonance and the response of the upper raker beams to spectator movements (particularly those of a rhythmic nature which might occur during, say, a pop concert).

The fundamental frequencies of vibration of the fixed roof were extracted from a three dimensional eigenvalue analysis of a full quadrant of the stadium.

The predicted response of the grandstand raker beams to rhythmic forces



resulted in the addition of intermediate columns to the upper raker beams in order to maintain the potential resonant forces and accelerations in these beams to within acceptable limit states.

2.3 Fabrication and Erection

The steelwork of the fixed roof was shop assembled and welded into component lengths up to 20m long for transportation to site. Once on site components were erected by mobile crane, the maximum lift being 6.1 tonnes. All field connections were made with Grade 8.8 high strength structural bolts tensioned to act in a bearing mode. The roof was designed on the basis that propping of the radial trusses would be unnecessary. The radial trusses were precambered by amounts varying up to 180mm in order to allow for approximately 80% of the permanent theoretical dead load deflections.

Erection of the fixed roof followed erection of the retractable roof runway girders and commenced simultaneously at the East and West sides of the stadium and progressed towards the North and then the South ends of the stadium sequentially. Radial truss erection was followed immediately by the adjoining circumferential trusses in a predetermined order. Tensioning of bolts was left until the completion of all steelwork at each end of the stadium. The entire erection procedure was enhanced by the use of purpose-designed mobile working platforms covering the full area beneath two of the longest radial trusses. These platforms were adjustable vertically to provide access for the later installation of the ceiling.

3. RETRACTABLE ROOF AND RUNWAY

3.1 Layout and Geometry

The retractable roof comprises 2 separate sections, each consisting of an exposed framework spanning 98.3m and supporting a suspended roof system 75m x 30m, sufficient to cover half the fixed roof opening. Each retractable roof section is supported on 4 electrically driven 4 wheel bogies capable of opening or closing the roof in about 23 minutes. The bogies run on twin rails mounted on a substantial runway girder.

The tubular framework of each roof section is made up essentially of two primary longitudinal trusses at 12m centres supported on disc bearings at bogie locations, with semi-circular shaped transverse frames at 9.1m centres to support the extremities of the 30m wide suspended roof system.

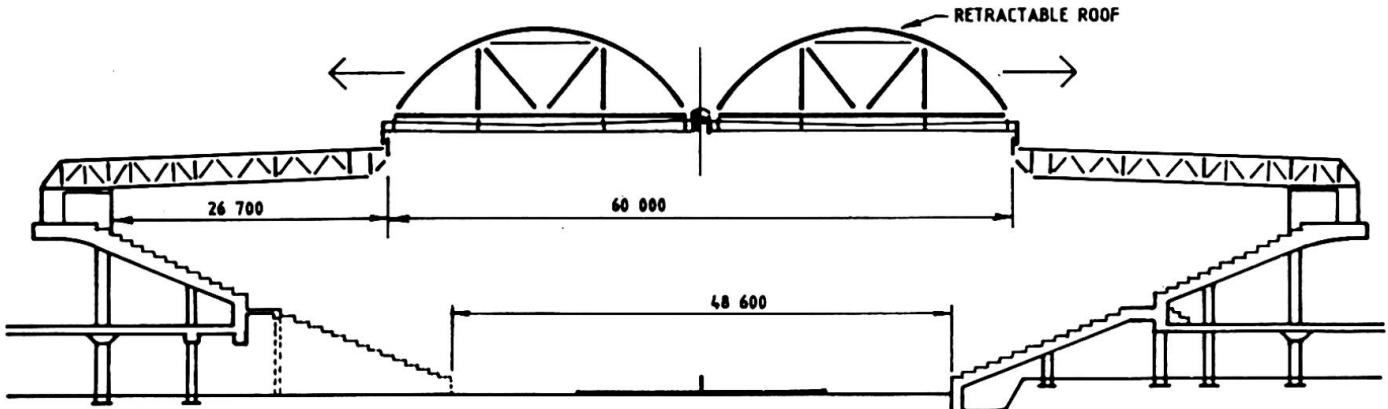


Fig. 2 North-South Section through Stadium

The two runway girders upon which the retractable roof bogies travel are located 98.3m apart and are each 109m in overall length. The term runway girder is used to describe collectively a 760mm x 460mm box girder to which the twin rails are attached and its support system which varies over its length. The runway girder is located primarily within the confines of the fixed roof except for a 20m length exposed at each of its ends. Within the stadium the support is a parallel-chord truss spanning between the shear walls, whilst outside the stadium structure the support is a truss with a curved bottom chord spanning between two 16.2m high braced tubular steel columns.

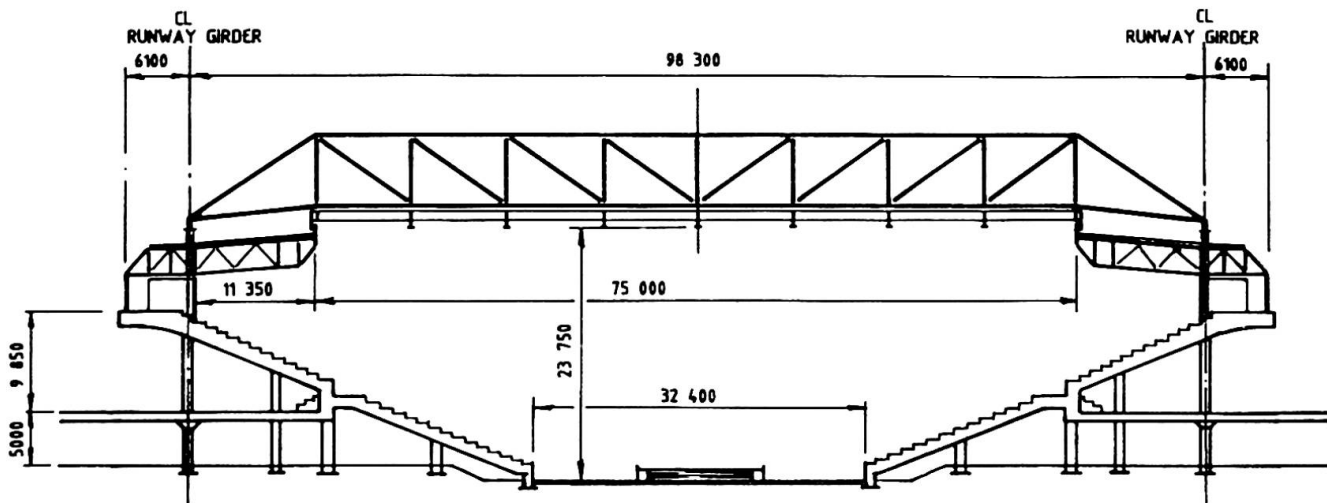


Fig. 3 East-West Section through Stadium

The runway girders are structurally independent of the fixed roof, but are restrained longitudinally by means of disc bearings at the lift wells located at each corner of the stadium.

The retractable roof bogies are supported on two 60 kg rails located 460mm apart directly above the webs of the box girder. The rails are placed on 7mm thick neoprene pads to suppress noise levels.

The total weight of structural steelwork in the retractable roof is 300 tonnes, excluding roof and ceiling purlins and the total weight of structural steelwork in the runway girder system is 190 tonnes, including the external support columns.

3.2 Design

The retractable roof was analysed for vertical and horizontal loading as a 3-dimensional space frame.

The critical wind loading case for the retractable roof occurs with the roof in the fully open position when one corner of the roof is exposed to updraughts.

Each roof truss can accommodate up to 24 tonnes of performance related equipment, suspended from 7 monorail beams located just below ceiling level. Monorail beams have up to 4 no. 3 tonne electric hoists accessed from retractable platforms contained within the fixed roof.

The runway girder system is designed to accommodate lateral and vertical loading from the retractable roof support bogies. Each retractable roof



section is supported on disc bearings at each of the four bogies, with one fixed bearing and three undirectional sliding bearings provided. A support system with a single point of translational fixity was adopted to minimise skewing forces normal to the runway girder.

During operating conditions each roof section is driven by only two of the bogies and these in turn are speed synchronised with a multiple control system to ensure that they do not differ in relative position by more than an absolute maximum of 500mm. Operation of the roof is not permitted for winds gusting above 15m/s.

When the roof sections are in the fully opened or closed positions mechanical locks are engaged automatically to ensure that the drive bogies are immobilized for any wind condition.

For the full 210m perimeter of each retractable roof section a unique yet simple sealing system, utilizing various configurations of natural rubber flaps, is provided to weatherproof and acoustically seal the interface between the retractable and fixed roofs. The sealing arrangement is designed to accommodate large vertical and horizontal relative movements between the various components, and to minimise both the forces exerted on conjugate parts and the power requirements of the drive motors.

3.3 Fabrication and Erection

The framework for each section of the retractable roof was largely field assembled and welded on site 40m South of the stadium perimeter and subsequently jacked up to final elevation prior to being moved laterally into its permanent position above the fixed roof. The jacking system used for raising each of the 260 tonne roof sections was based on the standard BBR system. The 20m lift was completed in approximately 9 hours.

The primary connections of the main trusses involving up to 7 intersecting tubular sections were generally facilitated by the use of central gusset plates in the plane of the main longitudinal trusses and diaphragms at each node. This form of connection gives a direct means of connection of primary truss members and provides sufficient rigidity to the main tubes to enable the direct tube to tube connection of secondary members.

Following shop assembly and welding of the primary frame nodal assemblies, the erection procedure for each retractable roof section involved assembly and welding of nodes and frame elements between nodes in a sequence from mid-span toward each end. Roof and ceiling purlins and diagonal bracing were then installed with bolts left loose. The structure was then jacked up to a height of 2m, where the roof and ceiling cladding and acoustic insulation were installed and bolts tensioned before jacking the roof to its full height. Temporary runway girders and the bogies were then fixed in place, the roof lowered onto the bogies and driven laterally into its final position.

The longitudinal trusses of each roof frame were precambered upwards by 280mm to accommodate approximately 80% of the full theoretical dead load deflection and this assumption was validated by the actual deflections recorded.

4. ACKNOWLEDGEMENTS

The National Tennis Centre was constructed for the National Tennis Centre Trust. Project Manager for the development was Civil and Civic Pty. Ltd.

Überdachung des Wiener Praterstadions

Roof of the Praterstadion of Vienna

Toiture du stade du Prater de Vienne

Heinz PIRCHER

Dipl.-Ing.

TDV – Pircher und Partner
Graz, Österreich

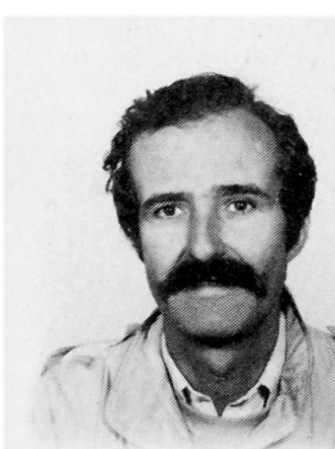


Heinz Pircher, geboren 1942, absolvierte sein Bauingenieurstudium an der TU Graz. Nach fünfjähriger Tätigkeit als Assistent am Institut für Stahlbau, Holzbau und Flächentragwerke gründete er 1970 TDV. Er beschäftigt sich mit der Entwicklung von Software und deren Anwendung für das Ingenieurwesen. Weiters ist er Lehrbeauftragter an der TU Graz.

Albert P. RAUNICHER

Dipl.-Ing.

Ing. büro Zemler + Raunicher
Wien, Österreich



Albert P. Raunicher, geboren 1944, studierte Bauingenieurwesen an der TU Wien und ist in der Statik und Konstruktion des Hoch- und Industrieanlagenbaus sowie des konstruktiven Ingenieurbaues tätig. Seit 1979 selbständiger Zivilingenieur für Bauwesen. Spezialgebiet: weitgespannte Flächentragwerke.

ZUSAMMENFASSUNG

Die im Herbst 1986 fertiggestellte Überdachung des Wiener Praterstadions überspannt, nur am Außenring aufgelagert, frei eine Ellipse mit 270 x 215 m und ist damit eine der weitest gespannten Dachkonstruktionen der Welt.

SUMMARY

The roof of the Prater stadium in Vienna was completed in autumn 1986. The construction, only supported by the outside ring, is spanned over an ellipse of 270 x 215 m. It is one of the largest constructions of this type in the world.

RÉSUMÉ

La nouvelle toiture du stade du Prater de Vienne a été complétée en octobre 1986. La construction, supportée seulement par l'anneau extérieur, est une ellipse de 270 x 215 m. Il s'agit d'une des plus vastes toitures tendues du monde.



1. ALLGEMEINE BESCHREIBUNG DER KONSTRUKTION

Das Tragwerk ist als Stabschale ausgebildet. Der Außenring, von 112 lambdaförmigen Rahmen am äußeren Tribünenrand über Pendelstäbe unterstützt, wirkt als Druckring. Der Innenring, ca. 13 bis 17 m tiefer angeordnet und in ca. 48 m Entfernung parallel auf einer kleineren Ellipse verlaufend, wirkt als Zugring.

Zwischen Zug- und Druckring sind radiale Speichen und die Stabschale angeordnet, gebildet aus weiteren 4 Zwischenringen und Diagonalstäben. An jedem Knoten schließen somit im allgemeinen 6 Stäbe an (Fig.2).



Fig.1 Fertiges Stadion

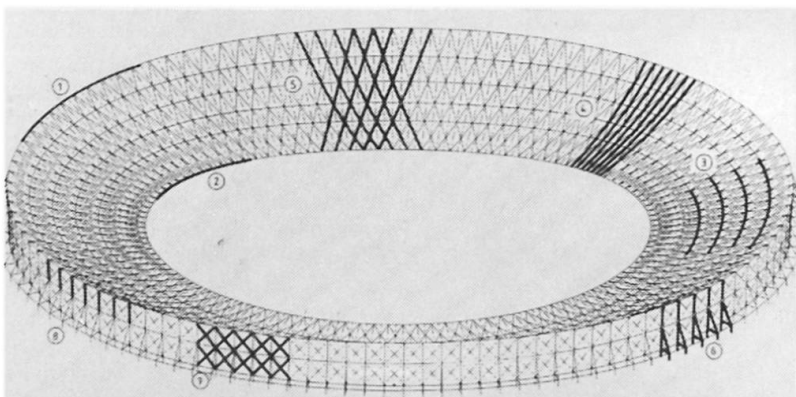


Fig.2 Komponenten des statischen Systems

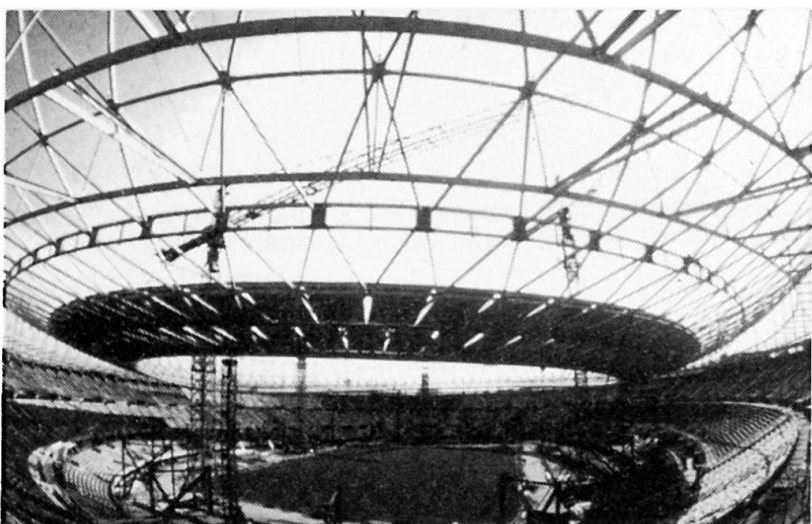


Fig.3 Montagezustand

Legende :

- 1 Außenring
- 2 Innenring
- 3 Zwischenringe
- 4 Speichen
- 5 Diagonalen
- 6 Lambda-Rahmen
- 7 Auskreuzung
- 8 Pendelstützen

Die Dachhaut liegt zwischen Innenring und mittlerem Zwischenring auf dem tragenden Stabwerk auf. Zwischen Mittel- und Außenring ist die Dachhaut vom Stabwerk abgehängt. Es ergibt sich ein flaches Satteldach, während die tragende Stabschale mit gleichmäßig konkaver Krümmung vom Innenring zum aufgeständerten Außenring verläuft (siehe Fig.6).

Die ästhetisch reizvolle Konstruktion stellt eine besonders wirtschaftliche Lösung dar :

- sie ist mit 1700 Tonnen Stahl (53 kg/m^2) in Relation zur Stützweite sehr leicht.
- aufgrund des geringen Gewichtes und der weiträumig verteilten Lasteinleitung war keine Verstärkung der bestehenden Tribünenkonstruktion notwendig.
- die Montage konnte ohne Hilfsunterstützungen innerhalb der Dachfläche nur von Kränen aus durchgeführt werden.
- Detailprojektierung und Bauausführung wurden in zusammen nur 15 Monaten durchgeführt.

2. DER "CONZEM" – KNOTEN

Der "CONZEM"-Knoten ist das Herzstück der Konstruktion : Ein ca. 80 cm großer Sphäroguß-Hohlkörper mit 6 Öffnungen, in welchen die 6 anschließenden Stäbe (Rechteckrohre 150/250 mm) vorerst nur lose gesteckt werden. Wenn alle Stäbe montiert sind, werden die verbleibenden Hohlräume mit Spezialbetonmörtel vergossen, nach Erhärten ist der Kraftschluß hergestellt (Fig.4).

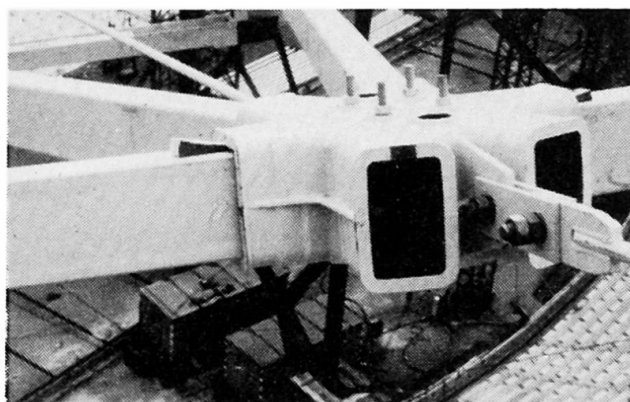


Fig.4 CONZEM-Knoten

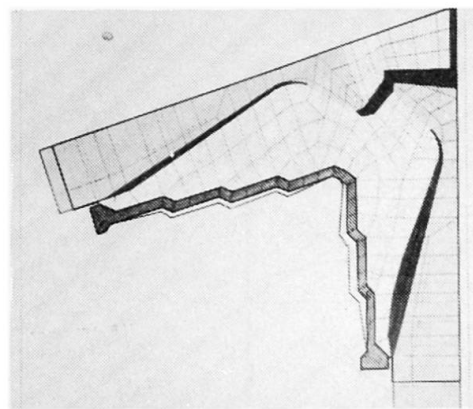


Fig.5 FE-Modell mit gerissener Betonzugzone

Auf der Baustelle müssen so weder Verschraubungen noch Schweißarbeiten durchgeführt werden. Die Geometrie der einzelnen Knoten ist verschieden, nur jeweils 4 sind zueinander symmetrisch. Das System lässt es aber zu, die Paßmaße so mit Toleranzmaßen zu erweitern, daß die Knoten für die gesamte Konstruktion aus 3 Grundtypen (Gußformen) gefertigt werden konnten.

Das Eigengewicht der Konstruktion wird nicht über die im Knoten verankerten Stäbe abgetragen (siehe Fig.3). Der Verguß-Beton in den Knoten wird daher nur durch kurzzeitige Lasten beansprucht. Kriechvorgänge sind daher nicht zu erwarten.

Die Biegesteifigkeit zwischen Knoten und Stäben ist entscheidend für die Abtragung der Windkräfte und die zugehörigen Stabilitätsnachweise (Durchschlagen der Stabschale nach oben !). Es wurden daher Festigkeitsversuche an Originalknoten durchgeführt. Parallel zu diesen Versuchen wurden auch Berechnungen nach der FE-Methode ange stellt. Zugspannungen im Füllbeton wurden dabei ausgeschaltet, die Reibung zwischen Stahl und Beton wurde mit 0.35 begrenzt. Es ergab sich gute Übereinstimmung zwischen Versuch und Berechnung, aus der statischen Auswertung der Versuche wurde eine Bemessungsvorschrift abgeleitet.



3. DIE MONTAGE

- zuerst wird der Außenring montiert, dann der Innenring auf einem leichten Hilfsgerüst ca. 0,7 m unterhalb seiner späteren Lage in Position gebracht.
- Montage der "Speichen": Jeweils 2 bzw. 3 Knotenstücke werden mit Rundstählen zu einer "Kette" verbunden und in radialer Richtung zwischen Außen- und Innenring eingehängt.
- anschließend werden die Diagonal- und Zwischenringstäbe vom Kran aus in die Knotenstücke eingeschoben. Das Eigengewicht der Stäbe spannt die "Ketten", über die Mechanik eines "Seileckes" stellt sich die Geometrie des Tragwerkes von selbst ein. Dabei hebt der Innenring automatisch vom Hilfsgerüst ab (Fig.6).
- jetzt werden die Knoten vom Kran aus mit Spezialmörtel gefüllt, nach Erhärten ist Kraftschluß hergestellt.
- zuletzt wird dann die Dachhaut (Trapezbleche) montiert.

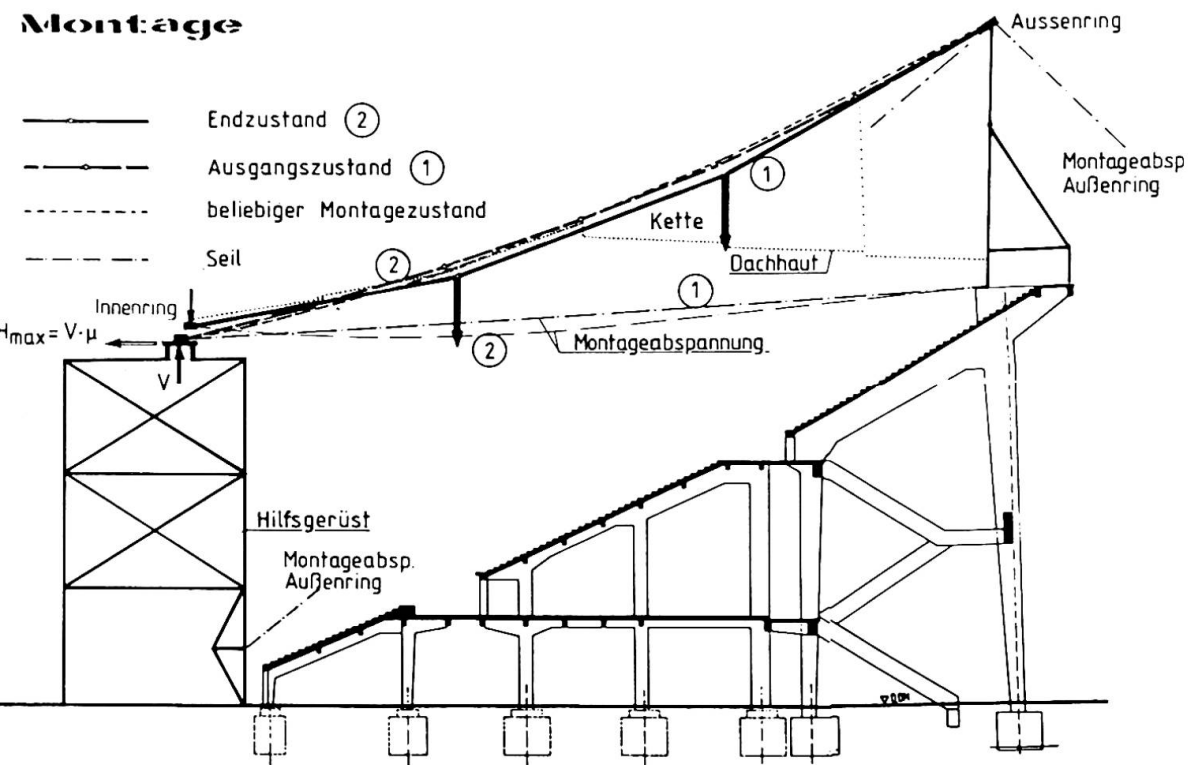


Fig. 6 Schnitt

Dieser Montagevorgang ist Voraussetzung für die wirtschaftliche und schnelle Herstellung der Konstruktion. Für Statik und Formgebung des Bauwerkes ergeben sich folgende Konsequenzen:

Vor Ausgießen der Knoten wirkt die Stabschale nicht im statischen System mit. Dieses besteht aus 2 elliptischen Ringen, die durch radiale Gelenkketten verbunden sind. Die vertikalen Knickwinkel der Gelenkketten entsprechen der Last, die in jeden einzelnen Knoten eingeleitet wird. Die beiden Ringe können ohne die aussteifende Wirkung des Stabwerkes nur eine geringe Biegewirkung abtragen. Daher muß die Ringzugkraft (innen) bzw. Ringdruckkraft (außen) mit den Zugkräften der Speichen im Sinne von "Umlenkkräften" im Gleichgewicht stehen. Die variable Krümmung des Außenringes bildet sich daher in einer variablen Höhenlage des Innenringes ab. Die elegante Raumkurve des Innenringes entspricht also nicht der architektonischen Gestaltung, sondern der Notwendigkeit einer biegungsfreien Abtragung des Eigengewichtes im Bauzustand.

Diese Idealgeometrie garantiert biegungsfreies Abtragen allerdings nur im Endstadium der Montage, wenn das volle Eigengewicht wirkt. In vorangehenden Montagephasen paßt das Kräftespiel der teilbelasteten Struktur nicht zur Geometrie des Innenringes. Es kommt daher zu großräumigen Verformungen, die durch die Hilfsauflagerung des Innenringes und zusätzliche Hilfsabspannungen begrenzt und behindert werden müssen.

4. DIE STATISCHE BERECHNUNG

wurde weitgehend am Computer abgewickelt und mußte unter anderem folgende Probleme lösen :

- Große Verformungen : Zwischen Ausgangslage im Montagezustand und verformter Lage extremer Lastzustände bestehen Differenzen bis zu 2,5 m. Daher wurde die gesamte Berechnung unter Berücksichtigung der Effekte großer Verformungen (Theorie III. Ordnung) durchgeführt.
- Bauzustände : Das verwendete Programm mußte in der Lage sein, alle Verformungen und Schnittkräfte über die ständig wechselnden statischen Systeme zu akkumulieren. Dabei ist zu beachten, daß die "Ketten" im Montagezustand im Sinne einer Seilnetzkonstruktion wirken. Für alle wichtigen Bauphasen waren Spannungen, Verformungen, sowie die Stabilität des äußeren Druckringes nachzuweisen. Dazu mußten die Effekte von Seilabspannungen inkl. Zug-Druck-Ausschaltung, das Abheben von Auflagern zusammen mit der automatischen Berechnung der horizontalen Reibungskräfte in der Iterationsrechnung gemäß Theorie Großer Verformungen berücksichtigt werden. Bei der Berechnung des fertigen Systems (Stabschale mit nun biegesteifen Knotenverbindungen) mußte beachtet werden, daß die Beanspruchung aus Eigengewicht im Sinne des Bauzustandes verbleibt und nur später aufgebrachte Lasten (Wind, Schnee usw.) am Gesamtsystem wirken.
- Knicken des Außenringes im Bauzustand : Die lambdaförmigen Stützrahmen sind zum Außenring mit einem Pendelstab angeschlossen. Der Außenring ist also radial frei beweglich. Jede denkbare Knickfigur des Außenringes hat aber auch tangentielle Bewegungskomponenten. Auf diesem Wege dienen die Auskreuzungen zwischen den Lambdarahmen zur Knicksicherung. Wegen dieser tangentiellen Verformungsbehinderung hat die kritische Knickfigur eine relativ kurze Wellenlänge.
- Stabilitätsnachweis : Hierzu wurden für mehrere Lastkombinationen die Lastwerte in mehreren Stufen gesteigert. Dadurch wurde sichergestellt, daß die Lasten mit normgemäßer Sicherheit aufgenommen werden, ohne daß im System Instabilitäten auftreten. Dabei wurde besonders auf das Problem des "Durchschlagens" bei Windsog geachtet. Die erforderliche Sicherheit konnte nur dadurch erreicht werden, daß die Rundstäbe der Ketten am Außenring wechselweise oben und unten exzentrisch angeschlossen wurden. Benachbarte Knoten erhalten so einen Niveau-Unterschied und die Stäbe des Stabwerkes bilden mit den Rundstäben der Ketten ein Sprengwerk, das dann für Biegung in radialer Richtung die erforderliche Steifigkeit bringt (Fig.7).

5. DIE SCHWINGUNGSBERECHNUNG

Zur Beurteilung der Auswirkungen von Windböenbelastungen wurde eine dynamische Berechnung durchgeführt. Es wurden alle Eigenfrequenzen und Eigenschwingformen bis zur Frequenz von 2 Hz ermittelt. Zur



Festlegung der Erregerkräfte standen die Ergebnisse eines Windkanalversuches zur Verfügung :

- Druckverteilung für das "Stundenmittel"
- Spectrum für die "Standardabweichungen" der Winddrücke vom Stundenmittel.

Auf Basis der "Modalen Analyse" wurden Standardabweichungen der Schnittkräfte und Verformungen zu den Werten des Stundenmittels berechnet. Inzwischen vorliegende Beobachtungen für einige extreme Windereignisse haben die Vorausberechenbarkeit der winderregten Schwingungen bestätigt. Rechnung und Wirklichkeit unterscheiden sich bezüglich der Kraftübertragung durch Reibung zwischen der Tragkonstruktion und den Trapezblechen der Dachhaut. Daher steht der errechneten niedrigsten Eigenfrequenz von 0,4 Hz eine gemessene von 0,5 Hz gegenüber. Die Dämpfung, für die Rechnung mit 7% angenommen, wurde am fertigen Bauwerk mit 12% gemessen. Wenn man diese beiden Parameter (Dämpfungskonstante und verschobene Eigenfrequenz) in der modalen Analyse entsprechend korrigiert, stimmt die Rechnung im Rahmen der Beobachtbarkeit mit dem tatsächlichen Verhalten der Struktur überein.

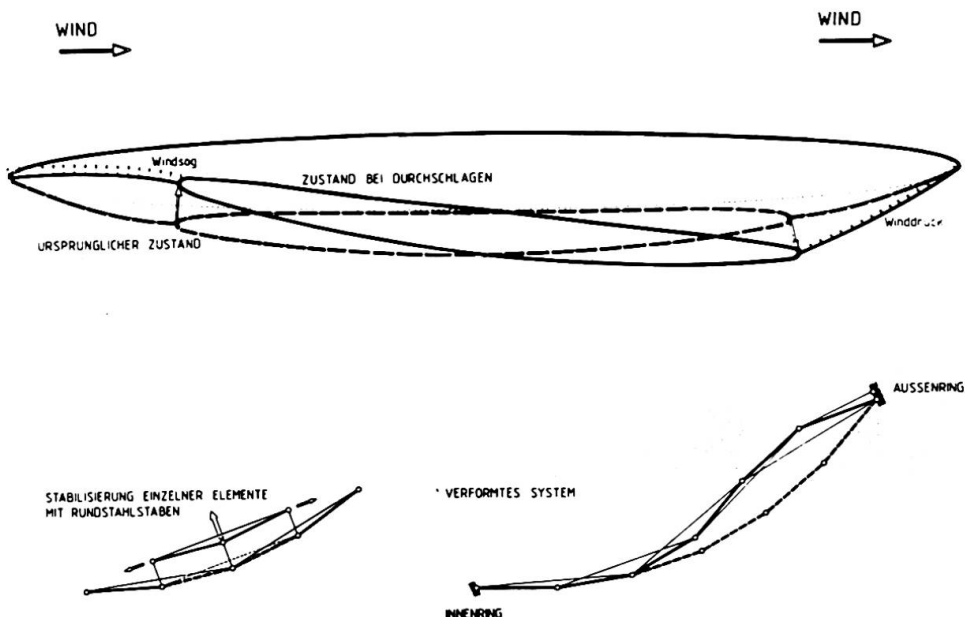


Fig. 7 Durchschlagen bei Windsog

Abschließend sei noch allen am Projekt Beteiligten für die gute Zusammenarbeit gedankt :

Gesamtplanung und Bauüberwachung :
Ingenieurbüro CONPROJECT
Ing. Erich Frantl
Ing. Peter Hofstätter

Statik :
Dipl.-Ing. Willibald Zemler
Dipl.-Ing. Albert P. Raunicher
EDV - Statik :
TDV-Dipl.-Ing. Heinz Pircher

Bauherr :
Wiener Stadthalle - KIBA
Generalunternehmer :
VOEST-ALPINE-HEBAG, vormals
Wiener Brückenbau A.G. (WBB)

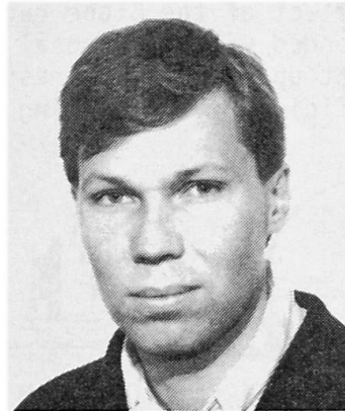
Prüfingenieure :
Univ.Prof.Dipl.-Ing.
Dr. Peter Klement
Dipl.-Ing.Dr. Kurt Kratzer
Schwingungstechnische Beratung :
Doz.Dr.-Ing. Hans Ruscheweyh

Unique Thin Walled Shells with Large Span Used as Roofstructures

Dünnwändige grosspannige Schalen verwendet als Dachstrukturen

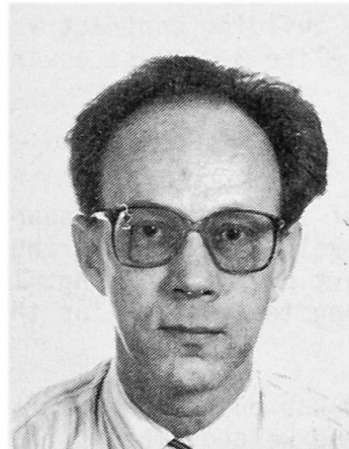
Coques de mince épaisseur à grande portée employées comme structure de toit

Lars HAMMARSTRÖM
Götaverken Arendal AB
Gothenburg, Sweden



Lars Hammarström received his Masters degree in Civil Engineering from Chalmers University of Technology, Gothenburg 1986. He has been working with marine structures at GVA since then. Mainly off-shore structures as for example Tension Leg Platforms and the new Swedish Icebreaker.

Lars Å. SAMUELSON
Swedish Plant Inspectorate
Stockholm, Sweden



Lars Å. Samuelson received his Masters degree from the University of Technology, KTH, in Stockholm 1961 and his Ph D in Engineering in 1969. Worked 1961–1979 for the Aeronautical Res Inst of Sweden. He is presently responsible for research and development in stability of shells at the Swedish Plant Inspectorate. Member of ECCS TWG 8.4.

SUMMARY

A unique design of the spherical roof of the Stockholm Globe Arena was proposed by the Engineer based on years of experience in shipbuilding. Vertically stiffened thin-walled plates welded to form spherical segments were to be assembled on site and hoisted in place on the supporting ring of the base structure. The design work primarily concentrated on the stability of the shell structure, utilizing linear bifurcation, non-linear collapse and non-linear dynamic analyses for a number of static and dynamic load case, including accidental loads.

ZUSAMMENFASSUNG

Die in seiner Art einzige Konstruktion von dem sphärischen Dach für die Stockholm Globe Arena gründet auf langjährigen Erfahrungen im Schiffbau. Vertikal verstifte dünnwändige Stahlbleche, on site zusammengeschweisst zu sphärischen Segmenten, sollten auf ihren Platz auf den tragenden Ring von der Grundstruktur gehoben werden. Die Konstruktionsarbeit wurde primär auf die Stabilität der Schalenstruktur eingerichtet.

RÉSUMÉ

Un projet unique du toit sphérique de la Stockholm Globe Arena basé sur plusieurs années d'expérience dans l'architecture navale a été proposé. Des lames de mince épaisseur, avec raidissement transversal, soudées pour former des segments sphériques, devaient être assemblées sur place et finalement levées pour montage sur le cercle de support de la structure de base. Le projet traite essentiellement de la stabilité de la structure de la coque.



1. BACKGROUND

In the development of light-weight structures, the tendency has been towards use of unstiffened and stiffened shells. Examples are aircraft and automobile structures. Steel ships were always built as shell structures and, when GVA moved into the offshore branch of floating constructions it was natural to utilize true shells rather than the current compromise between beam and plate structures. This was appreciated by the market.

When approached by the architect of the Globe regarding the possibility to build the spherical roof GVA responded with a proposal for a stiffened shell structure. The design was not optimized with respect to weight but with respect to the total cost through efficient manufacturing and erection procedures.



Fig. 1.1 Conception of the STOCKHOLM GLOBE ARENA

In the final competition the building contract was awarded to MERO and the GLOBE was finally built as a shell-like 3-D truss covered by prefabricated panels.

2. BASIC GVA DESIGN

The GLOBE is a half sphere of 110 m diameter supported by a heavy ring at the equator 35 m above ground level. Fig 2.1 The ring is supported by 48 arched columns forming the lower part of the building. The GVA design included a heavy ring at the 80 m level forming the support for the suspended equipment weighing approximately 200 tons.

The shell structure proposed was built up from 144 singly curved sheets to which the vertical T stiffeners were welded. The stiffened sheets were to be manufactured at the GVA plant and shipped to Stockholm. On site three by four sheet were to be joined together into segments by a special zig-zag welding technique developed by GVA in order to minimize distortions.

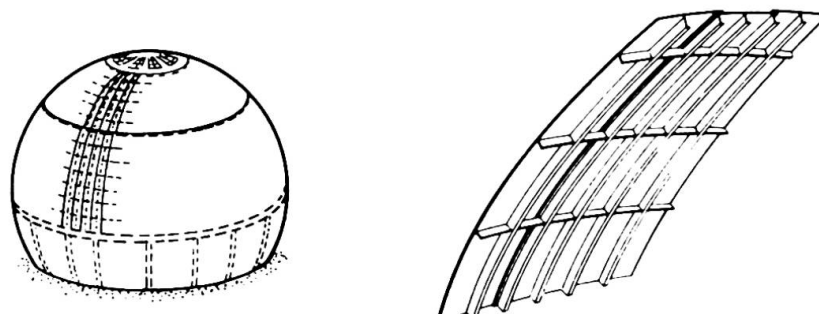


Fig. 2.1 Overview and detail of proposed structure

Erection of the structure was planned according to Fig. 2.2. First the central cap and the upper ring would be assembled on the ground and lifted to the final position by four large cranes. Subsequently, the shell segments were to be hoisted into place and welded.

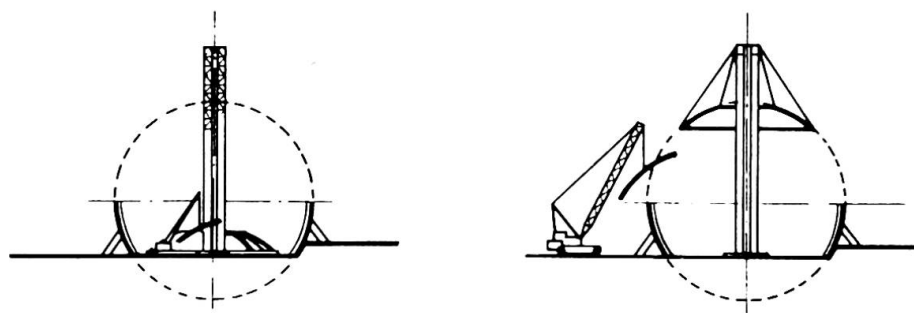


Fig 2.2 Main phases of construction

3. DESIGN PHILOSOPHY

The manufacturing technique for the proposed dome structure is based on well established ship building practice. Since the structure may be characterized as a thinwalled shell, the design analysis differs from that of the shipbuilding technology where, mostly, plane panels are used. Shell analysis requires consideration of imperfection sensitivity and the effect of local forces and nonuniform pressure distributions. A safe design may be based on the following criteria:

The basic structure treated as a ring stiffened orthotropic shell of revolution may be analyzed by use of special purpose computer programs. Initial estimates of the elastic buckling loads are obtained for an equivalent axisymmetric pressure distribution and, the carrying capacity is estimated by application of realistic reduction factors. Such factors may be approximately extrapolated from codes and experimental results presented in the literature. Final verification of the design is achieved through extensive non-linear analyses of the collapse behavior for a number of static and dynamic forces including catastrophic load cases. The design requirements are summarized in Fig 3.1.

The stability limit may be determined by use of bifurcation or collapse analysis or a combination of the two methods. Since the globe structure may be characterized as a shell of revolution, buckling analysis by use of linear bifurcation is easily carried out by use of special purpose programs. However, the calculated buckling load may be a very poor estimate of the carrying capacity and an appropriate reduction factor must be applied. According to Det norske Veritas (DnV) a reduction factor of 0.05 would apply for the unstiffened sphere, whereas a value of 0.1 to 0.2 may be realistic for the stiffened shell being proposed.

In a non-linear collapse analysis considering the nonsymmetric load distributions, initial deflections and other disturbances a reduction factor should not be necessary. However, it is strongly recommended to apply a factor of safety exceeding the value of 2.

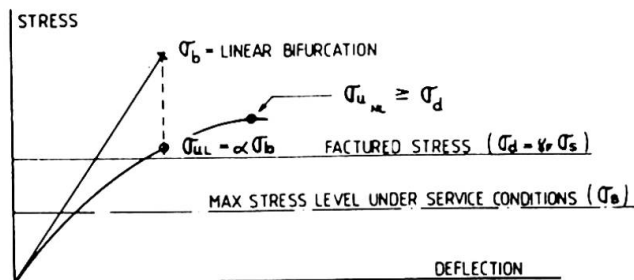


Fig 3.1 Definition of safety requirements



4. LOADS AND DISTURBANCES

The Swedish building code requires design with respect to a number of acting forces including wind and snow loads. The actual load distributions for the Globe were interpreted as shown in Fig 4.1, where the wind pressure distribution was taken from the Swiss code, 1 . In addition, two accidental load cases were considered. The first one simulates the loss of one of the support columns and the second an impact of a small airplane (see Fig 4.2). The load cases are numbered as follows:

Table 1. Definition of load cases

Load case no	acting loads
1	Eigenweight
2	Eigenweight + snow load
3	Eigenweight + wind pressure
4	LC 2 removal of support leg
5	LC 2 impact of small airplane: Shell section 5x5 m removed when max stresses reached in impact area

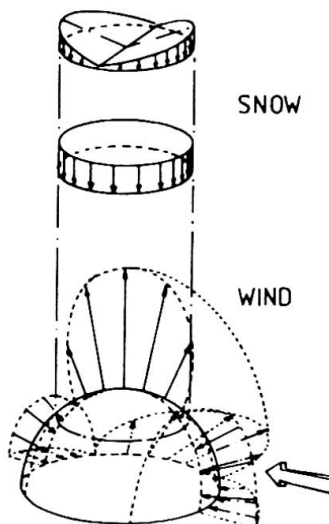


Fig 4.1
Environmental loads

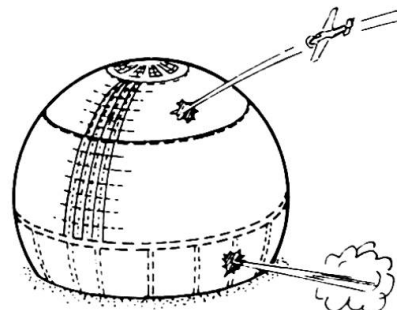


Fig 4.2
Accidental loads

5. MODELS AND METHODS OF ANALYSIS

Two basic models where used in the analysis. Since the Globe may be characterized as an orthotropic shell of revolution, certain stability problems may be readily treated by use of special purpose programs such as BOSOR4, 2 . The model, as shown in Fig. 6.1 includes discrete rings (horizontal) and 288 vertical stiffenes treated as smeared. This model was used for preliminary design of the stiffening system.

BOSOR4 does not have the capability to analyze buckling under nonsymmetric loads. Such cases were modeled in SOLVIA, (ADINA) 3 . Fig 6.2 shows the two FE models used in the analyses performed, including dynamic response. By necessity the shell and beam elements were lumped in order to reduce the size of the problem to a reasonable level.

BOSOR4 was used to analyze axisymmetric load cases including an approximation of the wind pressure distribution in the manner deviced in the German DAST rules, 4 . The program gives the stresses in the shell and the bifurcation buckling loads and it is a powerful tool in the early design phase. The program has a branch for computation of the eigenmodes and eigenfrequencies of the structure.

The sphere is very sensitive to imperfections and nonsymmetric loads, and it was essential to evaluate the influence of these parameters by use of nonlinear, large displacement theory. SOLVIA was used for this purpose and, for instance, discrete support loads, weights attached to the upper ring etc could be easily modeled. In addition linear eigenvalue problems can be handled by SOLVIA.

6. RESULTS

The BOSOR4 analysis showed that load case no 2 is the most critical since the wind produces suction at the crown. Typical results are shown in Fig. 6.1, indicating that buckling occurs above the ring in the area where two way compression exists. BOSOR4 was used in the preliminary design and Table 2 includes results for the unstiffened and vertically stiffened only designs. Dynamic analysis indicated a minimum eigenfrequency of 7 Hz.

Table 2 Linear bifurcation buckling analyse

		Load factor	Waves	
Unstiffened	LC 1	2.4	3	BOSOR4
432 Stiffener no rings	LC 1	6.3	90	BOSOR4
432 Stiffener no rings	LC 3	85.0	30	BOSOR4
288 Stiffener 10 rings	LC 2	38.0	25	BOSOR4
288 Stiffener 10 rings	LC 2	13.0	2	SOLVIA

Table 3 Non-linear large displacement analyse SOLVIA

	Load factor	Displacement nod D mm	Max eff. stress MPa
LOADCASE 2	1.0	20.0	35.5
LOADCASE 2	3.0	64.0	107.2
LOADCASE 3	1.0		
LOADCASE 3	3.0		

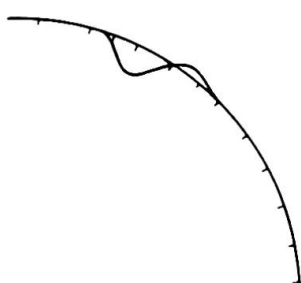


Fig 6.1 BOSOR Model and LC 2 critical buckling mode

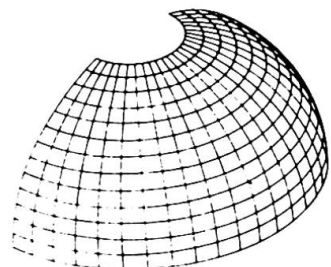


Fig 6.2 FE Model

The SOLVIA/ADINA program was utilized for linear bifurcation analysis of load case no 2, Fig 6.5 where the effect of the suspended point load could be included. The load factor of 13 is probably a slight underestimation since the cap was not included in the model.

Non-linear analyses were carried out for load cases 2 and 3. Sample results are shown in Figs 6.3 and 6.4. It was found that deflections and stresses are small and that their dependence on the load is practically linear up to a factor of three times the base load. The results are summarized in Table 2.

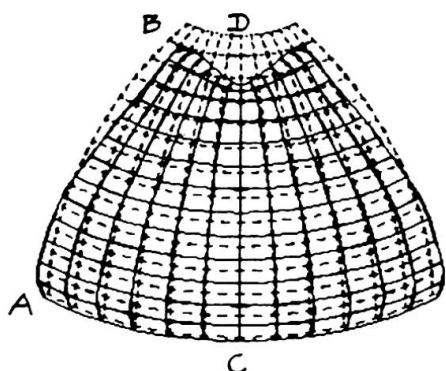
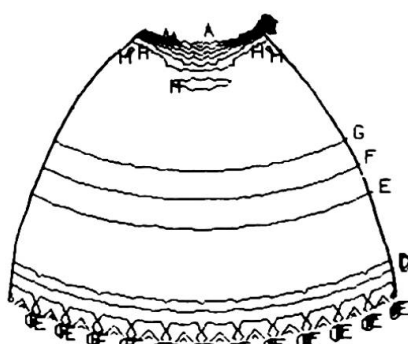


Fig 6.3 Deformation plot for LC 2



EFF. STRESS SHELL TOP MAX 0.3553E8	
A	0.3376E8
B	0.3022E8
C	0.2668E8
D	0.2313E8
E	0.1959E8
F	0.1605E8
G	0.1251E8
H	0.896E7

Stress plot for LC 2

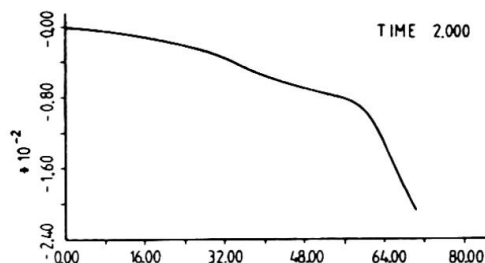
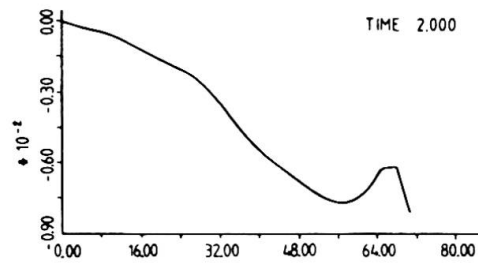


Fig 6.4 Displacement along line AB see Fig 6.3



Displacement along line CD

Finally a number of dynamic analyses were run simulating load cases 4 and 5. Case No 4 proved not to be critical. In case 5 the analysis was run in two steps. First the deflections of the intact shell due to the impact were calculated. At the time of maximum stress the impactor was assumed to rip a hole in the shell and the analysis was carried out for a few cycles. The shell was pre-loaded as in case No 2. Sample results are shown in Fig 6.6.

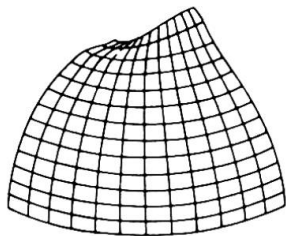
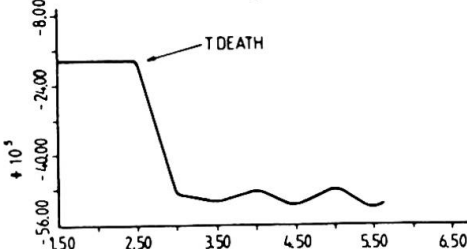


Fig 6.5

Fig 6.6



Buckling modes LC 2

Axial stress response at edge of hole, LC 5

7. DISCUSSION

The proposed stiffened shell design of the GLOBE was shown to fulfill all requirements of the Swedish Building Code and additional accident/sabotage related load cases. Because of the extreme dimensions of the structure - the r/t ratio of the shell plating equals 7000 - extra safety margins were considered. As a matter of fact, optimization of the structure would lead to some weight reduction but, handling and assembly would require more sophisticated procedures. The total cost of the proposed GLOBE design may thus be assumed to be reasonably close to the optimum.

REFERENCES

1. SIA 160, Swiss Building Code
2. BOSOR4, Users Manual, 1986
3. SOLVIA-IN, Users Manual, 1987
4. DEUTSCHE AUSSCHUSS für STAHLBAU Ri 013
5. SBN 80, Swedish Building Code, 1982:3

Design of Long Span Prestressed Concrete Railway Bridge

Conception d'un pont de grande portée en béton précontraint pour voie ferrée

Auslegung einer Spannbeton-Eisenbahnbrücke großer Spannweite

Iwao YOSHIDA

Director
Honshu-Shikoku Bridge Auth.
Tokyo, Japan

Born in 1925, obtained his engineering degree and doctorate at University of Tokyo.

Dairoku MATSUDA

Manager
Sakaide
Construction Office
Kagawa, Japan

Born in 1946, graduated from Central Railway Training School, Tokyo Japan.

Hiroo JIN

Chief of Research Div.
Honshu-Shikoku Bridge Auth.
Tokyo, Japan

Born in 1942, obtained his engineering degree at Kyushu University.

Masayuki OTSUBO

Deputy Manager
Kojima Construction Office
Okayama, Japan

Born in 1949, graduated from Central Railway Training School, Tokyo, Japan.

SUMMARY

This report summarizes the design of a five-span continuous PC box girder bridge having a span length of 120 m, the longest in Japan serving as a railway bridge. The safety of the structure and the reliable running of trains were examined using seismic response analysis. PC steel bars were used to resist for dead load of cantilever-erected girder and PC steel stranded wires were used for the completion system of train load. Low friction sheaths were used for the PC steel stranded wires.

RÉSUMÉ

Le rapport présente la conception d'un pont en poutre-caisson en béton précontraint à cinq travées continues d'une portée de 120 m, le plus long pont en béton précontraint pour voie ferrée du Japon. La conception est caractérisée par l'étude de la sécurité de l'ouvrage et la stabilité de roulement du train au moyen d'une analyse de réponse séismique, l'adoption des barres de précontrainte pour supporter le poids propre de la poutre en console, l'utilisation du toron de précontrainte pour le système de charge due au train, l'utilisation de la gaine à faible friction pour le toron de précontrainte.

ZUSAMMENFASSUNG

Dieser Bericht faßt die Auslegung einer fünffeldrigen Durchlauf-Hohlkastenträgerbrücke aus Spannbeton zusammen, die mit einer Spannweite von 120 m die längste Eisenbahnbrücke Japans ihrer Art ist. Die Auslegung ist dadurch gekennzeichnet, daß 1. eine seismologische Reaktionsanalyse der Bausicherheit und der Befahrbarkeit des Bahntrasses durchgeführt wurde, daß 2. für die Eigenlast des Freiträgers Spannbetonbalken mit Stabverspannung verwendet wurden und für die Fertigstellung des Geleisstreckenvorbaus für die Spannbetonstruktur Kabel verwendet wurden, sowie daß 3. für die Hüllrohre reibungsarme Ausführungen verwendet wurden.



1. PREFACE

Kitaura-ko Bridge is located on the Shikoku side of the Honshu-Shikoku Bridge (for combined highway and railway use) connecting Honshu with Shikoku and is a railway bridge that spans over Kitaura fishing port.

The superstructure consists of a five-span continuous box girder having a span length of 120 m, the longest in Japan (refer to Fig-1).

The substructure consists of a cast-in-site diaphragms wall foundation that was adopted for the first time in Japan as a foundation for a marine structure (Fig-2).

This report describes the points of consideration in improving the aseismicity, economy and constructability of long bridges in the design of this bridge.

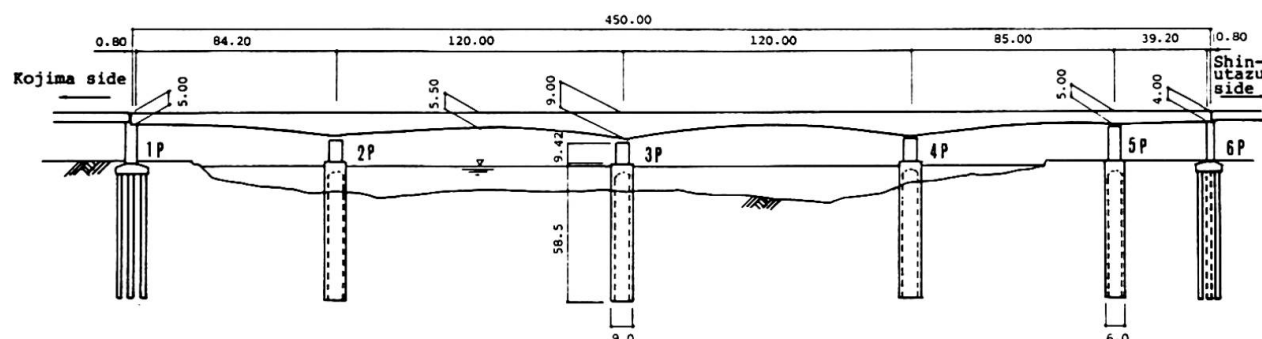


Fig-1 General drawing of the entire Kitaura-ko Bridge (m)

2. SEISMIC RESPONSE ANALYSIS

2.1 Analysis model

Recorded acceleration wave at the Kaihoku Bridge was used as a seismic wave and 4 cases were examined, i.e. longitudinal direction and transverse direction for both when completed and during construction. The input acceleration at the foundation bed (TP-91 m) was obtained using the multiple reflection theory so as to become 200 Gal. (100 Gal. during construction) at the aseismatic ground surface. As a result, the input acceleration at the foundation bed was measured to be 94 Gal.

The analysis model used was a total system model of superstructure-foundation-ground, a multiple mass point system vibration model that consists of concentrated mass points and the rod members

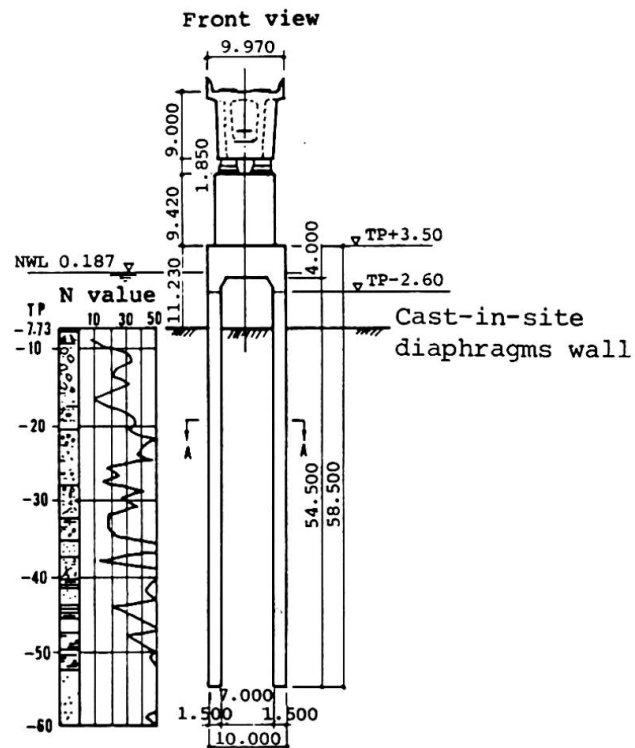


Fig-2 General drawing of superstructure and substructure at 3P (m)

connecting them for structural members, and similarly, a multiple mass point grid model of a concentrated-tie spring system for ground. In order to express semi-infinite ground, a viscous damper was used to evaluate dispersion effect at an interface.

2.2 Analysis results

Table-1 shows the maximum value of response acceleration of the completion system. The reason for the response value in the transverse direction being slightly larger at both ends (1,6P) is considered due to the effect of the girder terminating there.

For the generated sectional force, a comparison was made with the ultimate strength of members and the safety thereof was checked.

The ground spring used in the seismic response analysis was made an elastic spring. Although the response value may vary slightly, this was coped with by compensating the sectional force after comparing the elastic spring and elastic-plastic spring in the static analysis. In this connection, the maximum bending moment of the elastic-plastic spring was 1.20 times that of the elastic spring at 2-4P and 1.08 times at 5P, and the maximum shearing force, 1.45 times at 2-4P and 1.15 times at 5P.

2.3 Runnability of trains

Running trains might be endangered if the amplitude of lateral vibration of the bridge becomes extremely large. To judge this safety limit for runnability quantitatively, the runnability curve as shown in Fig-3 was obtained by means of vibration analysis and model tests.

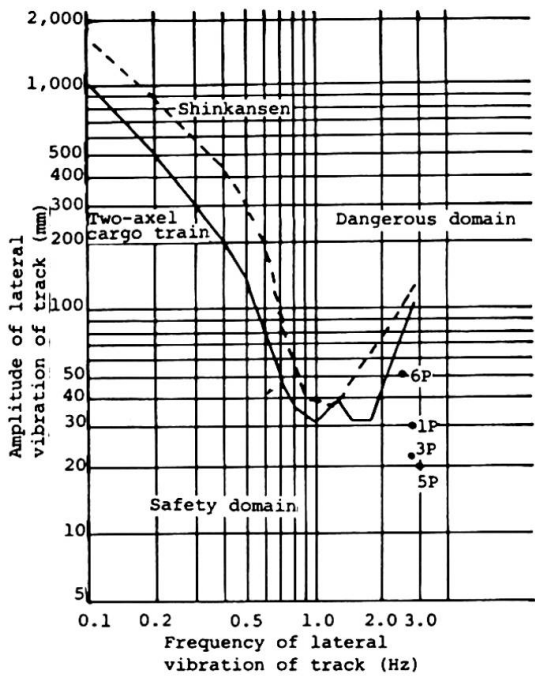


Table-1 Maximum value of response acceleration (Gal)

	bridge axis direction	direction at right angles to bridge axis
1P Center of girder	252	302
2P Center of girder	247	196
3P Center of girder	247	174
4P Center of girder	254	194
5P Center of girder	264	247
6P Center of girder	268	319

Fig-3 Runnability curve

The results of analysis for this bridge were plotted in Fig-3 and the safety of running trains at the time of an earthquake was confirmed.

3. DESIGN OF THE CAST-IN-SITE DIAPHRAGMS WALL FOUNDATION

Because the cast-in-site diaphragms wall foundation has an advantage which does not loosen the peripheral ground as do caisson foundations, it is considered a



foundation structure that excels in bearing capacity and aseismicity. Also, there are several advantages from the viewpoint of constructability, such as it is a low noise and vibration method, it can be excavated anywhere from soft and weak soil to gravel layers and rockbeds, it is possible to excavate to a large depth, it allows mechanized construction from ground level, etc.

In consideration of these points, an cast-in-site diaphragms wall foundation was adopted as the foundation structure of this bridge, particularly because a large depth marine excavation at a water depth of 12 m was called for during construction.

The cast-in-site diaphragms wall foundation was designed by obtaining a balance between the external force and restitutive force of members and the reaction force of ground springs.

The ground springs used in this analysis were elastic-plastic springs that deform plastically as they exceed the elastic limit value. In order to evaluate the effect of plasticization of ground at the time of an earthquake on the safer side, examinations were performed using a method in which an analysis was made by applying a seismic horizontal force of 1.5 times and multiplying the sectional force obtained by 2/3 times (except axial force).

Box sections were analyzed by applying the ground reaction force obtained by the analysis of vertical direction as a load on a box rigid frame.

4. SUPERSTRUCTURE

Table-2 shows the allowable stress of PC girders and Fig-4 shows the cross-section of a girder.

The design was performed based on the cantilever erection method using travelling forms with a block length of 3.0-4.5 m in consideration of construction period, capacity of the travelling forms, constructability, etc.

Photo-1 shows the completed Kitaura-ko Bridge.

4.1 PC Steel

In general, one kind of PC steel is used in a PC continuous girder, but in this bridge, PC steel bars, SBPR95/120, were used to resist for the dead load of cantilever erected girder and a steel stranded wire, SWPR7B12T15.2 for train load, etc. after the completion of the bridge.

This was done to reduce the necessary quantity of steel material, thereby lowering the cost of construction and improving constructability by making use of the features of steel bars and steel stranded wires. In other words, it is possible to lay out the steel bars delicately and the tensioning tools can be small and highly maneuverable. In addition, because the stranded wires have a large tensioning force, the number of tensioning and grouting works can be reduced, bending layout is easier, and as they are inserted after the casting of concrete, the risk of damage and rusting of steel is smaller.

Table-2 Allowable Stress of PC Girder

		SI unit
	Design standard strength σ_{ck}	39.2 MPa
	Compressive strength at the time of introduction of prestress	27.4 MPa
Concrete	Allowable bending compressive stress intensity	At the time of introduction of prestress 17.6 MPa At the time of application of design load 13.7 MPa
	Allowable bending tensile stress intensity	At the time of introduction of prestress 1.47 MPa At the time of application of total load 0 MPa At the time of application of design load 0.95 MPa
	Allowable diagonal tensile stress intensity	Shear force or torsional moment 1.27 MPa Shear force and torsional moment 1.67 MPa
Standard allowable bonding stress intensity (deformed bar)		1.96 MPa
PC steel material	During the prestressing	0.80 σ_{pu} or 0.90 σ_{py}
	Immediately after prestressing	0.70 σ_{pn} or 0.85 σ_{py}
	At the time of application of design load	0.60 σ_{pu} or 0.75 σ_{py}

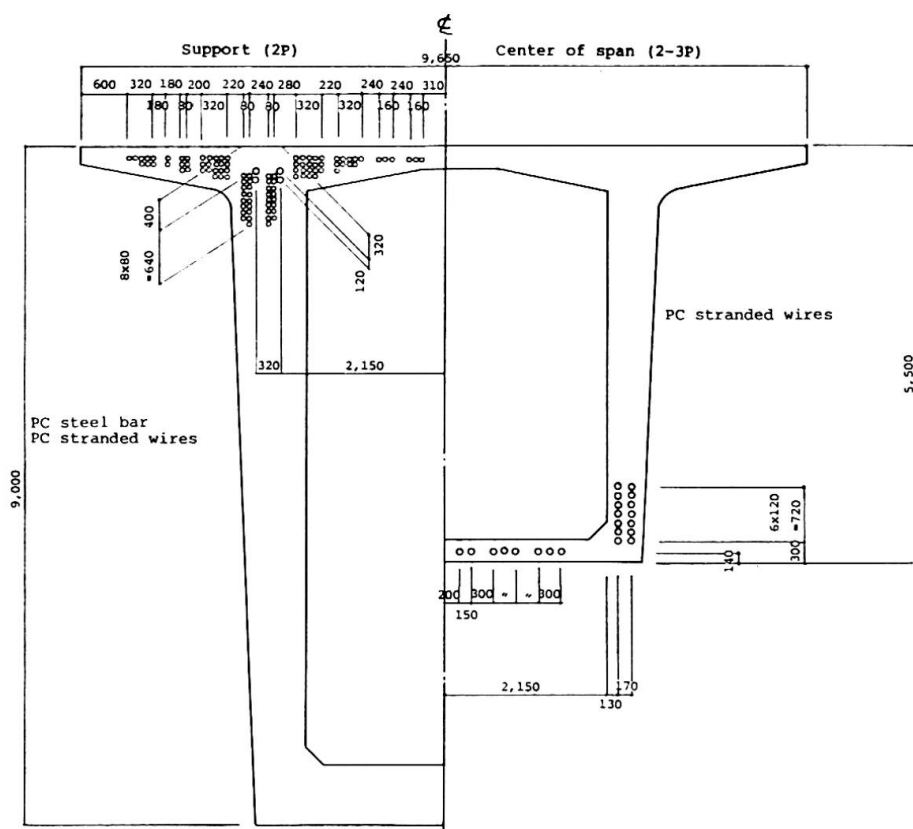


Fig-4 Cross section of girder and layout of PC steel bar and stranded wires (mm)



Photo-1 The completed Kitaura-ko Bridge.



As a result, the quantity of PC steel in the longitudinal direction was reduced by 20%, about 80 tons, also serving to improve the constructability.

4.2 Low friction sheath

Considering the fact that the length of a PC tendon was to be 130 m, the low friction sheath processed by fluoride was used. The tensile force was obtained by using the following formula. The design was performed using the coefficients of friction as $\mu = 0.3$, $\lambda = 0.004$ for the ordinary sheath and $\mu = 0.25$, $\lambda = 0.0033$ with reference to the test results, etc. for the low friction sheath.

In the construction, the PC tendon was tensioned as early as possible after insertion so as to reduce the rusting. As a result, the coefficient of friction was made smaller and the effect was fully demonstrated.

$$P_0 = P e^{-(\mu \alpha + \lambda l)}$$

where,

- P₀ : Tensile force of PC steel material at the position of l (m), the length of steel material, from the position where the tensile force is given
- P : Tensile force of PC steel material at the position where the tensile force is given, that is, the position of the jack
- α : Angular change (radian) in the length of l (m) of the PC steel material
- l : Length of PC material (m) measured from the position where the tensile force is given
- μ : Coefficient of friction per unit angle change (radian)
- λ : Coefficient of friction per unit length (m)

5. POSTSCRIPT

The Kojima-Sakaide route will be open for traffic for highway and railway on April 10, 1988 and train which shuttles between Honshu and Shikoku will run through the Kitaura-Ko Bridge. This paper introduced how to examine the runnability of train during earthquake, construction of cast-in-site diaphragms wall foundation and PC girder with two types of PC steel. We are convinced that these new technologies will contribute for more economical construction and seismic resistant design for long-span railway bridges.

Feasibility Study of Long Span Bridges in Chongqing, China

Etude de faisabilité de ponts routiers à grande portée à Chongqing, China

Machbarkeit der weitgespannten Brücke Chongqing in China

Rong-Quan XIU

Senior Engineer

Urban Bridge Commission of CCES
Chongqing China



Rong-Quan Xiu born 1918, received his Civil Engineering Degree at National Central University, China, in 1945. He has served as Civil Engineer of Chongqing Urban construction Bureau for more than 40 years. Since 1963, he is in charge of the technical work of several long span bridges in Chongqing.

SUMMARY

This paper studies some important aspects of the feasibility study of long span bridges, such as objectives, stage, content, scope, procedures and methodology. The alternative method of the bridge site and bridge type is briefly summarized. The paper is chiefly introduced on new construction and erection procedures for the long span bridges in Chongqing.

RÉSUMÉ

L'article aborde des aspects importants concernant les études de faisabilité sur les ponts routiers à grande portée, tels que des objectifs, contenus, domaines, procédures et méthodes des études ainsi que le choix du type de ponts et de leurs emplacements d'implantation. Les nouvelles méthodes appliquées à Chongqing pour la mise en oeuvre et la construction du pont routier à grande portée, sont présentées.

ZUSAMMENFASSUNG

Dieser Fachbericht untersucht einige wichtige Punkte der Weitspannbrücke, beschreibt Ziel, Inhalt, Bereich, Prozess und Methode der Machbarkeit der Weitspannbrücke sowie Auswahlmöglichkeiten des Brückenstandorts und der Brückenkonstruktion. Der Fachbericht gibt einen Überblick über die neue Bau- und Aufbauweise der Weitspannbrücke Chongqing.



1. INTRODUCTION

Chongqing is a mountain city with a long history of more than 3000 years. It is at the junction of the Changjiang and the Jialing rivers, which flow through the city proper. Chongqing consists of nine districts and twelve counties, covering an area of 22340 Km² with a population of 14.06 million, of which 3.36 million are urban inhabitants.

Since 1949 three highway bridges and two railway bridges have been built across the two rivers. In addition, more than 560 bridges have been built over the valleys and tributaries of the two rivers. The total length of these bridges is up to 20 Km.

The Niujiaotuo Jialing River Bridge which built in 1966 is a steel truss bridge; main span 88m, traffic capacity 4 lanes, and total length 600.56m.

The Beipei Jialing River Chaoyang Bridge which was built in 1969; its main bridge is double-cable suspension bridge; the main span is 186m, traffic capacity 2 lanes, and total length 233.24m.

The Changjiang River Bridge, with a total length of 1120m, traffic capacity 4 lanes was built in July 1980. It is a T-framed P.C. bridge, made up of a number of cantilever T-frames plus suspended spans of 35m each. The main span is 174m, which is the largest span among the same type of bridge in China.

Concrete : 3.48 M³/M² Steel : 260 Kg/M² Cost : RMB 1900 Yuan/M²

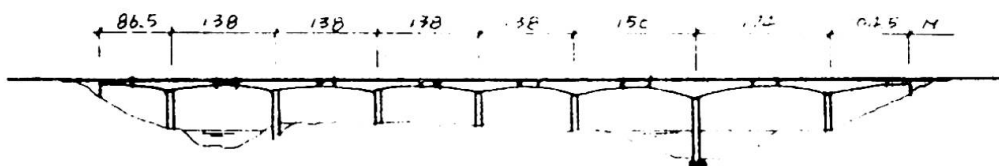


FIG 1 ELEVATION OF CHANGJIANG BRIDGE



Photo 1. General view of Changjiang River Bridge

Steel : 370 Kg/M² CONCRETE : 2.36 M³/M²
Cost : RMB 2450 Yuan/M²

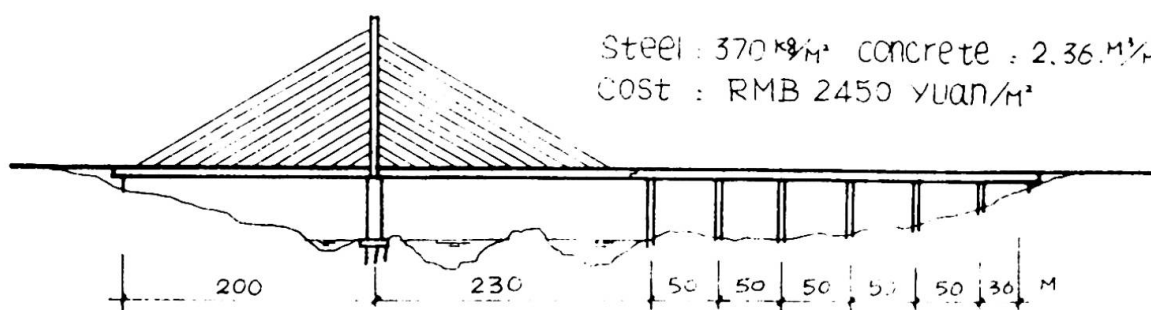


FIG 2 ELEVATION OF SHIMEN BRIDGE

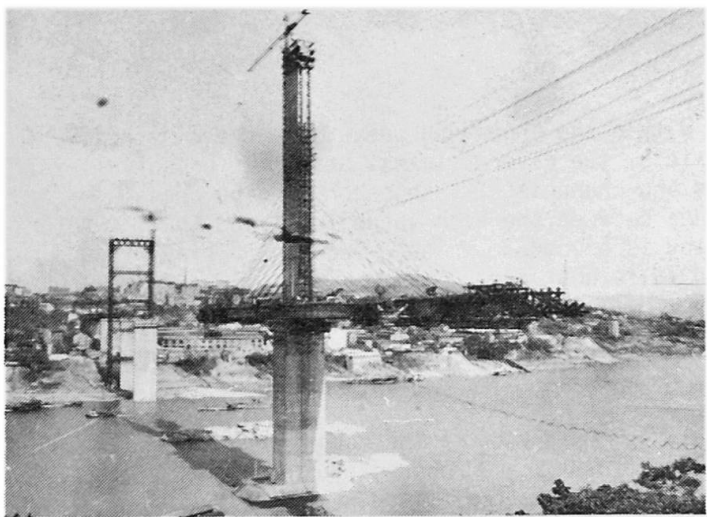


Photo 2. General view of Shimen Bridge
construction Commission, consists of Urban Construction
construction units, universities and colleges, etc.

2. OUTLINE OF THE FEASIBILITY STUDY OF BRIDGES

2.1 The objectives and task of the F/S are to carry out the investigation, analysis and study in terms of economy, technique and finance so as to settle a scientific foundation for the proposed schemes and the decision to be passed on and fully prove the construction of this project is feasible economically, technically and financially.

2.2 The stages and scope of the feasibility study

Before 1980, the planning task book was used instead of the F/S report. Since the early 1980s, we have started to do the F/S on all large projects. The F/S of Shimen bridge was performed in 1984, the scope of F/S extended from the technical study which used to be the major basis before 1980 for economy and finance. The index of economy of Shimen Bridge is as follows: N.P.V.=252.4572 million yuan, the ratio of benefit and cost B/C=3.76, E.I.I.R.=21.93%.

Financially speaking, the passing fee used to repay the loan is calculated on the basis of the average of 1.88 yuan per vehicle per time. The period for the investment recovery is seven years. As a result of the F/S report, the Shimen Bridge is a beneficial project. The benefit is remarkable and it is feasible economically, technically and financially. However, for the Shimen Bridge, only the F/S was performed, and the pre-F/S was not performed during the stage of project alternative, while for the Second Changjiang River Bridge, the pre-F/S and final F/S are arranged in two steps in accordance with the international common method and requirement.

2.3 The content of F/S should be include the following:

- a). General outline--including the task basis, construction address, project manager, construction scale, project history and background and the outline of F/S.
- b). The importance and necessity of the construction of the project.
- c). Traffic survey and forecast--including the social and economical survey and study which will indicate the analysis and forecast of the future traffic volume through the bridge.
- d). Choice of the bridge site.
- e). The design and construction of the project.
- f). The investment budget and management expense.
- g). The implementation of the plan--studying the schemes of the implementation, arranging the schedule of the construction and material supply.
- h). Economic evaluation--the method of cost-benefit analysis is adopted.
- i). Financial evaluation--the surplus-loss analysis, fund expenditure analysis, determining the F.I.R.R..
- j). Conclusion and suggestion..

The Jialing River Shimen Bridge is under construction. Its main bridge is P.C. cable-stayed bridge, with single tower, the main span 200+230m, traffic capacity 4 lanes and the length 780m. It was designed by Shanghai Municipal Engineering Institute and constructed by Chongqing Bridge Co.. It will be completed in Dec.1988. The completion of this bridge will indicate that we have the ability to design and construct cable-stayed bridges with spans larger than 450m.

The project of the Second Changjiang River Bridge, which was approved in 1986, to build this bridge by making use of the third round of yen loan. The office of pre-construction preparation of the Second Chongqing Changjiang River Bridge which was organized by Chongqing con-Bureau Research Institute, design and



3. CHOICE OF THE BRIDGE SITE

3.1 The features of the river:

The Changjiang River and Jialingjiang River within the Chongqing areas have the distinctive natural features of rivers in mountain districts, the rivers zigzag; among the broad valleys, the river has distinguishable river shallows and channels of V-shape or U-shape cross section, and even some side beach. The difference between the high water level and the low water level is 30--35m. The maximum velocity of flow is 5--6m/sec.. The direction of flow is subject to change at the difference levels, and it is unstable.

3.2 The necessary conditions of the bridge site:

The choice of the bridge site should be decided on the basis of the comprehensive consideration of economy, social and scientific development and the demands of masses, taking new ideas and notions instead of old ones, and studying fully the following basic conditions:

- a). It should obey the plan of the traffic development. If the bridge sites to be compared are planned ones, and while the road network planning is being made for lacking of scientific basis, it should obey the economic benefit from quantitative analysis.
- b). It should obey the interests and demands of masses and serve to improve the people's life and make things convenient for people. And it must not imperil flood control measures or infringe upon the rights and interests of peasants. It should avoid demolishing valuable buildings.
- c). It should meet the demand of navigation clear height and width, and they should be decided according to the hydrological conditions of different river segments and the navigation development. During the flood period, the angle between the direction of flow and the pier's axis should be less than 5 degrees. The river near the bridge should be necessarily straight.
- d). The site must have good hydrological and geological conditions for construction without any harmful geological problems, such as faults, caves and slides.
- e). It should be supported with good construction conditions, including communications and transportation, material supply, water electricity resources, and construction ground concerned.
- f). The sites of special bridges for national defence, big enterprises, scenery and other purposes should meet the demands of their special functions.

3.3 Choice of the bridge sites of the Second Chongqing Changjiang River Bridge:

Egongyan Bridge site and Lijiatuo Bridge site are both planned bridge sites. After comparing according to qualitative analysis, the consensus has not been reached, but after studying by the standard and demands of economic evaluation for projects, we have concluded that the Lijiatuo site is better than the Egongyan site.

The comparision of two sites is as follows (according to the data of the pre-feasibility study):

- a). Estimated traffic: in 1992, (open to traffic) Lijiatuo site 4995v/d more than Egongyan site 3992v/d.
- b). Economic benifits: Lijiatuo site: N.P.V.=293.6697 million yuan, E.I.R.R.=10.3% B/C=1.80
Egongyan site: N.P.V.<0 E.I.R.R.<3% (interest rate of the loan) B/C<1
- c). Local economy and development: Lijiatuo site: 15 Km² of land will be developed.
Egongtan site: is not so favorable.
- d). Investment and demolition of houses: Lijiatuo site: 40 million yuans more than the Egongyan site, but the demolition of houses is 44000M² less than the Egongyan site.
- e). Improvement of traffic conditions in the downtown: Lijiatuo site is better than the Egongyan site.
- f). Meeting the need of trans. so as to promote industrial development of the south west district. Lijiatuo site is effectively, but the Egongyan site is not so effective.
- g). Financial income and repayment of the loan: Lijiatuo site produces more and is quicker than the Egongyan site, its income is more than the expenditure, but the Egongyan site's income is less than the expenditure.

4. FEASIBILITY STUDY OF THE DESIGN SCHEMES OF BRIDGE TYPES

4.1 The Chongqing Changjiang River Bridge:

In the comparision and choice of the six design schemes of three bridge types, we put the stress on (1) the cable-stayed bridge, double pylon, $L_{max}=276m$, (2) the continuous rigid frame bridge $L_{max}=240m$, (3) the T-frame bridge $L_{max}=174m$. Scheme (1) and scheme (2) can fully satisfy the demands of the navigation and avoid the construction of deep water foundation, but the construction of bridge is difficult for lack of experience and needs more investment. According to the condition, then scheme (3) has been adopted because it can satisfy the demands of navigation on the whole, needs less investment, and the design and construction techniques are ready.

4.2 The Jialing River Shimen Bridge:

On the basis of 14 schemes of 5 bridge types, the Shanghai Municipal Engineering Institute offers 10 schemes, 4 of which have been taken for comparision and choice: (1) the P.C. cable-stayed bridge, double-pylon $L_{max}=265m$, (2) the single tower cable-stayed bridge with the main span $200+230$, (3) the flexible pier and continuous rigid frame concrete bridge $L_{max}=220m$, (4) the flexible pier and continuous rigid frame concrete bridge with span of $4x105m$. All things considered, scheme (2) is better. It can satisfy the demands of navigation. Within the port and wharf region of the south bank, there is no need to build any piers, which can ensure the coexistence of the wharf and the bridge in favour of the organization of construction. Its construction period is shortest, and it can push ahead with the development and advancement of the cable-stayed bridge. Its design and construction can reached the first rate level in the world, and its increase of investment is less than 5%. That is why scheme (2) has been adopted.

4.3 The Second Chongqing Changjiang River Bridge (Lijiatuo Bridge Site)

4.3.1 The main design data:

Traffic capacity--4 lanes, each lane-- $850v/h$; the width of the bridge: $2x7.5m+1.5m(\text{divisor})+2x3m(\text{side-walks})$; the navigation clearance: $H>18m$ $B>400m$ and the model test allows the clear width to be $>240m$. Design load: $H-20t$ $T-100$ flatbed truck $300t$ (check load). Sidewalks load $350Kg/M^2$. Wind force: the maximum wind velocity - $27m/sec$. Earthquake force: the basic seismic degree for design is 6 degrees, but will be 7 degrees for antiseismic ($H=0.07g$).

4.3.2 The Design Schemes For Bridge Types:

The Office of the Second Chongqing Changjiang River Bridge and Sumitomo Construction Co. and I.H.H.I.Co. of Japan offer 14 deaign schemes of 6 bridge types. Among them S.C.Co. offers three schemes of the suspension bridge $L_{max}=870m$, the concrete cable-stayed bridge $L_{max}=480m$ and the T-frame bridge $L_{max}=240m$, and I.H.H.I. offers a scheme of the steel girder cable-stayed bridge $L_{max}=450m$.

We must to evaluate the schemes of bridge types, according to the principle of function, safety, economy and beauty.

After the comparison and analysis, we think the scheme of $L_{max}=870m$, suspension bridge demands high techniques and needs too much investment. Its construction period will last 4 years, so it is not considerable. The schemes of the arched truss bridge and the ribbed arch bridge are not considerable, because the piers are over $40m$ high and bulky, and they need complicated construction and a long period, though they require lower cost and less steel. In addition, the bulky piers will cause the river bed the great changes of scour and fill.

For each scheme of the bridge type, the following problems should be studied: the span allocation, the type and stability of foundation, the wind stability, the form of vibration, the shape of the cross section of the girder and pier, etc.

4.4 The alternative design schemes of bridge type and the main technical and economical index are shown as follows: (Remark: The cost of the projects is relatively for each other)

Alternative 1: $L_{max}=450m$, cable-stayed bridge (main span steel girder) span allocation: $2x50+160+450+160+10x50=1370m$ steel: $480Kg/M^2$ concrete: $2.86M^3/M^2$ cost: $1.20c$ yuan/ M^2



Alternative 2: $L_{max}=450m$ cable-stayed bridge (main span composite girder) span allocation: $216+450+216+9\times50=1332m$ steel: $457\text{Kg}/\text{M}^2$ concrete: $2.62\text{M}^3/\text{M}^2$ cost: $1.16\text{c yuan}/\text{M}^2$
 Alternative 3: $L_{max}=430m$ cable-stayed bridge span allocation: $2\times50+170+430+170+10\times50=1370m$ steels: $410\text{Kg}/\text{M}^2$ concrete: $3.07\text{M}^3/\text{M}^2$ cost: $c \text{ yuan}/\text{M}^2$
 Alternative 4: $L_{max}=240m$ cable-stayed bridge with single tower span allocation: $4\times50+2\times210+13\times50=1330m$ steels: $360\text{Kg}/\text{M}^2$ concrete: $2.88\text{M}^3/\text{M}^2$ cost: $0.98\text{c yuan}/\text{M}^2$
 Alternative 5: $L_{max}=240m$ P.C.T-frame bridge span allocation: $40+170+2\times210+180+4\times120+30=1440m$ steels: $490\text{Kg}/\text{M}^2$ concrete: $2.87\text{M}^3/\text{M}^2$ cost: $1.42\text{c yuan}/\text{M}^2$
 Alternative 6: $L_{max}=2\times240m$ continuous frame bridge span allocation: $3\times40+120+2\times240+171.5+3\times133+81.5=1372m$ steels: $360\text{Kg}/\text{M}^2$ concrete: $2.78\text{M}^3/\text{M}^2$ cost: $1.14\text{c yuan}/\text{M}^2$

5. THE NEW CONSTRUCTION AND ERECTION TECHNOLOGY FOR LONG SPAN BRIDGES

5.1 In the deep water foundation construction of the Changjiang River Bridge, we adopt a double-wall steel coffer dam with the inner diameter of 24m, and a self-made gear driver is used which is twice as efficient as the general driver. The 12 bored piles with the diameter of 2.6m, 10-12m deep in rockbed, are completed in one dry season. For the foundation of pier No.5, 5m deep in rockbed, the new technology of an electric blast in deep and dense holes into the required shape at one stroke is successful. For the high concrete piers, over 50m high. The hydraulic sliding form method is adopted. The average sliding speed is 2.87m/day, and the maximum speed for No.3 pier reaches 4.65m/day.

5.2 For the Chongqing Changjiang River Bridge, the new technique first used in construction of the cantilever by the fixed outer form and the sliding inner form causes high construction speed and good quality, and gives us new technology in construction of the bridge with the long span of over 200m.

5.3 The tower columns of the Jialing River Shimen Bridge are 113m high, and their cross section is $4.5\times9.5\text{m}$. They are influenced by wind and sunshine, and the stability and stiffness is worse for the dense reinforcements and rolled-steel section in the piers. There are a lot of pre-hidden stayed pipes and bar joints. After careful study, the new technology of sliding form is adopted, and the construction pace and quality is ensured. The transportation of concrete and materials through a 120m tower crane and a six cable crane with the span of 519m ensure continuous construction during the high flood period. The concrete box beam with a single box three cells is 4m high. In its construction, we adopt the method of balanced cantilever by cast-in-situ. The box beam is of 27 segments, and the standard segment is 15m long and built by the flow progress of middle box, side box and cantilever plate. The 15m stiffened steel frame is made by welding with the rolled-steel section hidden in the middle box, thus forming a stayed-cable structure as the supporting structure of side box and lengthening pouring segments. This reforms the old technology of big hanger method, and quickens the construction speed. The Shimen Bridge has 216 cables, the longest of which is 234m. Each cable is made of 265 galvanized steel wires of $\phi 5$. The cables are made and treated for protection in the factory. We have adopted the hypalon rubber as protection material combined with sectional sulphurization thermopressing forming technique instead of P.E. pipe casting press in grout mixture protection techniques. In this way, the cables are of high quality and low expenditure and easy to erect. The technical index of the protection material of the cable are as follows: tensile strength $>11\text{Mpa}$, the minimum rate of elongation is 300%, hardness IRDH is 70-85, the resisting ability of sulphuric acid, ozone and ageing satisfies the demands. The protection covering of the cables is 5mm thick and their working life last over 20 years. The continuous box girder of the approach with 5 span of 50m and a span of 36m, the girder is 4m high and it is of a single box with three cells. It is built by incremental launching on high flexible piers. The new technology ensures high quality and high construction speed.

References

1. UNIDO, Manual For The Preparation On Industrial Feasibility Studies (China Transportation & publishing corp 1985)
2. DCAS & UNIDO, Manual For Evaluation Of Industrial Projects (New York 1980)
3. I.M.D.LITTLE and J.MIRRLESS, Project Appraisal And Planning For Development Countries (Heinemann, London, 1974)
4. T.Y.LIN, Progress and Problem-Today And Tomorrow (12th Congress I.A.B.S.E. Sep.1984)
5. Treasury Board of Canada, Benifit-Cost Analysis Guide (Ottawa, 1976)
6. XIU RONG-QUAN, LIN JUN-YAN, QU QING-LU, Chongqing Yangzi River Bridge China (I.A.B.S.E. Journal J-26/85)

Weitgespannte Schrägseilbrücken anstelle von Hängebrücken

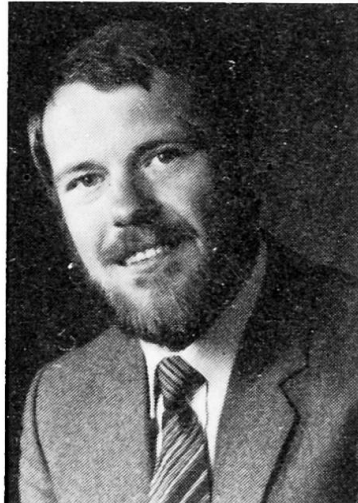
Wide Span Cable-Stayed Bridges instead of suspension bridges

Ponts haubanés de grande portée au lieu de ponts suspendus

Rolf KINDMANN

Dr.-Ing.

Thyssen Engineering GmbH
Dortmund, Bundesrep. Deutschland



Rolf Kindmann, geboren 1947, promovierte als Bauingenieur an der Ruhr-Universität Bochum. Er arbeitete in der Industrie als Statiker und Projektleiter im Stahlbrückenbau sowie in Forschung und Entwicklung. Seit drei Jahren ist er Leiter des Technischen Büros Brückenbau.

ZUSAMMENFASSUNG

Schrägseilbrücken dringen immer mehr in Stützweitenbereiche vor, die früher Hängebrücken vorbehalten waren. Der derzeitige Entwicklungsstand sowie die technischen und wirtschaftlichen Vorteile, die für den Bau von weitgespannten Schrägseilbrücken sprechen, werden aufgezeigt. Stützweiten bis etwa 1500 m sind durchaus technisch und wirtschaftlich ausführbar.

SUMMARY

Cable-stayed bridges are intruding more and more into ranges of span previously reserved for suspension bridges. The present state of development as well as technical and economical merits of construction of wide span cable-stayed bridges, are indicated. From both the technical and economical point of view, spans of up to around 1,500 m are absolutely feasible.

RÉSUMÉ

Les ponts haubanés sont réalisés pour des portées qui, autrefois, étaient réservées aux ponts suspendus. L'état actuel du développement, ainsi que les avantages techniques et économiques en faveur de la construction de ponts haubanés à grande portée, sont indiqués. Du point de vue technique et économique, des portées de 1.500 mètres sont absolument réalisables.



1. EINLEITUNG

Weitgespannte Brücken werden gemäß dem heutigen Entwicklungsstand in der Regel als Hänge- oder Schrägseilbrücken ausgeführt. Auch wenn in der Vergangenheit einige Bogen- und Fachwerkbrücken mit einer größten Stützweite von etwas über 500 m gebaut worden sind, so läßt sich doch allgemein feststellen, daß ab etwa 300 m größter Spannweite in der Regel die Schrägseilbrücke die wirtschaftlichere Alternative ist. Bei deutlich größeren Stützweiten dominiert zur Zeit noch die Hängebrücke.

Der häufigste Anwendungsfall für weitgespannte Brücken ist die Überquerung von Wasserstraßen in Form von Hochbrücken. Die freie Durchfahrt von Seeschiffen erfordert dabei die Hochlage der Brücke, so daß die Fahrbahn etwa 60 m über dem Wasserspiegel liegt. Die örtlichen Randbedingungen im Bereich der Brückentrasse beeinflussen entscheidend die Wahl des Brückentyps und der Konstruktion. Bei günstigen Voraussetzungen, geringe Wassertiefen und niedrige Geländehöhen, kann auch die Anordnung einer beweglichen Brücke als Kern eines Brückenzuges mit niedrigem Niveau Vorteile bieten, [1].

Beim Bau von Hochbrücken zeigen die Entwicklungstendenzen, daß Schrägseilbrücken gegenüber Hängebrücken in vielen Fällen technische und wirtschaftliche Vorteile bieten. Auch bei sehr großen Stützweiten lassen sich Schrägseilbrücken häufig kostengünstiger bauen. Sie sind außerdem steifer und aerodynamisch sicherer als Hängebrücken, [2]. Es ist daher zu erwarten, daß selbst dort wo zur Zeit noch Hängebrücken die Planungsgrundlage bilden, in vielen Fällen Schrägseilbrücken zur Ausführung kommen werden.

2. ENTWICKLUNGSSTAND

2.1 Hängebrücken

Die Brücke mit der größten Stützweite (1410 m) aller in Betrieb befindlichen Brücken ist die Hängebrücke über den Humber (Fig. 1) an der Nord-Ostküste von England, [3]. In Japan befinden sich zur Zeit mehrere Hängebrücken im Bau, von denen eine fast 2000 m als größte Stützweite erreichen wird.

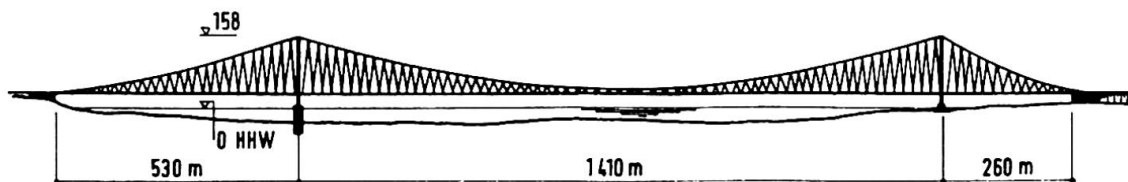


Fig. 1 Ansicht der Humber Brücke

Verschiedene Untersuchungen, siehe z. B. [4] und [5], zeigen auf, daß Bauwerke mit Stützweiten bis etwa 3500 m technisch realisierbar scheinen. Diese Extremwerte kommen aber schon aus Kostengründen nur für einige wenige Projekte mit besonderen Randbedingungen in Frage, wie z. B. bei der Meerenge von Messina oder der Straße von Gibraltar.

Die Tragkabel der neueren, großen Hängebrücken bestehen aus einer Vielzahl von verzinkten Einzeldrähten, deren Durchmesser bei etwa 5 mm liegt. Die Montage erfolgt vor Ort im sogenannten Luftspinnverfahren. Dazu werden auf die bereits fertigen Pylone Schleppseile montiert, an denen sich die Spinnräder ständig zwischen den beiden Widerlagern hin und her bewegen. Wegen der aufgefächerten Verankerung in den Gründungskörpern wird jeweils eine gewisse Anzahl von Einzeldrähten zu Strängen gebündelt. Der Zeitbedarf für das Luftsponnen ist relativ groß. Je nach Länge der Tragkabel und Anzahl der Einzeldrähte werden mehrere Monate benötigt. Bei ungünstigen Witterungsverhältnissen, z. B. starken Wind, müssen die Arbeiten unterbrochen werden.

Die Hänger werden senkrecht oder schräg angeordnet. Bei schrägen Hängern sind

die Durchbiegungen der Brücke etwas geringer, die innere Dämpfung gegen Schwingungen etwas erhöht und die Biegemomente im Versteifungsträger kleiner. Bezuglich der Materialermüdung liegen jedoch bei den schrägen Hängern ungünstigere Beanspruchungen vor, [4]. Die Tendenz scheint zur Zeit etwas mehr die Ausführung von vertikalen Hängern zu sein. So hat z. B. die erste Brücke über den Bosporus in Istanbul (max. $l = 1074$ m) schräge Hänger. Die zweite Bosporusbrücke (max. $l = 1090$ m), die zur Zeit im Bau ist, erhält dagegen vertikale Hänger. Bei der zweiten Bosporusbrücke liegen übrigens sehr günstige Voraussetzungen für den Bau einer Hängebrücke vor. Die Gründungsverhältnisse für die Pylone und Verankerungskörper der Tragkabel sind sehr gut (Fels). Außerdem ist nur zwischen den Pylonen eine Brückenkonstruktion erforderlich und keine Vorlandbrücken. In den Vorlandbereichen kann die Straße in Einschnitten auf festem Untergrund gebaut werden.

Für die Querschnitte der Versteifungsträger von Hängebrücken werden strömungsgünstige Formen gewählt, da die Brücken überwiegend in exponierter Lage gebaut werden, wo hohe Windgeschwindigkeiten auftreten können. Darüber hinaus kann die Bauhöhe wegen der geringen Hängerabstände klein gehalten werden. Fig. 2 zeigt mit der ersten Bosporusbrücke einen typischen Querschnitt, [6].

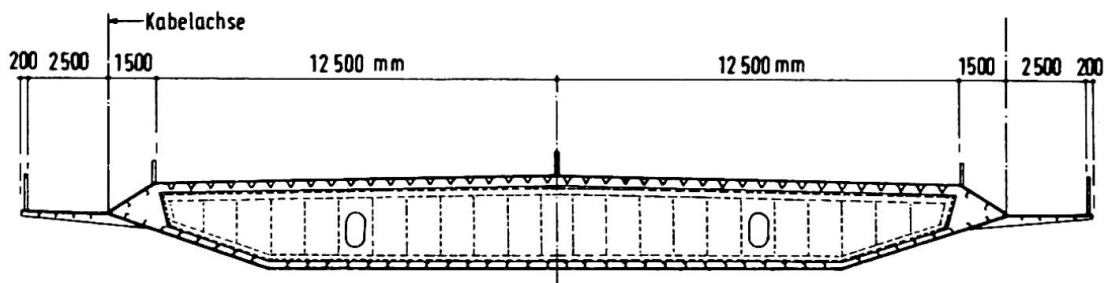


Fig. 2 Querschnitt der ersten Bosporusbrücke

2.2 Schrägseilbrücken

Bei der Ausführung von Schrägseilbrücken sind bisher max. fast 500 m als größte Stützweite erreicht worden. Viele Projektstudien belegen aber, daß auch deutlich größere Stützweiten mit diesem Brückentyp wirtschaftlich realisiert werden können.

Die Entwicklung im Schrägseilbrückenbau ist in den letzten beiden Jahrzehnten stürmisch verlaufen. Dies belegen die vielen technischen Lösungen, die aufgrund der jeweiligen Anforderungen für die Ausführung entwickelt worden sind. Neben der Vielfalt der Konstruktionen für die Versteifungsträger fallen insbesondere folgende Unterscheidungsmerkmale auf:

- eine oder zwei Seilebenen,
- einhüftige Lösungen oder zwei Pylone,
- Anordnung der Seile als Fächer oder Harfen sowie zahlreiche Variationen,
- Wahl der Materialien und Bauarten für Pylone, Seile und Versteifungsträger.

Ein Ausführungsbeispiel zeigt Fig. 3.

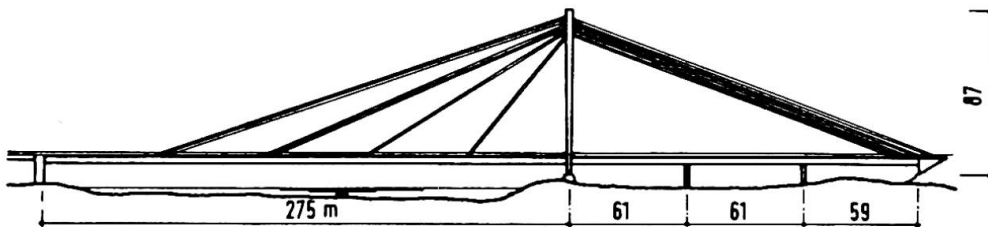


Fig. 3 Einhüftige Schrägseilbrücke über den Rhein bei Speyer



Als Seile werden vollverschlossene Spiralseile oder Paralleldrahtbündel eingesetzt. Die Verankerung erfolgt i. d. R. im Versteifungsträger und den Pylonen mit zylindrischen Seilköpfen. Der Seilkopf an jeweils einem Seilende hat dabei meist ein Außengewinde und ein Innengewinde. Auf das Außengewinde wird die Stützmutter geschraubt. Das Innengewinde dient zur Befestigung der Anspannvorrichtung.

Die Montage des Versteifungskörpers und der Seile erfolgt überwiegend im Freivorbau von den Pylonen aus, etwa symmetrisch zu beiden Seiten hin. Dabei werden jeweils sukzessive die Fahrbahnschüsse des Versteifungsträgers und die zugehörigen Seile montiert.

3. EINSATZ WEITGESPANNTER SCHRÄGSEILBRÜCKEN

3.1 Vorbemerkungen

Der im vorhergehenden Abschnitt grob skizzierte Entwicklungsstand für Hänge- und Schrägseilbrücken gibt bereits erste Anhaltspunkte für den vermehrten Einsatz von Schrägseilbrücken. Anstelle der in Fig. 4 dargestellten Hängebrücke über den Rhein in Köln-Rodenkirchen würde bei einem heutigen Neubau sicherlich eine Schrägseilbrücke zur Ausführung kommen. Dies wird offensichtlich, wenn man z. B. die einhüftige Schrägseilbrücke über den Rhein bei Speyer quasi symmetrisch ergänzt, siehe Fig. 5.

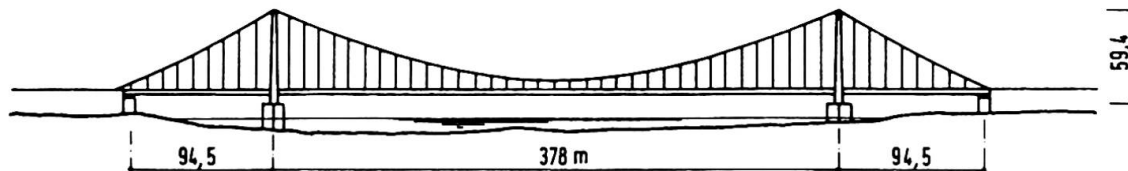


Fig. 4 Hängebrücke über den Rhein in Köln-Rodenkirchen

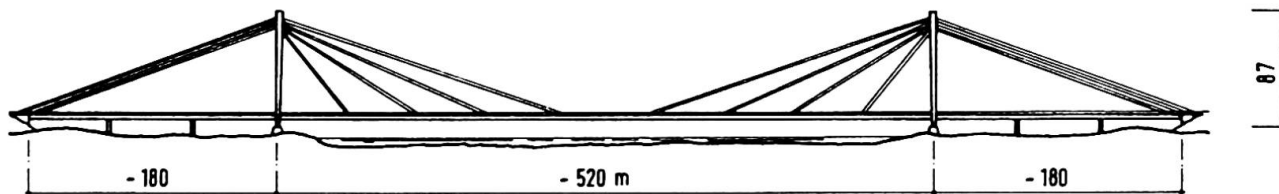


Fig. 5 Fiktive Ergänzung der Rheinbrücke Speyer

Andere ausgeführte, einhüftige Schrägseilbrücken belegen, daß Stützweiten von ca. 700 m ohne weiteres erreichbar sind. Bei günstiger Wahl des Tragsystems können aber durchaus auch die besonders großen Stützweiten realisiert werden, bei denen bisher Hängebrücken gebaut worden sind.

3.2 Systemwahl

Zum Erreichen großer Stützweiten ist die Anordnung von zwei Pylonen mit jeweils zwei Seilebenen erforderlich. Als Pylonform empfehlen sich der A-Bock oder das auf den Kopf gestellte Y. Mit diesen Pylonformen und einer Verankerung der Seile an den äußeren Rändern des Versteifungsträgers sind die Seile auch im Grundriß leicht geneigt, was sich günstig auf das Verformungs- und Schwingungsverhalten auswirkt. Die Schrägseile sollten als Vielseilsystem aufgelöst werden, damit der Versteifungsträger in möglichst engen Abständen gestützt wird und die Bauhöhe klein gehalten werden kann. Die Anordnung der Seile als Fächer, d.h. mit einer Konzentration der Seilverankerungen am Pylonkopf, gewährleistet große Vertikalkomponenten der Seile und daher große Stützkräfte für den Versteifungsträger. Darüber hinaus sind bei möglichst steiler Führung der Seile die Druckkräfte im Versteifungsträger geringer. Die Seile sollten nicht flacher als 1 : 3 geneigt

werden, damit ausreichend große vertikale Seilkraftkomponenten aktiviert werden können.

Wenn man große Stützweiten erreichen will, sind höhere Pylone als bei einer vergleichbaren Hängebrücke erforderlich. Mit zwei etwa 300 m hohen Pylonen, einer maximalen Seilneigung von 1 : 3 und der Annahme, daß die Fahrbahn ca. 60 m über dem Wasserspiegel liegt, läßt sich eine Stützweite von etwa 1400 m erreichen (siehe Fig. 6). Rechnerische Untersuchungen zeigen, daß diese Lösung technisch realisierbar und wirtschaftlich ist.

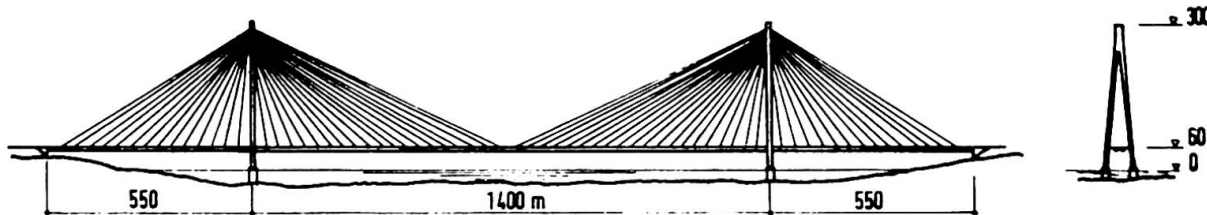


Fig. 6 Schrägseilbrücke als Vielseilsystem mit einer Stützweite von 1400 m

3.3 Materialeinsatz

Mit dem Vielseilsystem der Schrägseilbrücke kann der Versteifungsträger in ähnlichen Abständen gehalten werden wie bei der Hängebrücke durch die Hänger. Für beide Brückentypen kann prinzipiell die gleiche Querschnittsform verwendet werden, z. B. nach Fig. 2. Damit liegt die Gesamttonnage für den Versteifungsträger bis auf die Einflüsse aus den Seilverankerungen und Querschnittstabstufen aufgrund der jeweiligen Schnittgrößen in gleicher Größenordnung. Große Unterschiede ergeben sich aber beim Materialbedarf für die Seile und Kabel. Während das Vielseilsystem der Schrägseilbrücke eine sehr gute Anpassung an den Schnittgrößenverlauf bietet, ist eine "Abstufung" bei den Tragkabeln der Hängebrücke nicht möglich. Daraus resultieren erhebliche Einsparungen bei der Schrägseilbrücke, die insbesondere deshalb ausschlaggebend sind, weil die Materialkosten für Seile und Kabel sehr hoch sind.

3.4 Bauzustände und Montage

Die Montagekosten haben bei jeder Brückenbaumaßnahme einen besonders großen Anteil. Hinzu kommt, daß die Bauzustände und das Montageverfahren aus wirtschaftlichen Gründen möglichst geringen Einfluß auf den Materialbedarf für das Brückenbauwerk haben sollten. Dies wird durch die in Abschnitt 2 beschriebenen Montageverfahren bei Hänge- und Schrägseilbrücken in vergleichbarer Weise gewährleistet. Auch die Montagekosten für die Versteifungsträger bleiben in ähnlicher Größenordnung.

Die Montagekosten für die Tragkabel einer Hängebrücke sind aber extrem hoch. Dies ist leicht vorstellbar, wenn man bedenkt, daß ein Tragkabel (je nach Größe der Brücke) aus etwa 10000 bis 30000 Einzeldrähten im Luftspinnverfahren auf der Baustelle hergestellt werden muß. Dagegen werden die Seile bei der Schrägseilbrücke während der Montage im Freivorbau sukzessive mit eingezogen.

In den Material- und Montagekosten für Seile bzw. Kabel liegen daher auch in erster Linie die wirtschaftlichen Vorteile der Schrägseilbrücke begründet.

3.5 Verformungsverhalten und Windeinflüsse

Die vertikalen Durchbiegungen unter Verkehrslasten sind bei Schrägseilbrücken deutlich geringer als bei Hängebrücken. Aber nicht nur vertikal, auch in Querrichtung verhält sich die Schrägseilbrücke steifer, was zu geringeren Verformungen führt.

Dies wirkt sich besonders bei schmalen Brückenquerschnitten günstig aus, da dann die Windlasten in Brückenquerrichtung großen Einfluß auf die Bemessung haben.

Durch eine planmäßige Schrägstellung der Seile im Grundriß und die weitere Schrägstellung durch die Verformungen in Querrichtung (Theorie II. Ordnung) wird



der Versteifungsträger gut in seiner Sollage gehalten. Der Einfluß der Querschnittsform bezüglich der Windeinflüsse wird hier nicht weiter betrachtet, da, wie bereits erwähnt, für Hänge- und Schrägseilbrücken die selben Formen gewählt werden können.

Vergleichende, rechnerische Untersuchungen zum Schwingungsverhalten haben gezeigt, daß sich Schrägseilbrücken aufgrund der inneren Dämpfung sehr günstig verhalten.

Bei beiden Brückentypen können aber die Bauzustände von ausschlaggebender Bedeutung sein. Diese müssen daher in jedem Einzelfall im Detail untersucht werden.

3.6 Bauwerksunterhaltung und Korrosionsschutz

Seile bzw. Kabel bilden das Herz der Schrägseil- bzw. Hängebrücken. Da die Brücken für mehrere Jahrzehnte gebrauchsfähig bleiben müssen, ist der dauerhafte Schutz dieser Tragglieder besonders wichtig. Die Verwendung verzinkter Drähte gehört heute zum Stand der Technik. Die Entwicklung bezüglich der Beschichtungen, Umhüllungen oder Auspressen von Zwischenräumen ist dagegen noch nicht abgeschlossen.

Die Hängebrücke hat einige systembedingte Nachteile. Die Anschlüsse der Hänger an die Tragkabel bilden Störstellen, die die Dauerhaftigkeit des Korrosionsschutzes beeinträchtigen. Darüber hinaus ist das Auswechseln der Tragkabel bei Schäden praktisch kaum durchführbar. Die einzelnen Seile der Schrägseilbrücke können dagegen ohne weiteres ausgetauscht werden.

Im Sinne der Bauwerksunterhaltung sind stets gute Besichtigungsmöglichkeiten erforderlich, damit kleine Schäden frühzeitig erkannt und ausgebessert werden können. Für die Schrägseilbrücken in Deutschland wurde daher vor kurzem ein Brückenseilbesichtigungswagen entwickelt, von dem aus auch kleinere Ausbesserungsarbeiten vorgenommen werden können, [7].

Weitere kritische Punkte sind bei den Hängebrücken die Sattellager auf den Pylonen und die Verankerungen in den Gründungskörpern. Auch hier sind die konstruktiv einfachen Verankerungen mit zylindrischen Seilköpfen bei den Schrägseilbrücken wesentlich günstiger zu beurteilen.

LITERATURVERZEICHNIS

1. KINDMANN R., Movable bridges - an alternative economic solution instead of elevated bridges. Thyssen Technische Berichte, Heft 2/88, Duisburg 1988.
2. LEONHARDT F., Developments in bridge design. International Symposium on strait crossings, Tapir-Verlag, Trondheim, Norwegen 1986.
3. HOTZ R., Humber Brücke - Weitestgespannte Brücke der Welt. Der STAHLBAU 50 (1981), S. 129 - 133.
4. FISCHER M., Stahlbrückenbau. Stahlbau Handbuch, Band 2, Stahlbau-Verlagsellschaft, Köln 1985.
5. HERZOG M., Das Projekt einer Hängebrücke über die Meerenge von Messina mit 3500 m Spannweite. Der STAHLBAU 51 (1982), S. 33 - 36.
6. SCHRÖTER H.-J., Zum Bau der Bosporus-Brücke. Der STAHLBAU 42 (1973), S. 87 - 91.
7. BOUË P., In-situ inspection device for cable-stayed bridges. International conference on cable-stayed bridges, Bangkok, Thailand 1987.

Teilweise unterspannte Schrägkabelbrücke über die Obere Argen

Cable-stayed Bridge, Partially Supported From Below – over the Obere Argen River

Pont haubané, supporté partiellement par des câbles inférieurs, sur le Obere Argen

Jörg SCHLAICH

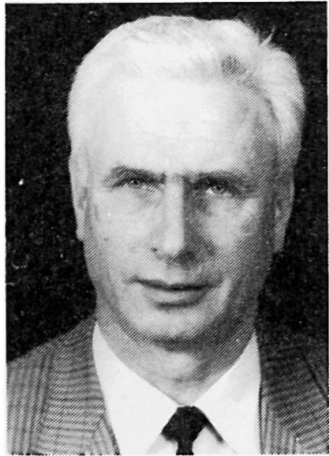
Prof.Dr.
Univ. of Stuttgart
Stuttgart, BR Deutschland

Jürgen SEIDEL

Structural Engineer
Schlaich und Partner,
Stuttgart, BR Deutschland

Dieter SANDNER

Structural Engineer
Schlaich und Partner,
Stuttgart, BR Deutschland



Jörg Schlaich, born 1934, studied Architecture and Civil Engineering at Stuttgart, Berlin and Cleveland, Ohio.



Jürgen Seidel, born 1941, studied Civil Engineering at Stuttgart and at Stanford University, California, USA.



Dieter Sandner, born 1949 studied Civil Engineering at Stuttgart University.

ZUSAMMENFASSUNG

Die südliche Flanke des Oberen Argen Tales lässt auf Grund der geologischen Verhältnisse keine Gründung zu. Zur direkten Überbrückung dieses 260 m-Feldes kam nach einem Entwurfswettbewerb eine teilweise unterspannte und teilweise direkt aufgehängte Schrägkabelbrücke mit Stahldeck zur Ausführung.

SUMMARY

Due to geological conditions no foundations were allowed on the southern slope of the Obere Argen valley. A design competition led to a cable-stayed bridge, partially supported from below and partially with direct suspension from the steel deck, in order to bridge the resulting 260 m span.

RÉSUMÉ

Les conditions géologiques du côté sud de la vallée de l'Obere Argen ne permettent pas de fondation. Le résultat d'un concours d'étude était un pont haubané avec un caisson en acier et une portée principale de 260 m, supporté partiellement par des haubans inférieurs. Cette solution est actuellement en cours de réalisation.



1. DER ENTWURF

In den süddeutschen Voralpen, zwischen Memmingen und Lindau, kreuzt die Autobahn A96 das Tal der 'Oberen Argen'. Die geologischen Verhältnisse und damit die Gründungsmöglichkeiten beider Talseiten sind völlig unterschiedlich. Während am nördlichen Talhang normale Gründungen möglich sind, findet sich am südlichen Talhang eine 15 m mächtige, instabile Rutschmasse aus Grundmoränenmaterial, welche eine Gründung ausschließt. Zur Überspannung dieses Rutschhangs war eine Brücke mit einem ca. 260 m weit gespannten Endfeld zu entwerfen. Während das zweite Feld direkt über der Oberen Argen auch noch 86 m lang sein mußte, gab es für die weiteren Felder bis zum gegenüberliegenden Widerlager keine besonderen Randbedingungen mehr.

Um für diese ungewöhnlichen Randbedingungen nicht nur eine technisch-wirtschaftliche, sondern ebenso gestalterisch befriedigende Lösung zu finden, welche diese schöne, unter Naturschutz stehende Landschaft möglichst wenig belastet, veranstaltete das Landesamt für Straßenwesen Baden-Württemberg unter Leitung von LtRBD E. Hoffmann einen Entwurfswettbewerb, der zum Bau der hier beschriebenen Brücke führte (Fig. 1).



Fig. 1 Brückenmodell

Im einzelnen wurden von den Verfassern die in (Fig. 2) dargestellten Varianten untersucht.

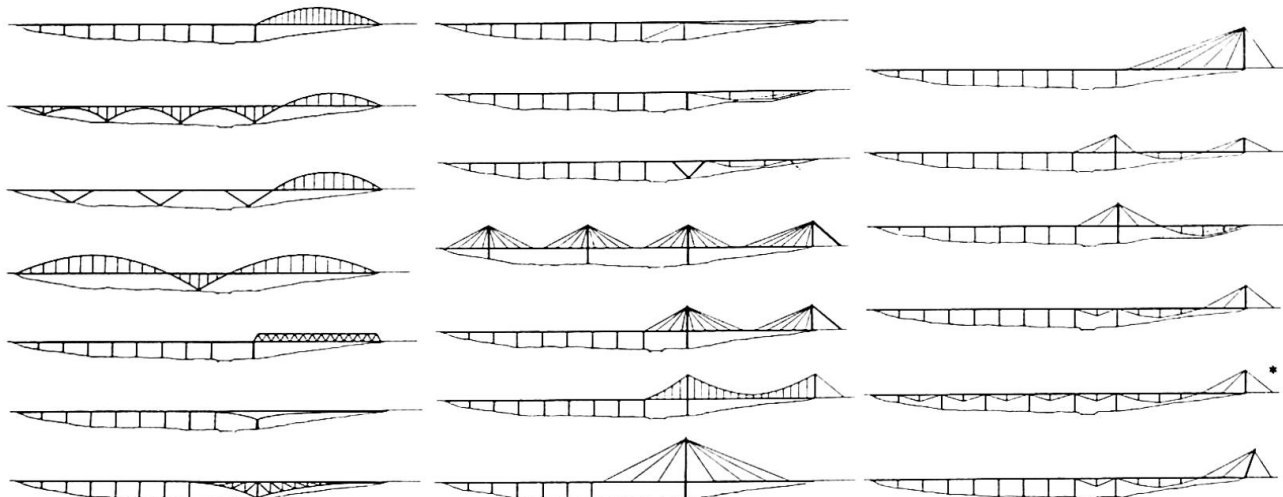


Fig. 2 Untersuchte Lösungsmöglichkeiten des Entwurfswettbewerbs

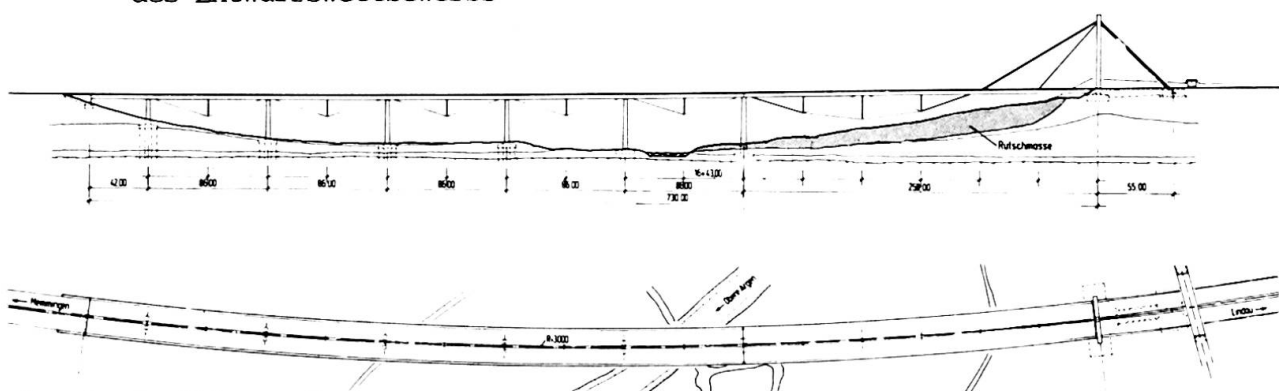


Fig. 3 Gewählte Brückenkonstruktion

Die gewählte Lösung (Fig. 3) passt sich mit einem sehr schlanken Überbau am unauffälligsten dem natürlichen Gelände an und führt mit der Kombination einer Schrägaufhängung und Unterspannung im Endfeld sowie der systematischen Fortsetzung der Unterspannung bis zum gegenüberliegenden Widerlager zu einer konstruktiven und gestalterischen Einheit. Wegen der Krümmung der Brücke im Grundriß bot sich für den Pylon die Λ -Form an, die zugleich als Tor dem Autofahrer die Brücke ankündigt.

Mit der Kombination von Aufhängung und Unterspannung im Bereich des Endfeldes braucht der Pylon, bei gleichen Kräften nur halb so hoch zu werden, wie bei einer reinen Aufhängung in Form der einseitigen Schrägseilbrücke (Fig. 4). Er fügt sich so bescheiden in die Landschaft ein, wobei die Seilführung dem Gelände folgt.

Aus Kostengründen wurde allerdings beim Ausführungsentwurf auf eine Fortführung der Unterspannung in den Seitenfeldern verzichtet. Das 258 m Endfeld und das anschließende 86 m Feld wurden in Stahl ausgeführt, die Fortführung mit kürzeren Spannweiten ganz konventionell in Spannbeton, wobei die Bauhöhen beider Brücken mit 3,75 m gleich sind. Dieser Beitrag kann sich auf die Beschreibung der Stahlbrücke beschränken.

2. LÄNGSSYSTEM DES STAHLÜBERBAUS

Der gekrümmte, durchlaufende Brückenträger geringer Bauhöhe ($H = 3,75$ m) ist auf den Pfeilern sowie am Pylonquerträger starr gestützt; zusätzlich ist er elastisch gestützt durch eine Seilunterspannung mittels zweier stabförmiger und einer V-förmigen Stütze, sowie durch eine Seilüberspannung an zwei Verankerungspunkten (Fig. 5). Die Seilüberspannung wird von einer Rückhaltekonstruktion getragen, bestehend aus dem Pylon, dem Rückhaltefundament – wirkend als Ballastkörper – und zwei Druckgliedern, zur kraftschlüssigen Kopplung der Horizontalkräfte zwischen Versteifungsträger und Rückhaltefundament.

Bei einer Länge der Hauptöffnung von 258 m bewirkt die vorhandene Kurvenkrümmung $R = 3000$ m beachtliche, horizontale Umlenkkräfte der Seile. Kleine Seilkräfte bei gleichzeitiger geringer Pylonhöhe waren somit die Hauptentwurfsskriterien. Die horizontalen Umlenkkräfte aus den Seilebenen werden am Hochpunkt über den

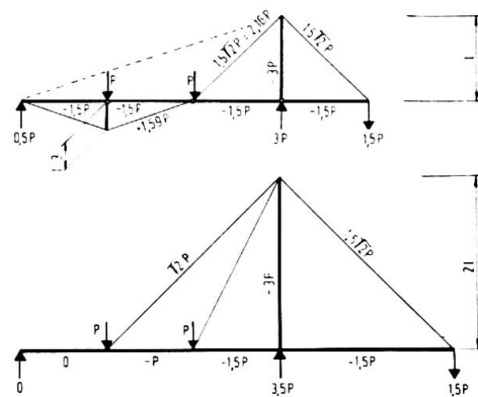
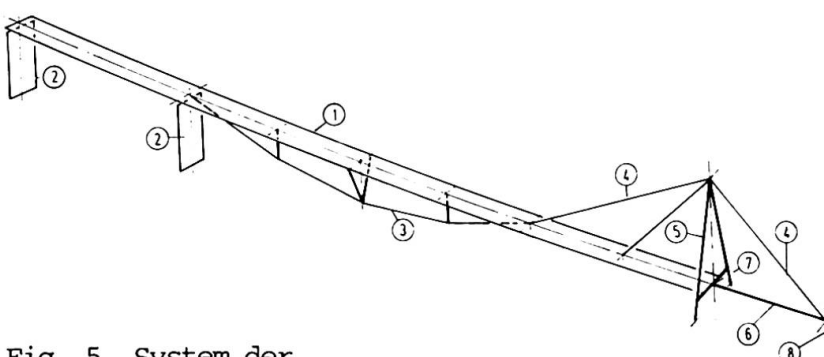


Fig. 4 Kräfte bei doppelter Pylonhöhe ohne Unterspannung



- 1 Versteifungsträger
- 2 Pfeiler
- 3 Unterspannung
- 4 Überspannung
- 5 Pylon
- 6 Druckglied
- 7 Pylonquerträger
- 8 Rückhaltekonstruktion

Fig. 5 System der ausgeführten Stahlbrücke



\wedge -förmigen Pylon und am Tiefpunkt über die V-förmige Luftstütze abgetragen. Weitere horizontale Umlenkräfte werden an den Silverankерungen in den Versteifungsträger bzw. in das Rückhaltefundament eingeleitet. Die stabförmigen Luftstützen liegen in der jeweiligen Seilebene und erhalten keine Umlenkräfte. Die Abtriebskräfte der gespreizten Pylonbeine werden über einen horizontalen Querträger kurzgeschlossen.

Am Pylonfuß befindet sich der horizontale Festpunkt bzw. Pol dieser Brücke (Fig. 6). Über den Pfeilern kommen Kalottenlager zur Anwendung; diese Lager sind auf den Pol ausgerichtet. Die horizontal geführten Lager befinden sich auf der Kurveninnenseite. Längsbewegungen werden am Fahrbahnübergang zur Spannbetonbrücke ausgeglichen.

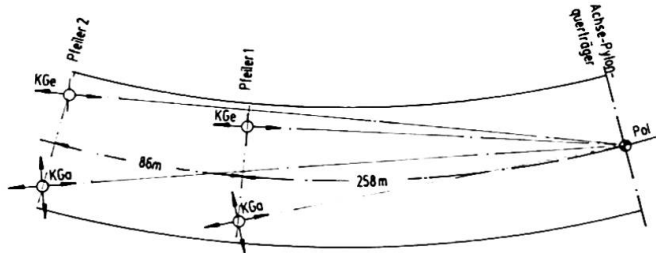
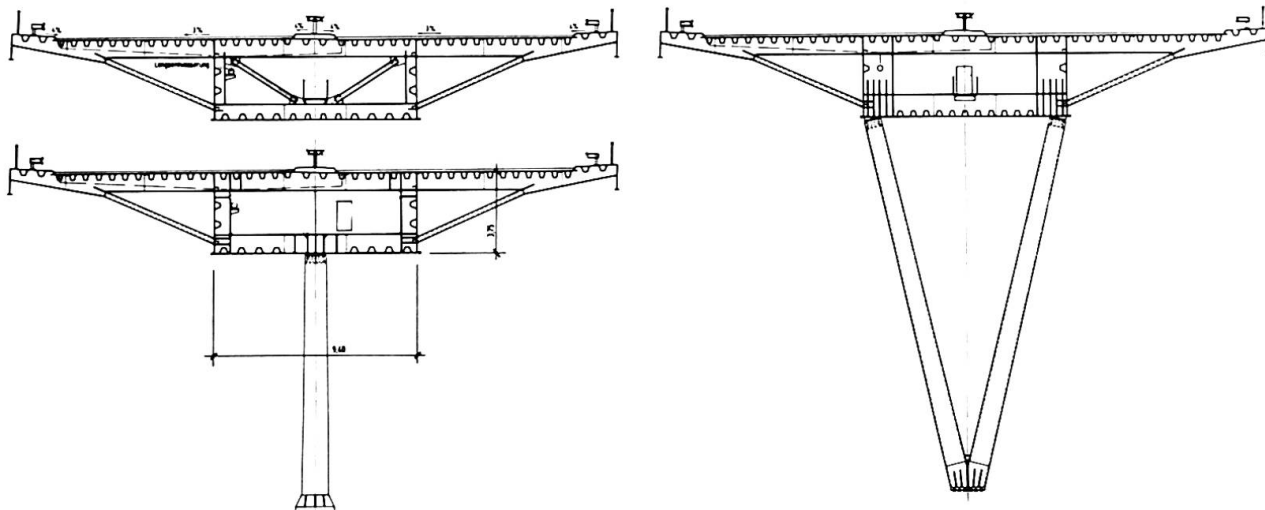


Fig. 6 Anordnung der Brückenlager

3. DIE KONSTRUKTION

Kurvenkrümmung, nur in Deckmitte angreifende Seilkräfte, sowie eingeschränkte Pfeilerbreiten machen einen torsionssteifen Versteifungsträger notwendig. Es wurde ein einzelliger Kasten mit Seitenstreben gewählt. Bei einer Breite des Brückendecks von 29 m ergibt sich aus einer Strebeneigung von 24° , sowie einem Stegabstand von 9,40 m, eine Bauhöhe von 3,75 m (Fig. 7).



Fahrbahn-, Boden-, Stegblech
Trapezstreifen, $h = 275 \text{ mm}$
Trapezstreifen, $h = 260 \text{ mm}$
Trapezstreifen, $h = 260 \text{ mm}$
Luftstützen, Querschotte
Verwendete Stahlgüte

: $t = 12-24 \text{ mm}$
: Fahrbahn , $t = 6, 8 \text{ mm}$
: Gehweg, Steg, Bodenblech , $t = 6-10 \text{ mm}$
: Mittelstreifen , $t = 6-10 \text{ mm}$
: $t = 20-70 \text{ mm}$
: St 52-3

Fig. 7 Überbauquerschnitte, frei sowie unterstützt

Aus der Überspannung wird vertikal eine Last von 89000 kN und horizontal eine Last von 1200 kN in den Pylonkopf übertragen. Durch die beiden hohen Pylonbeine werden diese Lasten über die Pylonsockeln in die Einzelfundamente eingeleitet. Als Zugglied zwischen den beiden Pylonsockeln nimmt der Pylonquerträger die horizontalen Spreizkräfte der geneigten Pylonbeine auf. Die Betongüte von Pylonkopf, Beinen, Querträger und Sockel ist B 45, die der Fundamente B 35 (Fig. 8).

Der Pylon ist mittels Abspannseilen am Rückhaltefundament verankert; die Summe der Seilkräfte beträgt hier 75000 kN. Auf das Rückhaltefundament wirkt eine abhebende Kraft von 52000 kN, welcher das Eigengewicht dieses Ballastkörpers gegenübersteht. Das Brückendeck ist mit der talseitigen Wand des Querträgers kraftschlüssig verbunden; die resultierende Druckkraft steht somit durch die beiden Druckglieder mit der Druckkraft des Stahlbrückenbalkens im Gleichgewicht.

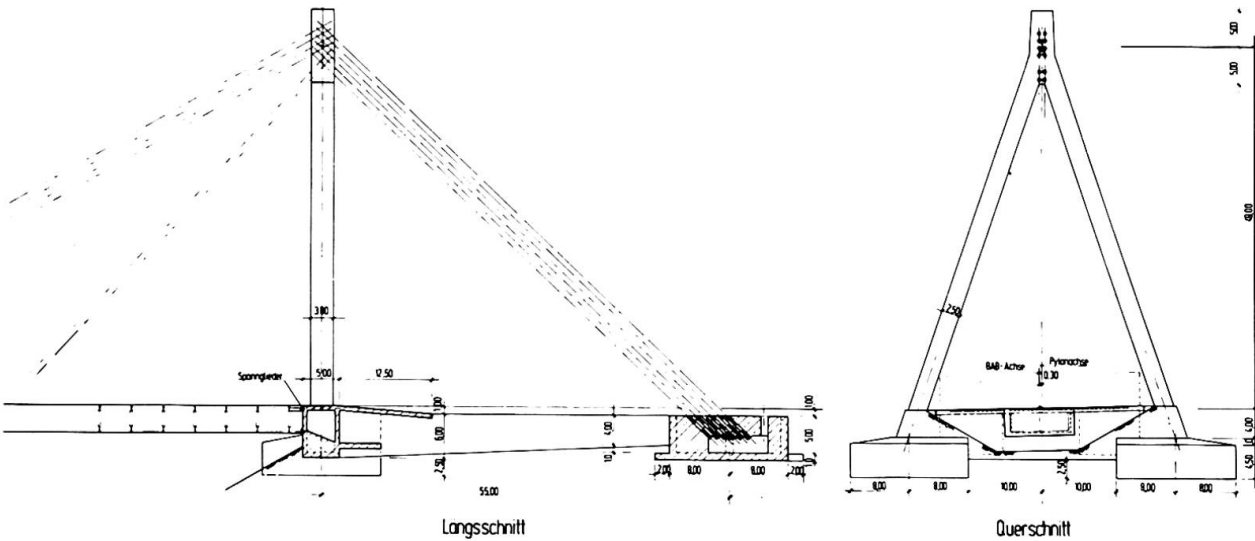


Fig. 8 Rückhaltekonstruktion

3.1. Der Pylonkopf

Die beiden Seilgruppen der talseitigen Überspannung 2x4 und 2x1, sowie die Rückhalteseile 2x6 werden in Nischen an der Pylonaußenseite verankert (Fig. 9). Die Seile werden vom Brückendeck bzw. vom Rückhaltefundament aus gespannt.

Die Seilköpfe sind über zwei geschlitzte Scheiben auf die Ankerplatten ($t = 70 \text{ mm}$) abgesetzt.

Am unteren Ende der Hüllrohre sind Seilhauben angeordnet. Innerhalb einer Stahlmanschette umschließt ein Elastomerkragen das Seil. Hier werden quer zum Seil wirkende Kräfte (70 kN) auf Grund von Änderungen der Seilachse aus Verkehrslasten aufgenommen und gegebenenfalls Windschwingungen gedämpft.

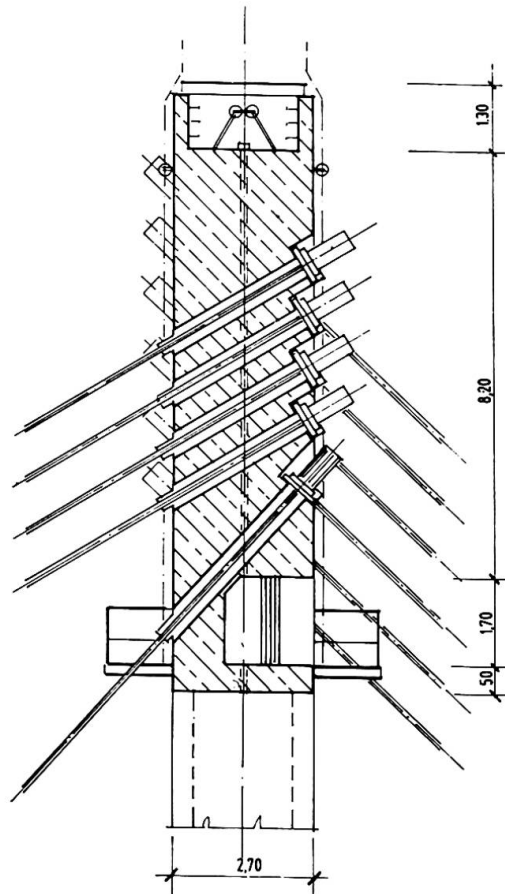


Fig. 9 Seilverankerung am Pylonkopf



3.2 Der Durchdringungspunkt von Über- und Unterspannung

Die Seilkräfte der Unterspannung 2x3, sowie die Kräfte der Überspannung 2x4 werden durch zwei Mittelstege ($t = 40 \text{ mm}$, lichter Abstand 1800 mm) miteinander gekoppelt. Die lokale Einleitung der Seilkräfte in beide Mittelstege erfolgt über Querscheiben ($t = 60 \text{ mm}$). Die lotrechten Seilkraftkomponenten stehen mit den Querkräften der Hauptträgerstege im Gleichgewicht. Diese Querkräfte müssen über verstärkte Querschottheit zu den Mittelstegen geleitet werden. Die horizontalen Umlenkkräfte der Überspannung werden mittels einer Längsaussteifung der Mittelstege ebenfalls in die Querschotte verteilt. Die Umlenkkräfte der Unterspannung werden durch eine direkte Verbindung der lokalen Querscheiben mit dem Bodenblech verbunden (Fig. 10.).

Schnitt A-A

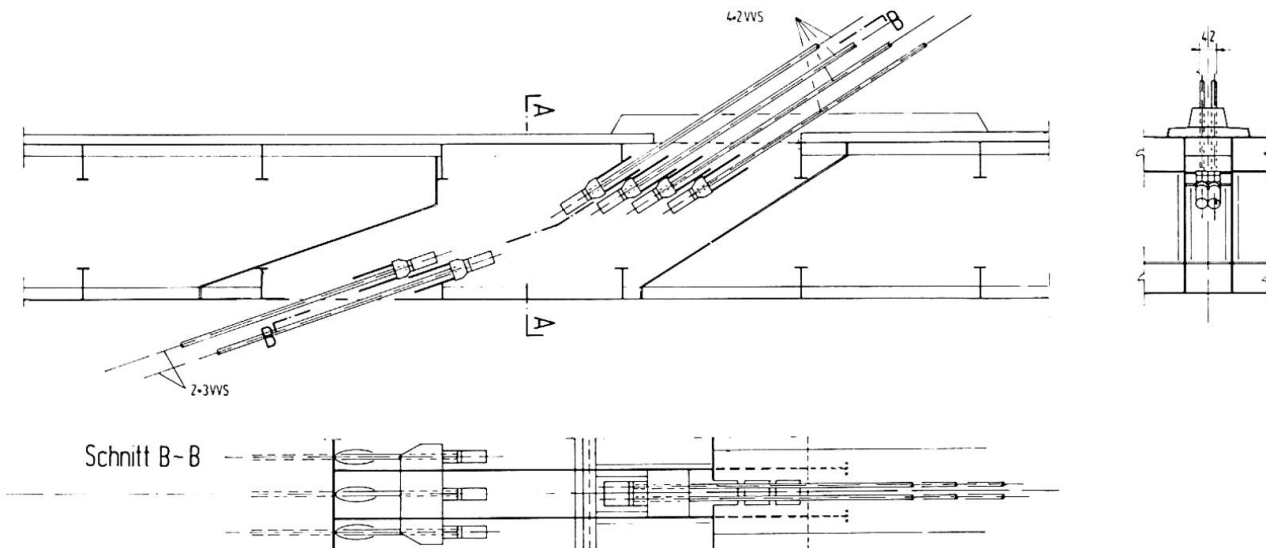


Fig. 10 Verankerungsbereich von Über- und Unterspannung im Brückendeck

3.3 Die Seile

- Aussendurchmesser: 126 mm
- sämtliche Drahtlagen aus feuerverzinkten Drähten
- blander Drahtquerschnitt 10775 mm^2
- erforderliche Minimal-Bruchlast 15563 kN
- Elastizitätsmodul: $160 \times 10^4 \text{ kN/cm}^2$

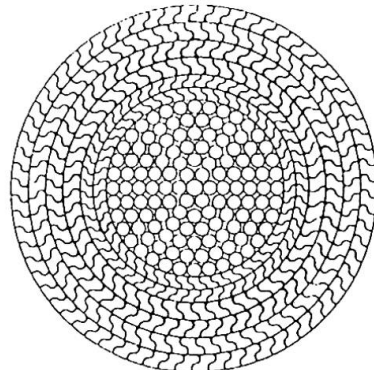


Fig. 11 Seilquerschnitt

4. DIE BETEILIGTEN

Landesamt für Straßenwesen Baden-Württemberg, Stuttgart

Entwurf und Ausschreibung: Schlaich und Partner, Stuttgart

Prüfingenieur: Schlaich und Partner, Stuttgart

Firmen: WTB Augsburg, D+W Lindau, CFEM Lauterbourg, TECNOR Bourg-en-Bresse

Projet du pont de Normandie – Conception générale de l'ouvrage

General Concept of the Normandy Bridge Project

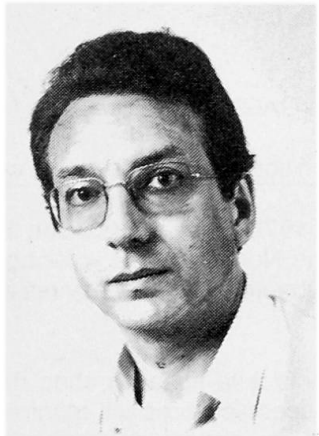
Konzept und Projekt der Normandie Brücke

Michel VIRLOGEUX

Professeur ENPC

SETRA

Bagneux, France



Michel Virlogeux, born in 1946 has been graduated at Ecole Polytechnique (1967) and Ecole Nationale des Ponts et Chaussées (1970), and is Docteur Ingénieur (Paris University, 1973). He received the 1983 IABSE Price in Venice. He is head of the Bridges Division of SETRA, and leads the design team for the Normandy Bridge project.

RÉSUMÉ

Cet article présente le projet technique du Pont de Normandie, sur l'estuaire de la Seine, entre Le Havre et Honfleur. Avec une portée principale de 856 mètres au-dessus du fleuve, ce sera l'un des plus grands ponts à haubans du monde si sa construction commence, comme prévu, en 1988. Cet article présente l'état final du projet, tel qu'il sera soumis à l'appel d'offres, en mars 1988.

ZUSAMMENFASSUNG

Das technische Projekt der Normandie Brücke über die Flussmündung der Seine zwischen Le Havre und Honfleur wird dargestellt. Mit einer Hauptspannweite von 856 m über den Fluss wird sie, wenn die Bauphase wie vorgesehen 1988 beginnt, eine der wichtigsten Schrägseilbrücken der Welt werden. Der Beitrag berichtet über den letzten Stand des Projekts, so wie er im März 1988 ausgeschrieben wird.

SUMMARY

This paper presents the technical project of the Normandy Bridge, over the River Seine mouth, between Le Havre and Honfleur. With a main span 856 m long over the river, it will be one of the most important cable stayed bridges in the world if the construction begins, as planned, in 1988. This paper presents the final state of the project, as it will be proposed for the invitation to bid, in March 1988.



1. GÉNÉRALITÉS

Le Pont de Normandie doit franchir l'estuaire de la Seine, légèrement à l'amont du Havre et de Honfleur. Sa construction et son exploitation ont été confiées par l'État à la Chambre de Commerce et d'Industrie du Havre, sous la forme d'une concession. Le Maître d'Oeuvre en est la Direction Départementale de l'Équipement de la Seine Maritime, qui a chargé une équipe pilotée par le SETRA de l'établissement du projet technique de l'ouvrage principal.

Cette équipe est constituée autour du SETRA par la SOFRESID, plus particulièrement chargée de la mise au point de la grande travée, par la SOGELERG, chargée de l'étude des travées d'accès en béton précontraint, et par l'ONERA à qui ont naturellement été confiées les études en soufflerie et de stabilité aéroélastique. L'architecte du projet est le cabinet Charles Lavigne.

2. CONCEPTION GÉNÉRALE DE L'OUVRAGE

2.1. Implantation des pylônes – Protection contre les chocs de navires

Un premier projet avait été établi entre 1976 et 1979, avec une travée principale de 510 mètres pour franchir le chenal de navigation. Outre le pylône Nord placé au voisinage de ce chenal, ce projet comportait quatre appuis en rivière, accessibles à marée haute à tous les navires de fort tonnage susceptibles de naviguer sur la Seine.

Mais les effondrements de grands ponts à la suite du choc d'un bateau se sont multipliés ces dernières années [1]. Certains de ces accidents spectaculaires ont montré qu'à la suite de conditions particulières des navires pouvaient s'écartier largement du chenal de navigation si aucun obstacle physique ne les en empêchait.

Il a donc été décidé de franchir la Seine sans appui en rivière, de la rive gauche à la Digue Basse Nord qui sépare le fleuve proprement dit des marais qui le bordent au Nord. La portée principale de l'ouvrage est ainsi de près de 900 mètres.

Le pylône Sud a été placé à terre, en rive gauche, à environ 25 mètres en arrière du quai, de façon à ce qu'un navire qui viendrait vers la rive avec un angle d'incidence important et une grande vitesse soit pratiquement arrêté par sa pénétration dans le sol avant de toucher les fondations du pylône.

De son côté, le pylône Nord est placé en avant de la Digue Basse Nord, pour ne pas augmenter la portée de façon excessive. Mais des bateaux de 130 000 tonnes et de douze mètres de tirant d'eau, arrivant avec une vitesse et un angle d'incidence déduits de simulations d'incidents établies par la SOGREAH, pourraient venir frapper violemment ses fondations. Jean Armand Calgaro a donc imaginé de constituer une enceinte de protection autour de ces fondations, formée par une longrine en béton armé de grandes dimensions (4 mètres de largeur sur 5 de hauteur) fondée sur une série de pieux rapprochés de gros diamètre (pieux de 2,60 mètre de diamètre espacés de 9 mètres), dessinant un demi cercle autour de la fondation de chaque fût (figure 2).

2.2. Principe du schéma statique longitudinal

La portée de la grande travée est ainsi de 856 mètres, ce qui constitue un bond en avant considérable par rapport au record du monde actuel, détenu par le pont d'Anacis au Canada, avec 465 mètres.

L'ouvrage a une longueur totale de 2 260 mètres. Il est constitué, de chaque côté de la Seine, par une série de travées d'accès à la travée principale. Ces travées d'accès sont construites en béton précontraint. Seule la travée principale doit être construite en acier (figure 1).

Les portées de ces travées d'accès en béton précontraint sont assez modestes : elles ne dépassent pas 58 mètres. De ce fait, les parties du tablier qui équilibrivent le poids de la grande travée, par l'intermédiaire du haubanage, sont beaucoup plus lourdes que la grande travée et portées par des pilettes rapprochées. Cette solution présente de nombreux avantages :

- le montage des travées d'accès en béton précontraint est classique et facile ; la grande travée peut être

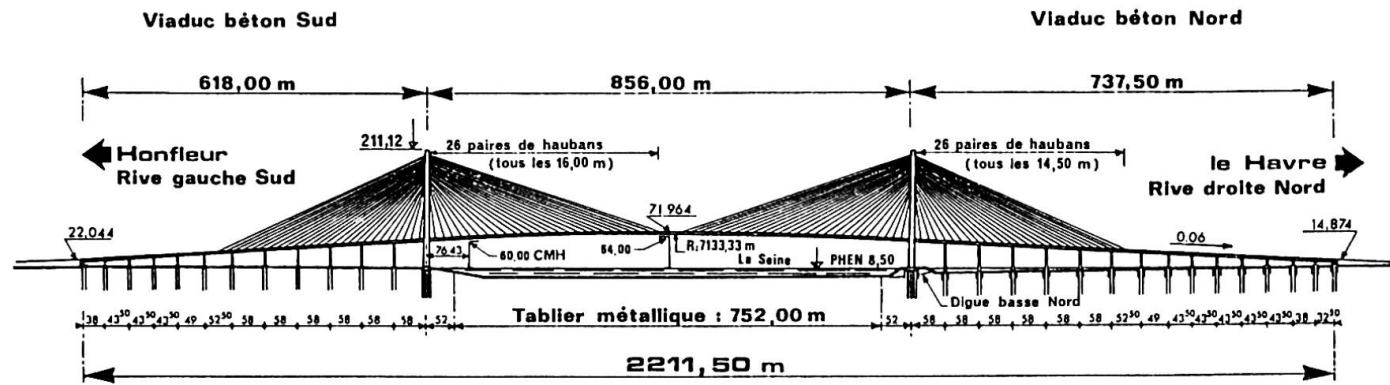


Figure 1 : Elévation longitudinale du Pont de Normandie.

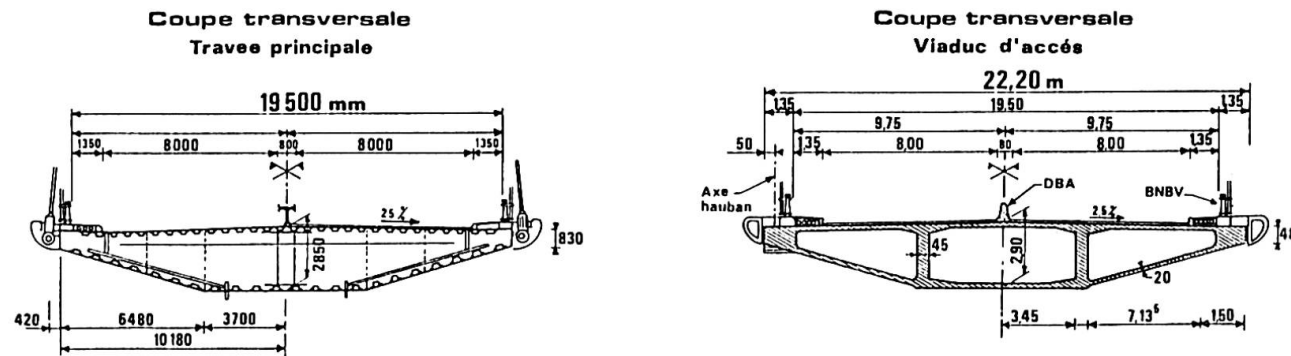


Figure 3 : Coupes transversales courantes du projet du Pont de Normandie.



- construite par encorbellements successifs à partir des pylônes ;
- cette solution permet de dessiner un haubanage aussi symétrique qu'on le souhaite par rapport aux pylônes, ce qui nous paraît plus élégant ;
 - la présence de nombreuses piles dans les accès en béton assure une multiplication du nombre des haubans "de retenue", qui sont répartis dans toute la nappe ; ce qui permet de répartir les ancrages sur une grande hauteur dans le mât ;
 - la différence de poids entre les "accès" en béton et la grande travée métallique élimine tout risque de soulèvement d'appui ;
 - la multiplication et la répartition des haubans "de retenue" rigidifie la suspension ; ce qui diminue les déplacements du tablier et surtout du pylône lors du chargement de la grande travée ;
 - lorsqu'on charge les travées d'accès, la travée principale ne subit pratiquement aucun effort ; la plage totale de variation des moments fléchissants dans la grande travée en est donc considérablement réduite ;
 - de même, les variations de tension dans les haubans de retenue sont fortement réduites, ce qui diminue les risques de fatigue ;
 - et, bien entendu, les variations de moment dans les travées d'accès sont considérablement plus faibles qu'avec un schéma classique à trois travées, ou même à plusieurs travées d'accès de moyenne portée.

Compte tenu de ce choix, il a été possible de dessiner un pylone en béton en forme de Y renversé, dont la hauteur dépasse 200 mètres et dont la crête permet de répartir les ancrages des haubans sur une hauteur d'environ 50 mètres.

2.3. Section transversale

Le principe d'un haubanage latéral a été retenu compte tenu de l'importance de la portée principale, pour améliorer la stabilité aéroélastique de l'ouvrage dans les phénomènes faisant intervenir la torsion.

La section transversale de la grande travée a été profilée en s'inspirant des ponts suspendus anglais projetés par le bureau Freeman-Fox and Partners. La hauteur du caisson métallique à dalle orthotrope a été choisie aussi faible que possible – 2,90 mètre à l'axe – et la largeur du bas de caisson a été réduite autant qu'il était raisonnable, sur les conseils d'Edmond Szechenyi, pour améliorer le profilage et augmenter le rapport largeur sur hauteur, déterminant dans les phénomènes d'écoulements tourbillonnaires. Mais aussi pour réduire la traînée, et donc les déplacements transversaux sous l'effet du vent (figure 3).

Cette section profilée a été conservée dans les travées d'accès en béton précontraint, pour assurer l'homogénéité technique et architecturale du projet.

2.4. Viaducs d'accès – Espacement des haubans

Il est envisagé de construire les viaducs d'accès en béton précontraint au moyen de voussoirs préfabriqués, et de les poser à l'avancement depuis les culées à l'aide d'un haubanage provisoire, travée par travée. La grande largeur du tablier a conduit à ne conjuguer les voussoirs qu'au niveau du caisson central, et à couler en place des joints armés dans les alvéoles latérales. Les bossages d'ancrage des haubans seraient aussi coulés en place pour faciliter la diffusion des efforts (figure 4).

Dans la grande travée métallique, les entretoises sont espacées de 4 mètres. De façon à limiter la puissance et la taille des haubans, leur entraxe a été fixé à 16 mètres dans la grande travée. Cet entraxe a été réduit à 14,50 mètre dans les travées d'accès en béton, parce que la pente importante des rampes aurait produit un effet désagréable : les haubans auraient été plus longs que dans la travée principale si l'on avait maintenu l'entraxe de 16 mètres, et les nappes de retenue auraient paru plus importantes que les nappes de suspension de la travée centrale.

La portée des travées d'accès a été choisie en fonction de l'entraxe des haubans. La valeur de 58 mètres, soit quatre intervalles d'ancrage, a été adoptée malgré la faible hauteur du caisson et son mauvais rendement géométrique. Car les haubans viennent aider la structure en béton des travées d'accès, comme s'ils réduisaient le poids propre du caisson en béton du poids du tronçon métallique central correspondant.

Cet avantage ne pouvait pas se retrouver dans les travées proches des culées, qui ne sont pas soutenues par des haubans de retenue. Ladislas Paulik et Jean Lawnicki ont donc dû raccourcir progressivement la portée des travées, depuis la fin de la zone haubanée jusqu'aux culées, Nord et Sud, en levant à chaque

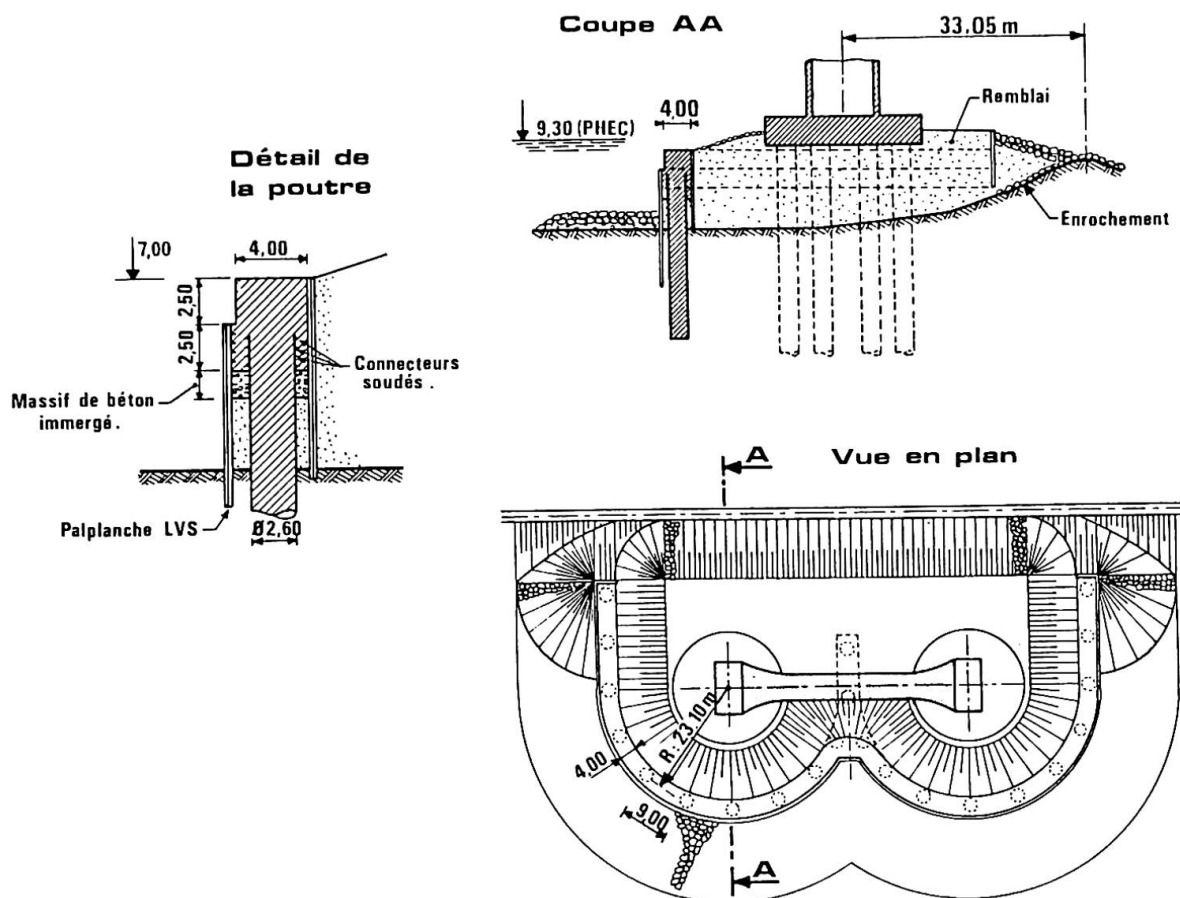


Figure 2 : Schémas de la protection du pylône Nord.

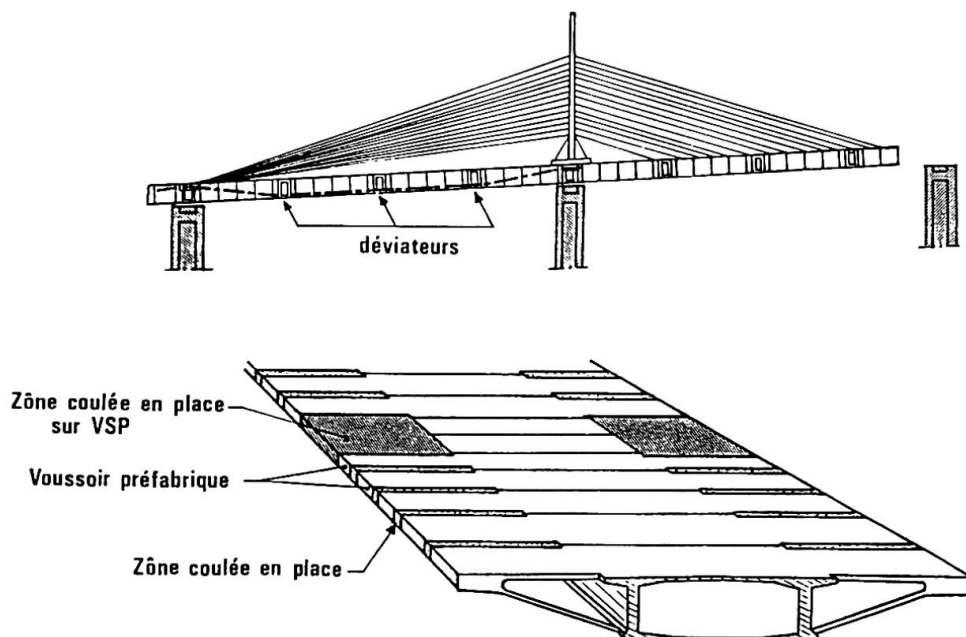


Figure 4 : Principe de la méthode de construction des travées d'accès.



fois un nombre entier de voussoirs de même longueur. Cela conduit à un schéma intéressant sur le plan esthétique puisque les travées les plus basses sont les plus courtes, ce qui assure une bonne harmonie des proportions des différents rectangles que découpent piles et tablier.

2.5. Liaison béton – acier

Pour assurer l'équilibre du tablier de part et d'autre de chaque pylône, la partie en béton a été prolongée de 52 mètres à partir de chaque pylône dans la grande travée. Cette longueur de 52 mètres a été choisie pour plusieurs raisons :

- une analyse économique comparative a montré qu'un allongement de la partie en béton était intéressant tant qu'il ne mettait pas en cause les méthodes de construction, à condition de ne pas dépasser une centaine de mètres ;
- plus la section de liaison béton – métal est éloignée du pylône, plus les efforts de flexion transversale dûs au vent y sont réduits ; ce qui limite les efforts de serrage à mettre en œuvre à la liaison ;
- la méthode de construction à l'avancement à l'aide de haubans provisoires permet de construire avec le matériel de construction des travées d'accès des consoles de 58 mètres, sans la moindre modification ; la longueur de 52 mètres est la plus grande en dessous de 58 mètres qui soit compatible avec la position des ancrages des haubans ;
- l'allongement des consoles au delà d'une trentaine de mètres permettra de lever directement depuis la Seine les tronçons successifs de charpente métallique, dont la longueur devrait être de 16 mètres.

L'analyse des efforts de flexion longitudinale a conduit Vu Bui à placer les premiers haubans très près du pylône, où ils sont peu efficaces sous charges d'exploitation mais permettent de diminuer les importants efforts de flexion dûs au poids propre de la partie en béton. Grâce à cette disposition et à un réglage judicieux des tensions des haubans, les moments fléchissants sont très faibles dans l'ouvrage, et la section métallique courante est partout suffisante, ne demandant aucun renfort local.

Sur le plan des détails techniques, la liaison entre la partie en béton et la partie en acier est assurée en garantissant un alignement aussi parfait que possible des fibres moyennes des différents voiles :

- en ce qui concerne les voiles latéraux inclinés et le hourdis inférieur, la tôle métallique ne vient qu'à 5 centimètres du bord du béton ; comme le centre de gravité des voiles métalliques, raidis par les augets, est à 4 ou 5 centimètres de la paroi, l'alignement est à peu près parfait avec des voiles en béton de 20 centimètres d'épaisseur ;
- il n'y a pas d'âmes verticales dans la section courante de la grande travée ; mais il y en a dans le prolongement des âmes en béton, sur une dizaine de mètres au delà de la liaison avec le béton, pour assurer un bon transfert des efforts ;
- en ce qui concerne le hourdis supérieur, les conditions de continuité de la surface de roulement ont interdit un parfait alignement des fibres moyennes, mais l'écart est fortement réduit par la puissance des augets de la dalle orthotrope.

La section de liaison entre les parties en béton et en acier est fortement sollicitée par le moment transversal dû au vent, et par le moment longitudinal dû aux charges d'exploitation, que l'effort normal produit par le haubanage ne suffit pas à équilibrer. La résistance est donc assurée par la mise en œuvre d'une précontrainte de serrage. Une partie de cette précontrainte est créée par des grands câbles qui dépassent la zone du pylône où ils sont utiles. Le complément est assuré par des barres de précontrainte courtes, ancrées sur des zones fortement raidies de la charpente, dans les mêmes conditions que pour la précontrainte de liaison d'un avant-bec de poussage.

2.6. Les pylônes

Les pylônes ont été dessinés de façon à permettre l'ancrage des haubans, en principe tendus depuis le tablier, et à permettre la visite ultérieure des pylônes et des ancrages, ainsi que le réglage éventuel de la tension des haubans depuis les mâts.

Les formes intérieures ont été choisies de façon à ne transmettre que des efforts d'appui au béton. Et à livrer passage, de chaque côté du voile central, à une échelle à crinoline – tantôt à gauche, tantôt à droite – et à une cheminée de descente du vérin de réglage.

Les haubans les plus bas ont été légèrement cintrés dans leurs passages dans le béton, par Hélène Abel et Jocelyne Jacob, de façon à remonter leurs points de sortie, pour les intégrer dans les formes architecturales définies en collaboration avec Charles Lavigne.

2.7. Conditions de liaison du tablier et des appuis

Pour assurer une excellente résistance au vent, et limiter autant que possible les déplacements de balancement transversal qu'il produit, il a été décidé d'encastrer dans chaque pylône le tablier, qui est en béton à ce niveau, et de placer sur les piles des travées d'accès des appareils d'appui fixes transversalement. Le vent crée donc, sur les piles voisines des pylônes, des réactions horizontales transversales qui peuvent atteindre 100 tonnes dans les conditions de service.

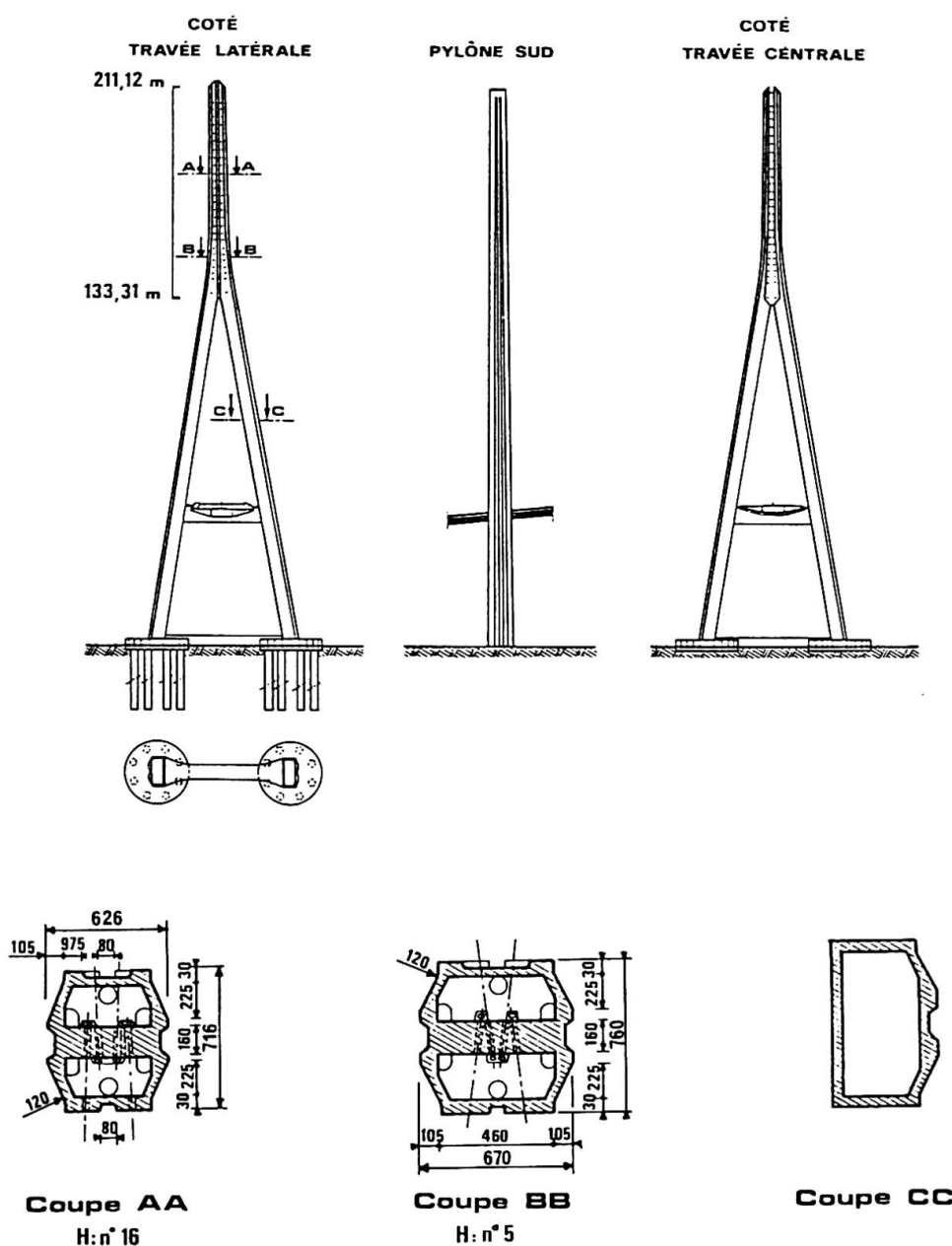


Figure 5 : Schémas de définition des pylônes.



Compte tenu du schéma statique longitudinal qui a été retenu, la travée centrale fonctionne en portique, si bien que les variations de température créent dans les pylônes des efforts de flexion non négligeables, mais acceptables.

Comme il n'est pas possible de créer des joints de dilatation dans la partie haubanée de l'ouvrage, il a été décidé de ne placer des joints qu'au droit des deux culées. Mais la rigidité des pylônes permet de limiter l'ouverture des joints à des valeurs raisonnables, de l'ordre de 70 centimètres (de + 30 à - 40 centimètres).

Enfin, comme les piles les plus proches des pylônes sont extrêmement souples du fait de leur grande hauteur, et comme les déplacements longitudinaux sont faibles au voisinage des pylônes où le tablier est encastré, il a été possible de placer des appareils d'appui fixes sur les premières piles à partir des pylônes. Sur les autres piles, les appareils d'appui sont fixes transversalement et glissants dans le sens longitudinal.

2.8. Choix du type des haubans

Le choix du type des haubans sera évidemment laissé à l'initiative de l'entreprise. Pour l'établissement du projet, Jean Claude Foucriat a choisi des câbles clos, avec des couches internes de fils ronds galvanisés de 5 millimètres de diamètre, deux couches extérieures de fils Z galvanisés, et une couche de protection en fils Z d'Almelec, un alliage d'aluminium qui assure une bonne protection contre la corrosion. Cette dernière couche ne participe pas réellement à la résistance mécanique du câble, compte tenu de la faible valeur du module de déformation de l'alliage.

Cette solution a semblé la meilleure dans la mesure où :

- le poids au mètre linéaire du câble est plus faible que pour toutes les autres solutions, pour une valeur donnée de la tension utile, ce qui limite l'effet de chaînette ; en particulier, toutes les solutions prévoyant l'injection d'une large gaine au coulis de ciment doivent être écartées ;
- le diamètre extérieur du câble est plus faible que pour toutes les autres solutions, pour une valeur donnée de la tension utile, ce qui limite les efforts dûs au vent, qui ne doivent pas être négligés compte tenu de l'importance considérable de la surface au vent de la nappe de haubanage.

En contrepartie, le module de déformation longitudinale des câbles constitués de torons ou de fils parallèles (ou légèrement torsadés) est supérieur à celui des câbles clos; mais les avantages que nous venons d'évoquer ont semblé suffisants pour compenser ce handicap.

3. CONCLUSION

Compte tenu de l'importance de l'ouvrage et de la valeur de la portée centrale, le Directeur des Routes a décidé de constituer une Mission d'Évaluation, chargée de donner un avis motivé sur le projet du Pont de Normandie. Cette mission, présidée par l'Inspecteur Général Marcel Huet, est constituée des Inspecteurs généraux Henri Mathieu et Charles Brignon et des Professeurs Roger Lacroix, Jorg Schlaich et René Walther.

Cette mission a déjà donné un avis favorable sur l'avant projet en juillet 1987, et suggéré un certain nombre d'aménagements, dont plusieurs ont été retenus par l'équipe d'étude pour l'établissement de l'avant projet détaillé, qui servira de base à l'appel d'offres qui doit être lancé en février ou mars 1988.

BIBLIOGRAPHIE

- [1] Ship Collision Problems with Bridges and Offshore Structures. IABSE Colloquium, Copenhague 1983. IABSE publications volumes n° 41 (Rapport Introductif), 42 (Rapport Préliminaire) et 43 (Rapport Final).
- [2] M. Virlogeux, J.C. Foucriat, B. Deroubaix : Design of the Normandie Cable Stayed Bridge, near Honfleur. Cable Stayed Bridges. Experience and Practice. Proceedings of the International Conference on Cable Stayed Bridges, Bangkok, novembre 1987 – p. 1123-1134.

Design of Long Span Suspension Bridges for Combined Highway and Railway

Conception d'un long pont suspendu mixte route et voie ferrée

Entwurf von Hängebrücken als kombinierte Eisenbahn- und Autobahnbrücken

Masamitsu OHASHI

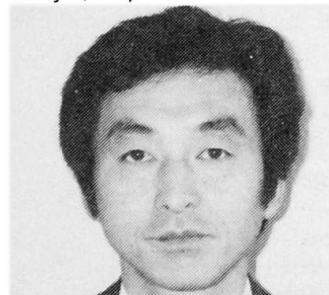
Dr.Eng.Dir.
Honshu-Shikoku Bridge Auth.
Tokyo, Japan



Born in 1928, obtained his Dr.Eng. degree in civil engineering at the Kyoto University, Japan. From 1969 to 1974, he worked for the construction of the Kanmon Bridge as a manager. Now, he is an executive director for the Honshu-Shikoku Bridge Authority.

Yuji FUJII

Civil Eng.
Planning Division, H.S.B.A.
Tokyo, Japan



Born in 1949, received his masters degree in civil engineering at the Hokkaido University. He was engaged in the construction of the Shimotsui Seto Bridge.

Shin NARUI

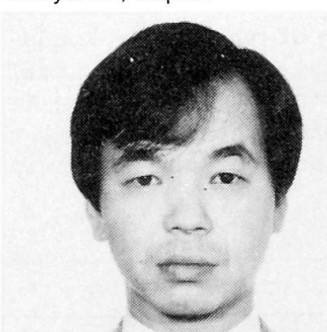
Cief of Bridge Eng.
Naruto Maintenance Office,
Tokushima, Japan



Born in 1948, received his Dr.-Ing. degree in civil engineering at the Stuttgart University, West Germany. He was engaged in the construction of Minami and Kita Bisan Seto Bridges.

Shigeru HIRANO

Subchief
Second Constr. Bureau
Okayama, Japan



Born in 1953, received his masters degree in civil engineering at the Tokyo Metropolitan University. He was engaged in the construction of Minami and Kita Bisan Seto Bridges.

SUMMARY

This report introduces the design problems and solutions of the bridges for combined highway and high-speed railway, taking the case of the Minami Bisan-Seto Bridge, the longest suspension bridge on the Kojima-Sakaide Route of the Honshu-Shikoku Bridges.

RÉSUMÉ

Le rapport présente des problèmes et solutions dans la conception d'un pont mixte route et voie ferrée à grande vitesse: le Pont Minami Bisan-Seto qui est le plus long pont suspendu dans la section Kojima-Sakaide du projet de liaison Honshu-Shikoku par ponts.

ZUSAMMENFASSUNG

Diese Arbeit befaßt sich mit der Darstellung und Lösung von Entwurfsproblemen, die bei kombinierten Eisenbahn- und Autobahnbrücken auftreten und geht hauptsächlich anhand der Brücke Minamibisan-Seto als Beispiel vor, welches die längste Hängebrücke der Honshu-Shikoku-Verbindung auf der Strecke Kojima-Sakaide ist.



1. INTRODUCTION

The construction of the Kojima-Sakaide Route, one of the three routes to link the Honshu (Mainland) and the Shikoku Island started in October 1978, and is scheduled to be opened to traffic in April 1988.

There are three long span suspension bridges on the route carrying both highway and railway; the Minami Bisan-Seto Bridge (center span: 1,100m), the Kita Bisan Seto Bridge (center span: 990m) and the Shimotsui-Seto Bridge (center span: 940m). (See Fig. 1)

At the very early stage of the project the Honshu-Shikoku Bridge Authority (to be called the Authority hereafter) faced many technical problems in design of the superstructures of the bridges such as the safety in the bullet train service, the establishment of the fatigue design criteria and the design against large deflection and forces.

This paper describes those problems we faced and the solutions we selected for the bridges for the combined use.

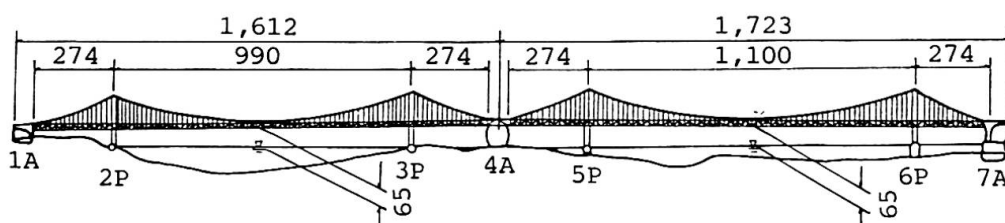


Fig. 1 General View of Kita and Minami Bisan-Seto Bridges (m)

2. DESIGN LOADS

We take the Minami Bisan-Seto Bridge as an example in this paper. We listed the designed loads for the bridge in Table-1. The significance in the design loading for the suspension bridge for such a combined use is considered to be live load, that is automobile traffic load and train load.

The intensity of the above loads was determined based on the actual surveyed data of highway and railway traffic. Although this suspension bridges are designed to carry four railway tracks, considering the actual service schedule and the traffic control system, the train load applied for the design purpose was of two tracks of the train instead of four.

Table-1 Design Loads (Minami Bisan-Seto Bridge)

Classification		Design Load
Dead Load : D	Uniform Load : D_0	434kN/m (Center span) 448 kN/m (Side span)
	Ununiform Load : D_1	Difference between actual dead load and D_0 .
Live Load	Car load L_H	Equivalent concentrated load : P Equivalent distributed load : p
	Train load L_R	Normally design For fatigue stress In times of an earthquake
Impact : I	Impact coefficient : i	i = 0.2 (Shinkansen) i = 0.1 (Ordinary train)
Temperature Change:T		±30deg
Others	Support displacement, Erection error, Wind, Earthquake	

3. STRUCTURAL FEATURES

3.1 3-span-continuous suspension bridge

Carrying the railway tracks, the geometrical continuity is a very important factor for this bridge, where the angular bends at towers and girder ends shall be limited in order to assure the safety in railway service.

Therefore, 3-span-continuous girder was selected. We listed the angular bend and the expansion joint movement of 2-hinged suspension bridge and 3-spanded continuous suspension bridge for comparison purpose in Table-2.

Table-2 Comparison of suspension bridge types

	Vertical angular Bend	Movement at Expansion Joints
2-hinge suspension bridge	3.1% at towers	±108cm at towers
3-span-continuous suspension bridge	1.1% at ends	±64cm at ends

The major design solutions are as follows.

1) Large bending moment at the intermediate support

The bending moment of the stiffening girder at the intermediate support is 1,450 MNm/Br., approximately four times as large as that at middle of the center span. The sectional dimension of the chord members at the intermediate support is 1,000mm wide x 1,200mm high with 75mm thick plates, while that of the typical section is 750mm x 750mm with 35mm thick plates.

2) Large reaction force at the intermediate support

As the reaction force at the intermediate support is as large as 34.3MN and the longitudinal movement is ±65cm, a solid-forged link structure was designed to link the tower and the stiffening girder with solid lubricant bushings in the contact surface to a sliding pin. Total weight of the link structure including the bushings is 637 kN.

Further, the tower link is connected to the lower chord member of the stiffening girder and is located between the lower and upper chords from an aesthetic point of view.

3) Negative reaction force (uplift) of the stiffening girder

As negative reaction forces due to live load would occur at the intermediate support and girder end, counterweights with concrete weighing 2,500 kN and 540 kN respectively, are placed in order to minimize the occurrence of the negative reaction forces.

4) Hanger bracket

In order to maintain the continuity of the stiffening girder through the two towers, the girder was designed with the hanger brackets where the hanger ropes are to be anchored (See Fig. 2).

3.2 Double deck structure

The stiffening girder has two layers of decks i.e. the lower deck for railway and the upper deck for highway (see Fig. 2).

Considering that the long-spanded girder is carrying both railway and highway, the dead load stress of the main cable comes up to 80% of its total stress.

As one of the approaches to reduce the above dead load, the upper deck for the highway is made up of the steel deck with 75mm thick asphalt pavement and the



lower deck for the railway is made up of tracks directly attached to the top flange of railway stringer with newly developed rail fasteners.

4. DYNAMICS OF TRAIN OPERATION

The runnability of trains was a major concern in this project. Our series of studies on this subject is summarized as follows.

4.1 Development of transit girder system

The problem of angular bend at the towers was solved by adoption of the 3-span-continuous bridge. Fig. 2 Typical Cross Section of the Suspension Bridge The angular bend at the girder ends which is calculated to be 1.1% max. and the longitudinal movement at the points which is calculated to be $\pm 64\text{cm}$ were, however still to be solved. The deflections at railway stringer and cross truss also lead to additional angular bend to that at girder ends. To solve this problem, the transit girder was developed. It has the capacity of the movement $\pm 75\text{cm}$ and dispersing the amount of angular bend at the two points (see Fig. 3). Further, the performance of this assembly was confirmed through the field running tests with real vehicles.

4.2 Restriction of stringer deflection

With the trains running at high speed on the railway stringers as they have deflection due to the train load, the wheel load is reduced and consequently it would increase the risk of derailing. The vibration of the train will also reduce riding comfort.

After analyses and simulations, it was decided to solve this problem that the stringer deflection shall be restricted to be $L/900$ max. for the ordinary train, where L is length between two supports.

4.3 Runnability against earthquake

The lateral vibration due to earthquake would threaten the safe running of the trains on the stiffening girder. The series of model testings on the shaking table and computer simulations were carried out to evaluate the reactions

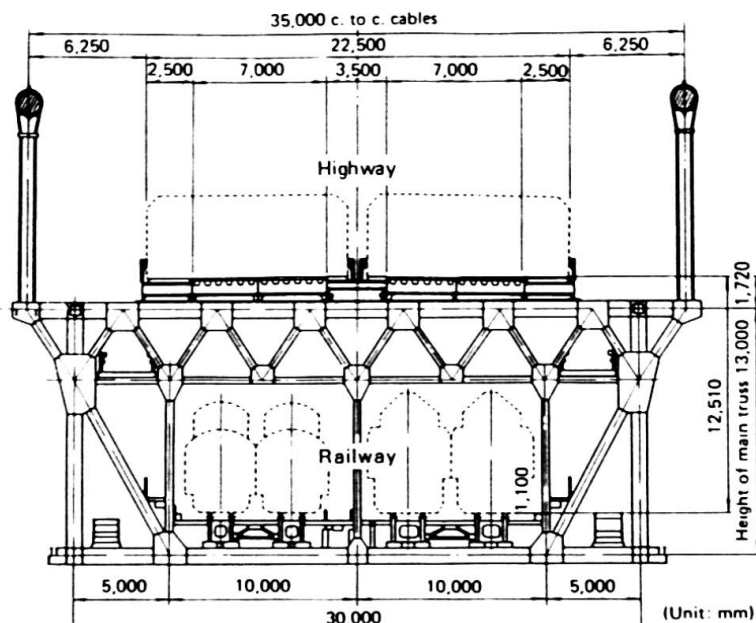


Fig. 2 Typical Cross Section of the Suspension Bridge

① : Expansion joint of rails

②, ③ : Angular bend portion

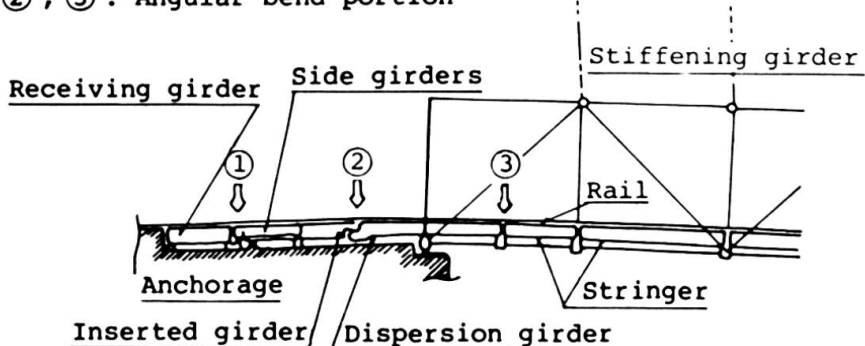


Fig. 3 Transit Girder System of Inserted Girder Type

against earthquake.

Based on the above studies, the running safety limit curve was prepared (see Fig. 4) to evaluate the runnability in case of earthquake.

4.4 Runnability against wind

In order to evaluate the influence of the disturbed wind blowing (30m/sec.) through trussed stiffening girder members to runnability, the series of the wind tunnel tests were carried out. The safety of the running on the bridge was confirmed through these tests.

5. FATIGUE DESIGN

The bridges designed for the Kojima - Sakaide route are expected to carry more than 6 million passages of the trains during the bridge life i.e. 100 years. Furthermore, considerable amount of the quenched and tempered high strength steel (570 ~ 790 MPa) whose structural fatigue behaviour was not fully clarified is used for those bridges' primary members. Therefore fatigue problem was considered one of most important subjects for the project. We carried out number of full-scaled fatigue tests for the structural elements and researches from the view point of fracture mechanics.

Based on the result of the above efforts, the fatigue design criteria for the project was established.

In actual design of the structural members, each detail was carefully examined in order to assure sufficient fatigue life. Especially the design of hanger bracket (see Fig. 5), which has relatively complicated detail, was supported by FEM analysis and full scaled fatigue tests.

In order to maintain the fabrication workmanship required for the project, the additional requirements such as welding procedure tests with full size member, selection of welding materials, additional requirements for welder qualification and severer dimensional tolerances of welding defects were specified.

The automatic ultrasonic testing was carried out for the primary members' corner welding to assure the quality of the weldment satisfies the above mentioned fatigue requirements.

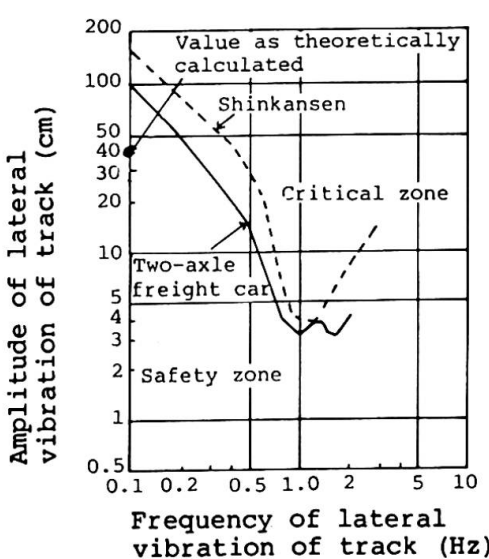


Fig. 4 Running Safety Limit Curve

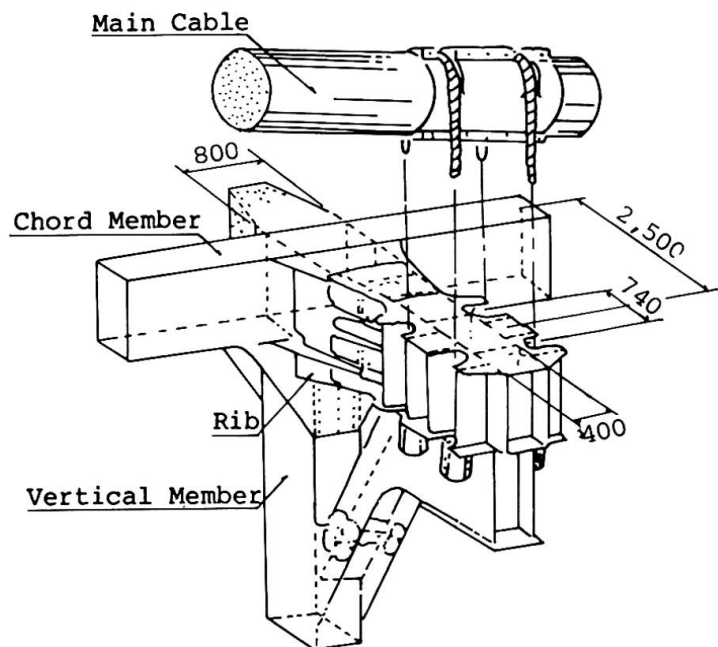


Fig. 5 Detail of Hanger Bracket



6. CONCLUSION

As stated in this paper, we have solved many problems we faced at the every early stage of the project through number of experiments, trial fabrications and so on clarifying the structural characters of long span suspension bridge for both highway and railway uses. In the following table (Table-3) we summarized dead load used for the bridges we designed and for other major bridges as a part of the results we gained through our efforts.

In comparing those listed in the table, it can be remarked that the intensity of train load is a significant factor to determine the dead load per unit bridge length.

After the completion of the bridges, deflection, stress and angular bend of stiffening girder etc. will be measured on the train running tests and the vibration tests of completed bridges to confirm the design concept we stated herein.

We sincerely hope that the results we gained through our projects can be any of assistance for those who share the field of suspension bridge for the combined use of highway and railway.

Table-3 Comparison of Dead Load

*: Lower deck added.

**: Shinkansen can be provided in future.

Name of Bridge		Innoshima Bridge	Minami Bisan-Seto Bridge	George Washington Bridge	Golden Gate Bridge	Verrazano Narrows Bridge
Year of completion		1983	1988	1931('60)*	1937	1964
Span (m)		250+770+250	274+1,100+274	190+1,067+186	343+1,280+343	370+1,298+370
Item	Number of Lanes	Highway	4	4	14	6
	Railway	-	2(4)**	-	-	-
Dead Load	Stiffening girder (kN/m)	156	314	423	165	379
	Cable (kN/m)	46	121	160	146	155
	Total (kN/m)	202	435	583	311	534

Railway Traffic on Long Span Suspension Bridges

Circulation ferroviaire sur les ponts suspendus de grande portée

Eisenbahnverkehr auf weitgespannten Hängebrücken

Fabio BRANCALEONI

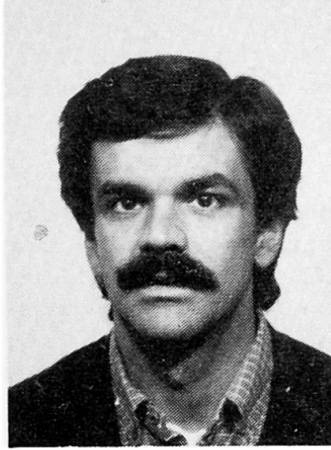
Assoc. Prof.
University "La Sapienza"
Rome, Italy



Fabio Brancaleoni, born 1949, received his civil engineering degree at the University of Rome, where he also had his academic career, but for a year spent at UMIST in UK. Fabio Brancaleoni authored numerous papers in the fields of Structural Mechanics and Dynamics, with several applications devoted to suspension bridges.

Federico CHELI

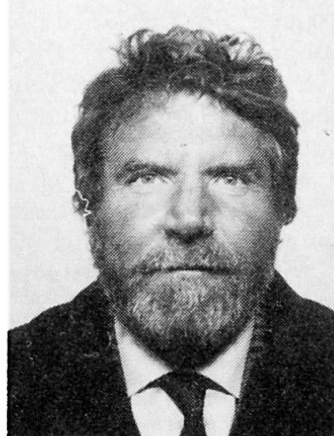
Researcher
Politecnico di Milano
Milan, Italy



Federico Cheli, born 1956, received his Mechanical Engineering Degree at the Politecnico di Milano in 1981, where he is presently researcher at the Dipartimento di Meccanica. His work is concerned with Structural Vibrations, Rotor-Dynamics and Railway Vehicle Dynamics.

Giorgio DIANA

Professor
Politecnico di Milano
Milan, Italy



Giorgio Diana, born 1936, received his Mechanical Engineering Degree at Politecnico di Milano in 1961 and became Professor of Applied Mechanics in 1971. He now gives the course "Vibration of Machines" at Politecnico di Milano. Giorgio Diana authored many papers in the fields of Fluidoelasticity, Rotor-Dynamics and Vibration Problems in Mechanical Engineering.

SUMMARY

General deformation aspects of suspension bridge response are discussed, proceeding subsequently to the examination of static runnability problems deriving from the elevate slopes which can occur for severe loading. The second part of the paper is devoted to dynamic runnability analyses where, beside the structural behaviour, structure-vehicle interaction and vehicle response are simulated, providing indications on transit comfort and safety.

RÉSUMÉ

Les aspects généraux de la déformation des ponts suspendus sont traités ainsi que les problèmes de circulation découlant de la pente élevée consécutive aux charges maximales. Des problèmes de circulation dynamique sont considérés en simulant le comportement de la structure, l'interaction entre la structure et le véhicule et la réponse du véhicule, en donnant des indications sur le confort et sur la sécurité.

ZUSAMMENFASSUNG

Dieser Beitrag behandelt die gesamten Aspekte der Verformung von Hängebrücken, mit Hilfe von Untersuchungen bezüglich der Probleme des statischen Verhaltens bei hohen Neigungen, die von Schwerbelastungen herstammen. Der zweite Teil behandelt Untersuchungen des dynamischen Verkehrs, das Verhalten der Struktur, die Wechselwirkung zwischen der Struktur und dem Fahrzeug. Das Verhalten des Fahrzeugs simulierend, können Angaben bezüglich der Sicherheit und des Komforts des Verkehrs gegeben werden.



1. INTRODUCTION

The debate on the possible performances of large span suspension bridges for railway use is active in the bridge engineering community since several decades [1, 2, 3, 4]. A milestone in the argument has now been set in '88, with the completion of the Kojima-Sakaide route of the Honshu-Shikoku Bridge project, comprising three suspension bridges open to full rail traffic. Not less interesting when progressing towards very large spans the theoretical and technical developments achieved during the feasibility analyses for other large crossings, such as the Great Belt and the Messina Straits.

The present paper, written in the context of the studies carried out for the second, presents nevertheless a full account of related topics for the entire range in which suspension bridge structures can be of interest for very large crossings.

General deformation aspects of their response are discussed first, proceeding subsequently to the exam of static runnability problems deriving from the elevate slopes which can occur for severe loading. Spans from one to three thousand meters are considered; effects of rail loads, road loads and temperature are shown.

A second part of the paper is devoted to dynamic runnability analyses where, beside the structural behaviour, structure-vehicle interaction and vehicle response are simulated. Indications regarding transit comfort and safety are given: railway loads running in different conditions on the bridge deck are considered, with the simultaneous presence of severe environmental actions, namely earthquakes and wind.

Brief attention is also given to relevant numerical procedures adopted in the different sections.

2. STATIC RESPONSE

The interest in the analysis of suspension bridges deformation aspects goes beyond a pure information on their displacement behaviour: it is known in fact that, in certain conditions, elevate displacements can imply slopes of the rail axis not compatible with operation. Besides, other significant deformation parameters, such as deck ends rotation, are of paramount influence on the train-bridge system dynamic response. A general discussion of the related topics cannot be restricted in the space of the present paper and can be found in [1]. Here a number of synthetic results are reported: fig.s 1 and 2 show the maximum and minimum vertical displacements of a suspension bridge deck versus its centre span length, in the hypotheses of anchoring side spans (no suspended deck in the side spans) and of 1/11 sag/span ratio. The loads considered, which are not intended to be design code conditions for safety or service, but indications for an understanding of the orders of magnitude involved in the behaviour of the structure, are:

- i) uniform 1 t/m load on half centre span
- ii) uniform load on half centre span, with a total of 1500 t (coincident with i) for a 3000 m span
- iii) one heavy train, with 300 m length and 1200 t total weight
- iv) temperature variations of the cable and deck (dependent on cable diameter, with a reference value of 20 °C)

The enormously varying influence of different loads for different spans is evident: over 1500-2000 m the temperature prevails among those considered, as the increase of cable geometric stiffness consequent to the increased axial force in the same decreases the others. As the slopes due to temperature are obviously constant for equal temperature variations, it can hence be stated that progressing towards very large spans railway slopes must become close to an asymptotic value, but for a minor decrease due to the smaller average temperatures of larger diameter cables.

The above conclusion is demonstrated in the graphs of fig.s 3 and 4, showing the maximum railway slopes at the reference and maximum temperatures for different train lengths, sag/span (f/l) ratios and centre span lengths.

+ 300 m length, 1200 t weight train; Δ live load, distribution i);
 \diamond live load, distribution ii); \square temperature

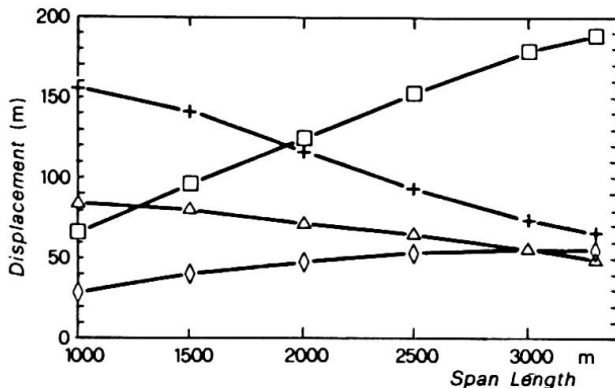


Fig. 1 - Maximum vertical displacements versus centre span length

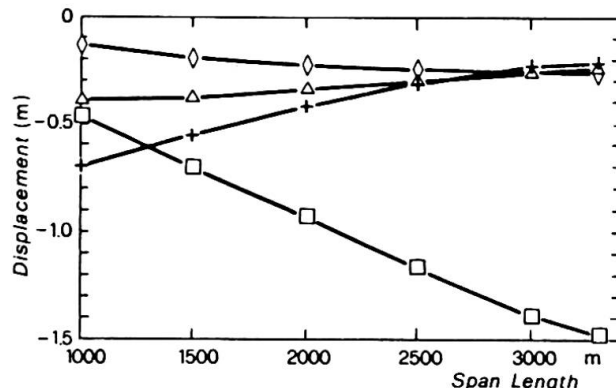


Fig. 2 - Minimum vertical displacements versus centre span length

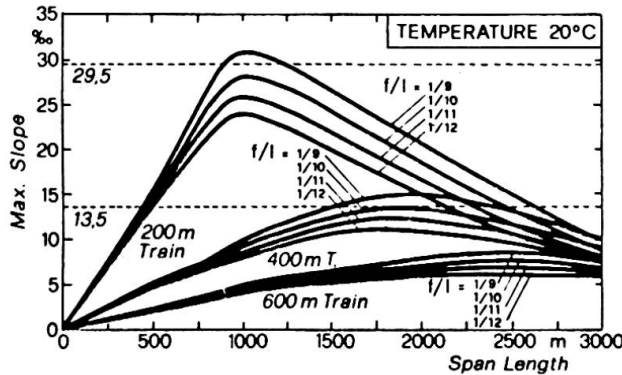


Fig. 3 - Maximum slopes versus centre span length, reference temperature

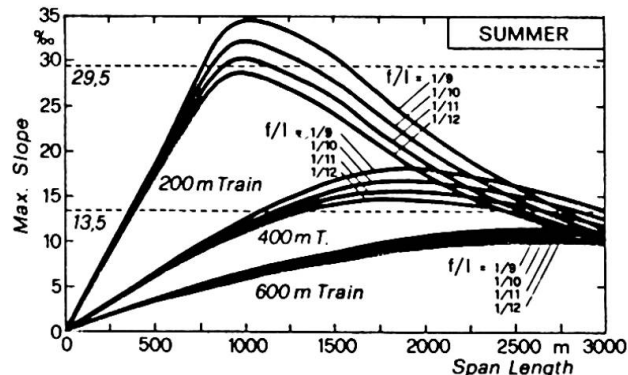


Fig. 4 - Maximum slopes versus centre span length, maximum temperature

The detailed load combinations adopted, which are those assumed for the analysis of service conditions in the Messina Straits crossing project feasibility, are discussed in detail in [1]. Two aspects must be stressed when examining the above results: first, the convergence of all the curves towards a common slope range, which confirms the conclusions drawn before even if the asymptotic values have certainly not been reached; second, and more important, the natural adequateness of the pure suspension scheme to railway needs as far as slopes are concerned for spans over 1500-2000 m, i.e. when temperatures effects become important. The admissible slopes go in fact from 1.3 to 1.5% and an opportune initial deck configuration can provide the necessary correction. It must also be noted that the corrections cannot be too large, as they could cause excessive slopes for minimum temperature conditions.

3. DYNAMIC RESPONSE AND VEHICLE-STRUCTURE INTERACTION

The dynamic response analyses have been restricted to the runnability of the 3300 m one span suspension bridge proposed within the Messina Straits crossing feasibility studied [5], see also [9,10]. The runnability problems derive from the bridge motion caused by wind, traffic and seismic actions: important components of rail generalized deformations are [11]:

- maximum slopes in the vertical plane;
- maximum transverse roll angle, due to deck twisting;
- rail deviation (cusps) in the horizontal plane in correspondence to the bridge-viaduct joint, when the bridge is laterally deflected;



d) minimum curvature radius of the rails in the horizontal plane.

Dynamic phenomena which warrant attention are:

e) possible resonance between the train natural frequencies and the transit frequency associated to the modulus of the deck girder supporting the rails, with subsequent dynamic amplification;

f) high frequency vibrations and noise induced by train transit.

A mathematical model of the train-bridge system, capable of simulating the behaviour of a railcar, was developed [7,8] and tuned through comparisons with the results obtained during a test campaign carried out on an existing steel truss railway bridge in Italy. The research was then extended to the suspension bridge response, obtaining the information summarized in the following.

3.1 The global bridge-train mathematical model

The procedure proposed is based on the separate but simultaneous direct integration in time of the bridge and train equations of motion, accounting for the compatibility conditions of the two systems in terms of displacements at the contact points and for the mutual contact forces. Within a displacement finite element approach to the bridge structure modeling [6,9,10] the associated equations of motion can be set as:

$$\underline{M}_p \ddot{\underline{X}}_p + \underline{R}_p \dot{\underline{X}}_p + \underline{K}_p \underline{X}_p = \underline{F}_{pc} + \underline{F}_{pe} \quad (1)$$

where \underline{M}_p , \underline{R}_p and \underline{K}_p are respectively mass, damping and stiffness matrices, while \underline{F}_{pc} are the external generalized contact forces due to interaction and \underline{F}_{pe} are other environmental actions, such as wind and seismic events.

Each railcar is treated as composed by a set of rigid bodies connected through springs and dashpots to form the 23 d.o.f. system shown in Fig. 5. The corresponding non linear equations of motion are derived, as shown in [7], in the form:

$$\underline{m}_j \ddot{\underline{Z}}_j + \underline{r}_j \dot{\underline{Z}}_j + \underline{k}_j \underline{Z}_j = \underline{F}_{vj} + \underline{F}_{yj} + \underline{F}_{zj} \quad (2)$$

At the left-hand side of eq.s (2) are located the linear inertia, damping and stiffness terms; \underline{F}_{vj} represents the external forces directly applied to the railcar (i.e. wind). \underline{F}_{yj} contains the generalized forces due to track displacements; \underline{F}_{zj} contains non linear terms and the generalized wheel-rail contact forces, dependent on train \underline{Z}_j and bridge \underline{X}_p displacements. Equations (1) and (2) are coupled, as the contact forces \underline{F}_{pc} , \underline{F}_{yj} and \underline{F}_{zj} are function both of \underline{X}_p and \underline{Z}_j variables. The direct time integration of the equations of motion is performed via a modified Newmark algorithm [8], with an iterative implementation whose convergence is controlled by the wheel-rail contact forces balance.

3.2 Simulation of railway-bridge system behaviour

The train transit on the suspension bridge was simulated, see [9,10] for further details, via a computer code based on the theory described. Beside the railway loads, simultaneous presence of wind or earthquake was accounted for.

3.2.1 Wind effects

Transverse turbulent wind acting on the bridge (average speed $U = 32$ m/s, turbulence index $I = 0.17$) was simulated: vertical forces due to the most unfavourable distribution of moving loads for the central span were also considered. A sensitivity investigation for variable forward speed V of the train was carried out, so as to evaluate the safety and comfort coefficients in different conditions. In Fig. 6 the time history of the overturning coefficient of a wheelset for the vehicle entering the bridge at $V = 130$ Km/h (i.e. in correspondence to an expansion joint) is shown: the C_{ovt} coefficient maximum value is well below the safety threshold ($C_{ovt} = 60\%$). The time history of the C_d derailment coefficient, evaluated on the left and right wheel of the same wheelset is shown in Fig. 7: also in this case the C_d coefficients are considerably lower than the limit value ($C_d = 120\%$).

The accelerations of the carbody for the train entering the bridge versus V are

shown in Fig. 8. Fig. 9 shows the shock (time derivative of the acceleration) trend on the carbody, while Fig. 10 shows the overturning and derailment coefficients: for any speed C_{ovt} is lower than 40%, while C_d does not exceed the value of 85%. Resonance effects on the train due to the modularity of the bridge deck structure were found to be negligible. Local effects, even on the wheelsets, proved to be modest. Railway runnability conditions are always acceptable, particularly along the span.

3.2.2 Seismic effects

Earthquake effects on a train, running either on ground or on the bridge at $V = 60$ km/h, have been simulated [9,10]. Seismic conditions are specified by means of acceleration, velocity and displacement time histories: max. ground acceleration of the event considered was 0.64 g. These values are assumed to describe the rail motion on ground: the rail motion on the deck is computed by imposing opportune time histories to one bridge tower foundation and to the relative anchor block. For the train running on ground, Fig.11 reports the time histories of C_{ovt} and C_d . In Fig. 12 the same quantities are shown for the train running over the bridge. It is apparent how earthquake effects are strongly attenuated over the bridge, which behaves like a low-pass mechanical filter.

4. CONCLUSIONS

The following main conclusions can be drawn:

- very large pure suspension bridge schemes become naturally adequate for railway service, due to their elevate geometric stiffness: this stand both for the dynamic and the static response
- as to the specific case of the 3300 m single span bridge proposed within the feasibility studies for the Messina Straits Crossing project, it has been set into evidence as the transit parameters are always favourable during severe wind action, while earthquake effects, which are filtered by the structure, are far more dangerous on ground than on the bridge deck.

5. REFERENCES

- [1] BRANCALEONI F., "Verformungen von Haengebruecken unter Eisenbahnlasten". Der STAHLBAU, N. 48, 33-39, february 1979.
- [2] SHINOARA, ASAMA, "Suspension Bridge for Railway". Proc. In. Symposium on Suspension Bridges, Lisbon, 1966.
- [3] LEONHARDT F., ZELLNER W., "Vergleiche zwischen Haengebruecken und Schraegkabelbruecken fuer Spannweiten ueber 600 m". IVHB Abhand., 32-1, 1972.
- [4] GIMSING N., "Cable Supported Bridges". John Wiley & Sons, 1983.
- [5] BRANCALEONI F., CASTELLANI A., D'ASDIA P., FINZI L., SANPAOLESI L. "Alternative Solutions to Contain the Deck Deformation in a Long Suspension Bridge", Proc. of IABSE Congress "Challenges to Structural Engineering", Helsinki, june 1988.
- [6] DIANA G., FALCO M., GASPERETTO M., CURAMI A., PIZZIGONI B., CHELI F. "Wind Effects on the Dynamic Behaviour of a Suspension Bridge", Report, Dipartimento di Meccanica, Politecnico di Milano, 1986.
- [7] DIANA G., CHELI F., PIZZIGONI B., DI MAJO F., BONADERO A. "A Method to Analyze the Dynamic Behaviour of a Railway Vehicle on a Movable Track", 3rd Seminar "Advanced Vehicle System Dynamics", Amalfi, may 1986.
- [8] DIANA G., CHELI F., "A Method to Define the Dynamic Behaviour of a Train Running on a Deformable Structure", under press, MECCANICA, J. of the Italian Association for Theoretical and Applied Mechanics.
- [9] DI MAJO F., BONADERO A., DIANA G., FALCO M., GASPERETTO M., CURAMI A., PIZZIGONI B., CHELI F., "Railway Runnability of a Single Span Suspension Bridge", Report, Dipartimento di Meccanica, Politecnico di Milano, 1986.
- [10] DIANA G., CHELI F., "Dynamic Interaction of Railway Systems with Large Bridges", VDI BERICHTE N. 635, 1987.
- [11] YASOSHIMA Y., MATSUMOTO Y., NISHIOKA T., "Studies on the Running Stability of Railway Vehicles on Suspension Bridges", J. Fac. of Eng., Tokyo Un., Vol.XXXVI, 1981.

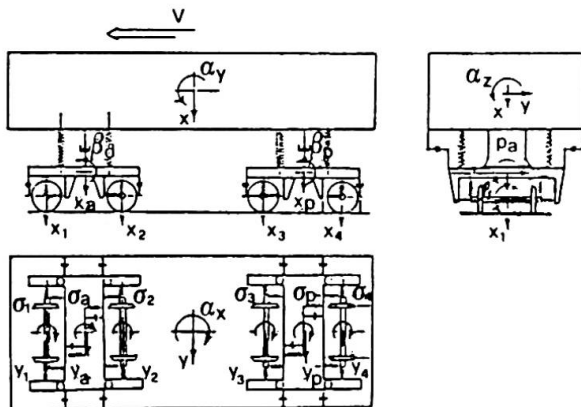


Fig. 5 - Railway car model

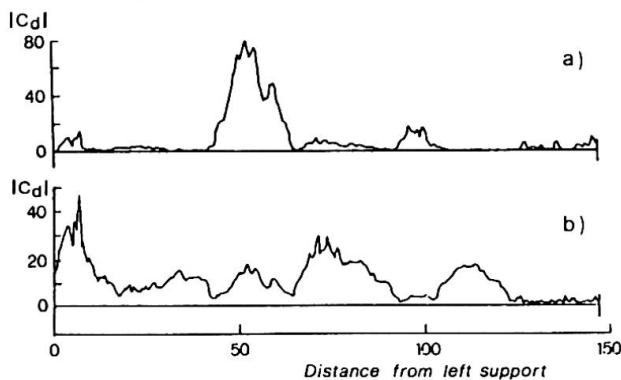
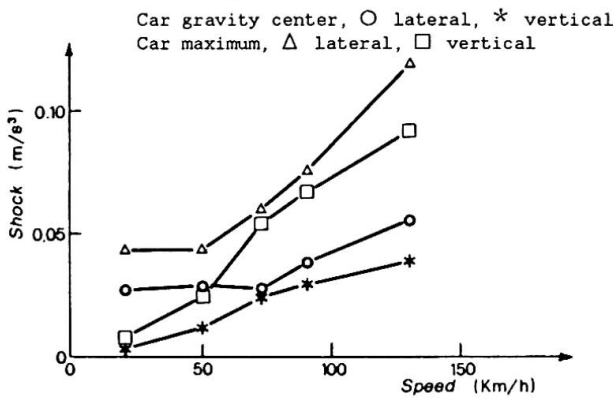
Fig. 7 - C_d , train entering the bridge: a) right wheel b) left wheel

Fig. 9 - Maximum carbody shock

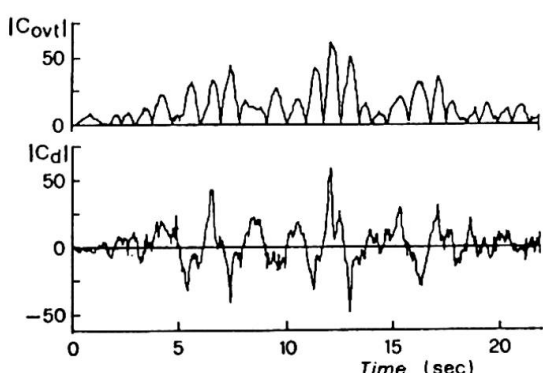
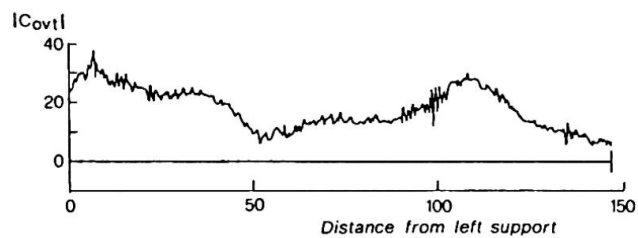
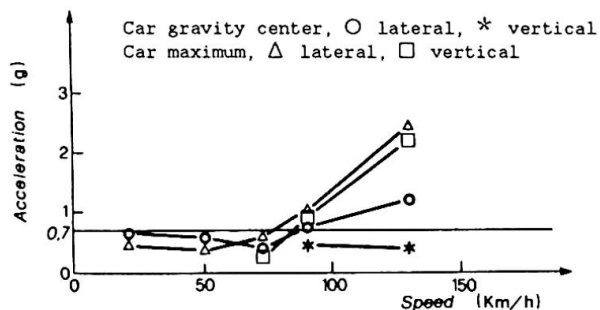
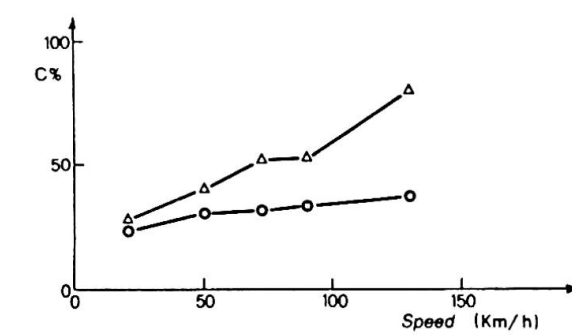
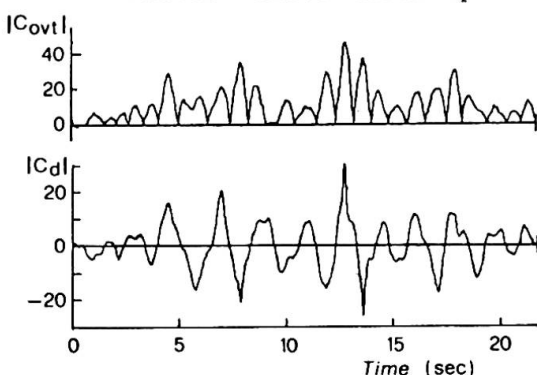
Fig. 11 - C_{overt} , C_d for train running on ground during a seismic eventFig. 6 - C_{overt} coeff. on a wheelset for the train entering the bridge

Fig. 8 - Max. lateral carbody accel.

Fig. 10 - C_{overt} (○) and C_d (Δ) maximum values versus train speedFig. 12 - C_{overt} , C_d for train running on the bridge during a seismic event

Long Span Structures for the Gibraltar Crossing

Structures à grandes portées pour le détroit de Gibraltar

Weitgespannte Tragwerke für die Strasse von Gibraltar

Javier MANTEROLA

Civil Engineer

Carlos Fernandez Casado,
Madrid, Spain

Javier Manterola, born 1936, graduated from the Polytechnic University of Madrid in 1961. His professional work has mainly been in the field of bridges and structural engineering. He was responsible for the design, among others, of the Barrios de Luna cable stayed bridge. He is professor of bridge engineering at the Polytechnic University of Madrid.

Miguel Angel ASTIZ

Civil Engineer

Carlos Fernandez Casado,
Madrid, Spain

Miguel A. Astiz, born 1950, graduated as civil engineer from the Polytechnic University of Madrid in 1973, and as Ph.D. at the same University in 1976. He joined Carlos Fernandez Casado S.A. in 1977. He is professor of mechanics of materials at the Polytechnic University of Madrid.

Klaus OSTENFELD

Project Director

Cowiconsult,
Virum, Denmark

K. H. Ostenfeld, P. E. born 1943, M.Sc. in Civil and Structural Engineering from the Technical University of Copenhagen and registered professional engineer in the U.S., has worked as bridge engineer in the United States and France for many years. With Cowiconsult in Copenhagen, responsible for the design of several long span bridges.

Georg HAAS

Consult. Engineer

Cowiconsult,
Virum, Denmark

G. Haas, born 1922, M.Sc. in Civil and Structural Engineering from the Technical University of Graz, Austria. Since 1953 he has been with Cowiconsult in Copenhagen, responsible for conceptual and detailed design of major suspension and cable stayed steel bridges, and other major steel structures.

SUMMARY

The paper summarizes the main results of an ongoing study regarding the technical feasibility of long span bridge superstructures for the Gibraltar Crossing. Different cable supported multi-span bridge systems and stiffening girder designs relevant for the crossing have been compared technically and economically. This includes evaluation of aerodynamic stability based on section model tests performed in wind tunnel.

RÉSUMÉ

L'article résume les résultats principaux de l'étude en cours relative à la faisabilité technique de superstructures de ponts de longue portée permettant la traversée du détroit de Gibraltar. Plusieurs systèmes de ponts à travées multiples suspendues et plusieurs conceptions de tablier rigide pour la traversée ont été étudiés sur le plan de l'économie et de la technique. Cette étude comprend une évaluation de la stabilité aérodynamique basée sur des essais sur modèle de section en soufflerie.

ZUSAMMENFASSUNG

Der Artikel fasst die Hauptresultate einer noch unbeendeten Studie über die technische Durchführbarkeit von Brücken grosser Spannweiten für die Strasse von Gibraltar zusammen. Verschiedene kabelgetragene Brückensysteme, alternative Formen des Versteifungsträgers sowie ihre aerodynamischen Eigenschaften an Sektionsmodellen im Windtunnel werden untersucht und getestet.



1. INTRODUCTION

The Spanish government agency SECEG, along with its Moroccan counterpart, SNED, was created in 1979 to launch studies with the purpose of establishing a fixed link between Europe and Africa across the Strait of Gibraltar. This agency has entrusted a group of engineering consultants and selected specialists lead by Carlos Fernandez Casado S.A. and Cowiconsult with a feasibility study for a long span bridge superstructure. This paper summarizes the main results of this ongoing study.

2. BRIDGE SITE AND TRAFFIC

The study comprises two options for the traffic conditions at the crossing. Either a 4 lane road bridge or a combined solution with a 4 lane road and a single track railway.

The most realistic bridge alignment is in the western part of the straits at a natural sill with maximum water depth of approx. 300 m. At this alignment the total length of the bridge will be 28 km. A shorter alternative alignment requiring a central bridge pier on a water depth of 450 m has also been considered.

Due to the very important water depths and problems regarding navigation, seismic activity and complex foundation conditions the economic optimum span length for the deep water section of the bridge is in the range of 2000-3000 m. For the shorter alternative alignment extreme spans of approx. 5000 m would be necessary.

3. STATICAL MAIN SYSTEMS

A number of statical main systems relevant for the actual span range considered have been studied and compared technically and economically (fig. 1).

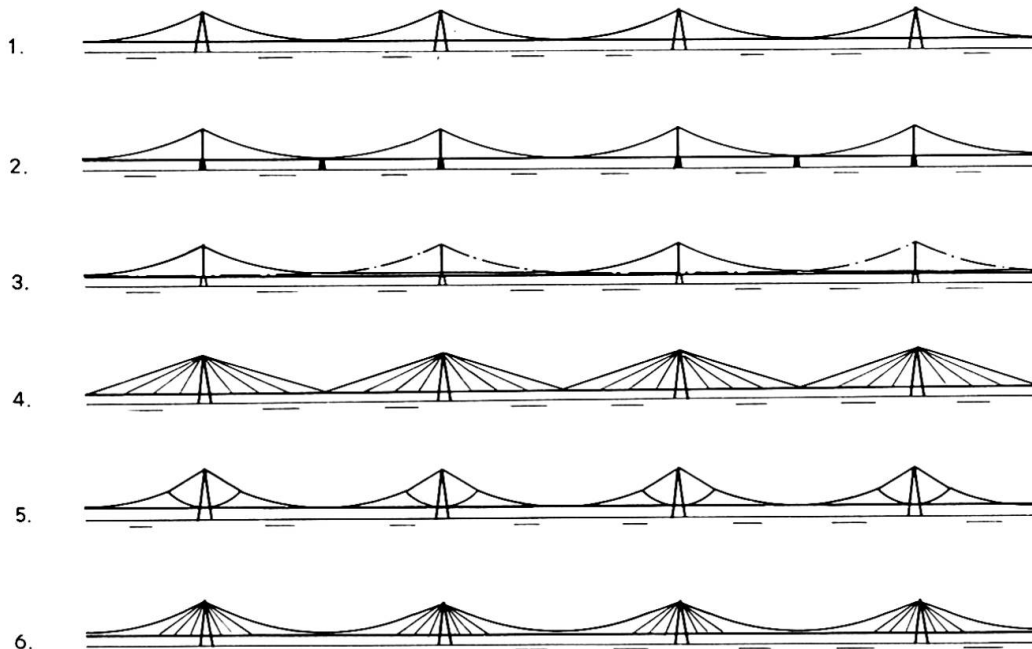


Fig. 1 Statical Main Systems

3.1 Multispan Suspension Bridge System With Rigid Pylons

(system 1)

This system consists of a row of 1-span suspension bridges with expansion joints at the rigid (A shaped) pylons capable of transferring differential unbalanced cable forces with small deformations at the top of pylon. The main cables runs continuously through cable saddles on the pylon tops from anchor block to anchor block, i.e. over a distance of approx. 18 km.

3.2 3-span Suspension Bridges in Series

(system 2)

This solution is composed of a number of classical suspension bridges - one main span and two symmetrical side spans - arranged in a row with common anchorage structures for neighbouring systems. The concept is known from the San Francisco Bay Bridge and latest from the Bisan Seto Bridge in Japan.

3.3 Multispan suspension Bridge System with Complementary Main Cables

(system 3)

Like system no. 2 this solution is based on flexible plane frame pylons. Instead of the intermediate anchor blocks this system is stabilized by means of special double, overlapping main cables. Each cable running continuously over two spans is anchored at the pylon bases. This means that the piers shall be able to transfer unbalanced cable forces as for system no. 1, however, at the considerably lower pylon base level.

3.4 Cable stayed Bridges in Series

(system 4)

This cable stayed bridge system is in principle composed as system no. 1 with expansion joints at the rigid (A-shaped) pylons, which requires that the girder acts as a tension element in the statical main system.

3.5 Multispan Suspension Bridge with Supplementary Stay Cables

(system 5)

Combined system where the girder in the areas near the pylons are carried by stay cables to the extent that the girder can be utilized as a tension element without special strengthening. The remaining part of the girder is carried by the suspension bridge cables. This system acts as a variant of system 1.

3.6 Multispan Suspension Bridge System with Alternative Cable Arrangement

(system 6)

By this special main cable arrangement the bridge span is divided into three load carrying sections by funicular cables. The topoints of the funicular cables (= 'fictitious saddle points') are suspended from high pylons by stay cables. The purpose by this arrangement is to achieve a stiffening of the main cable system by introducing "fixed nodes". Furthermore the length of the hangers near the pylons and thus the additional deflections of the girder due to hanger elongations are reduced.



3.7 Technical/Economical Comparison

The main conclusion of the comparison performed is that solution no. 1 and the related variant no. 5 can be considered as the most adequate. System no. 2 is approx. 10-15% more expensive as the savings for pylons and main piers cannot compensate the additional costs of the intermediate anchorages. Furthermore system no. 2 is more flexible due to the great sidespan - mainspan ratio of 0.5. This can of course be reduced such that system 1 and 2 are at the same level regarding stiffness, but in this case the differential cost will be increased. Accordingly system no. 3 will for comparable stiffness requirements be considerably more expensive than solution no. 1 among others due to the much greater amount of cable steel required. This difference is strongly increasing with the span length but already significant at 2000 m. Furthermore the erection and certain structural details for the interaction between main cables, girder and hangers are considerably more complicated and less clarified than for the two previously mentioned suspension bridge solutions. System no. 4 requires a smaller amount of cable steel than the other solutions. On the other hand a large additional amount of steel for the girder and higher pylons are necessary. Furthermore the girder cross section will be variable adapted to the variation of the great axial forces, which is a drawback for a rational industrial fabrication of girder elements and the erection procedure. System no. 6 implies a complicated joint connection at the 'fictitious saddle points'. The achieved improved stiffness for this system compared to e.g. system no. 1 is evaluated not to justify the problems regarding the detailed design of the joint and the erection work as a suitable stiffening can be obtained by other means at a relatively lower cost.

4. STATICAL MAIN SYSTEM, ALTERNATIVE ALIGNMENT

For the before mentioned shorter alternative bridge alignment the topographical conditions naturally leads to a solution with two main spans of each approx. 5000 m and two side spans of each approx. 2000 m (fig. 2). Thereby the anchorages can be placed on the shores of the strait. In order to achieve a satisfactory stabilization of the system it is necessary to design the centre pylon with an A-shape while the two side pylons can be conventional plane frame structures.

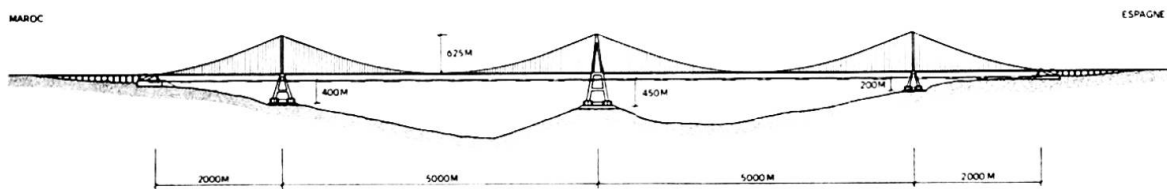


Fig. 2 Statical main system, alternative alignment

5. GIRDER DESIGNS

For bridges with very long free spans an essential aspect is to design the girder and suspension system so that sufficient safety against catastrophic oscillations due to wind induced effects is obtained. Sufficient stability can be achieved by using very heavy and stiff bridge girders, but aiming at reaching a more economical design various lighter girder designs representing different principles for obtaining aerodynamic stability have been investigated (fig. 3).

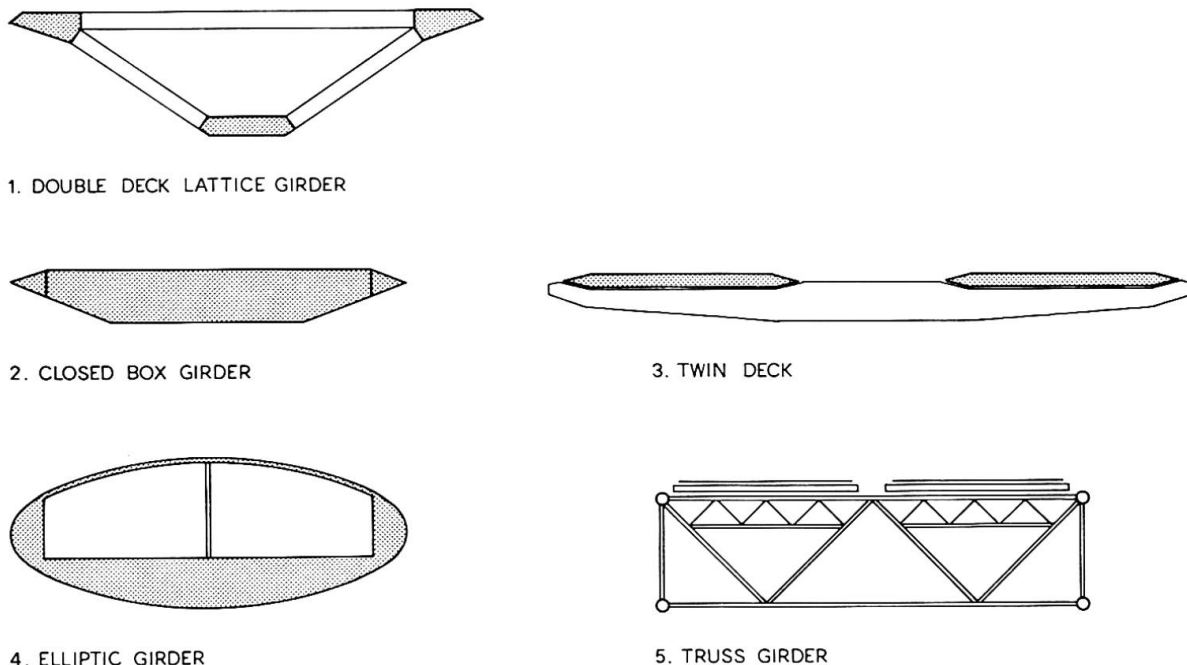


Fig. 3 Girder designs

5.1 Double Deck Lattice Girder

This is a 2-level torsional stiff lattice girder with a single track railway below and the road traffic on the upper orthotropic deck. Furthermore a variant of this cross section with a longitudinal 2 m wide slot in the upper deck allowing the wind to pass freely through the central part of the deck surface has been considered.

5.2 Closed Box Girder

This closed aerodynamically shaped box girder type for a road bridge is well known from a number of existing great suspension bridges in Europe.

5.3 Twin Deck

The twin deck girder principle for a road bridge can, as shown on the figure, be designed with two relatively small box girders interconnected by a horizontal truss system and supported on cross beams at each hanger plane. Other variants of this solution as e.g. direct suspension of the two closed box girders in four main cables as well as alternative designs of the cross beams will be possible.

5.4 Elliptic Cross Section

The elliptic solution is a very interesting alternative among others regarding aerodynamic aspects and, furthermore, it provides a total protection of bridge traffic (an important quality for a 28 km long bridge 80 m above the sea surface).

5.5 Conventional Truss Girder

The truss girder proposed for a road bridge is mainly composed of steel tubes. Alternatively the cross section can be designed as a 2-level solution with the single track railway placed on the lower truss. The principle for this traditionally very stiff girder design is wellknown from USA and the latest great Japanese suspension bridge projects.



5.6 Aerodynamic Stability

Aerodynamic section model test in wind tunnel are planned to be made for girder types 1, 2, 4 and 5 with dynamic properties corresponding to the statical main system no. 1 (see chapter 3) and a free span of 2000 m. Tests have been performed for the double deck and the closed box girder. The main result for both cross sections is that observed critical wind speeds are lower than the required critical design wind speed. However, it has been observed as expected that a longitudinal slot in the upper deck of the double deck cross section tend to increase the critical wind speed. When the test results for the two remaining girder types are available it will be decided whether modified solutions shall be investigated experimentally. A possible improvement could be to make the cross section wider introducing a 5-6 m central longitudinal slot. The two parts of the deck must at the slot be interconnected by a stiff horizontal truss such that the torsional stiffness of the cross section is maintained. The added weight and greater width for this modification will in itself also tend to improve the stability. Another possibility to increase the critical wind speed for classical flutter will be to obtain a greater difference between the system eigenfrequencies for bending and torsion. This can in principle be achieved by an alternative design of the main cable arrangement as illustrated below (fig. 4).

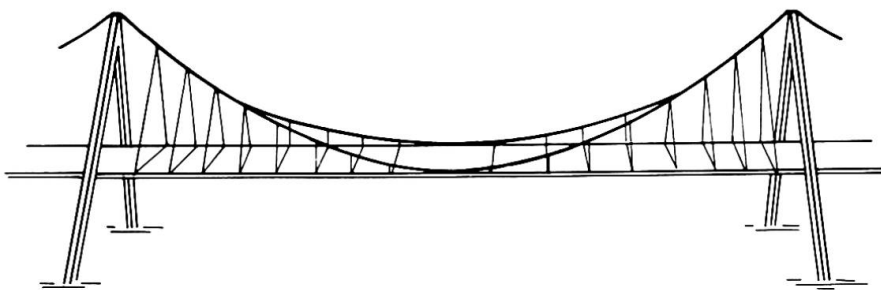


Fig. 4 Alternative main cable arrangement

6. PYLONS

For the actual span range between 2000 and 3000 m the pylons will reach a height of 300 to 400 m above sea level as a free navigation clearance of 70 m is required. Both solutions in concrete and steel have been investigated. Due to relatively great earthquake loads, concrete pylons have been considered less suited as their great weight generates large horizontal seismic forces, which among others makes the pier structures considerably more expensive. A design with big legs without cross beams built up by rings of steel tubes has been proposed for the actual project. Nevertheless other solutions are currently being proposed.

7. ERECTION OF MAIN CABLES

The erection of the main cables is an important aspect in the construction of the bridge types considered. The proposed erection principles are based on fabrication of parallel wire strands on the site at one of the anchorage structures and pulling the individual strands in one continuous operation over the entire bridge length to the opposite anchorage. Both pulling of strands and arrangement of these to form the final cable are known techniques which can be performed with suitable economy and safety. The advantages by this concept is especially that the operations with the cable material are performed close to the shore and that no unbalanced forces from cable erection are introduced on the pylons. The following erection of the stiffening girder can be performed in stages with a distribution of suspended girder elements in the individual spans corresponding to the capacity of the pylons to transfer unbalanced horizontal forces.

Limitation of Deformations of Long Span Suspension Bridges

Limitation des déformations des ponts suspendus de grande portée

Deformationsbegrenzung bei weitgespannten Hängebrücken

Georg HAAS
Consult. Engineer
Cowiconsult,
Virum, Denmark

G. Haas, born 1922, is M.Sc. in Civil and Structural Engineering from the Technical University of Graz, Austria. Since 1953 he has been with Cowiconsult in Copenhagen, responsible for conceptual and detailed design of major suspension and cable stayed steel bridges, and other major steel structures.

Flemming PEDERSEN
Civil Engineer
Cowiconsult,
Virum, Denmark

F. Pedersen, born 1950, M.Sc. in civil and structural Engineering from the Technical University of Copenhagen. Since 1974 he has been with Cowiconsult in Copenhagen, involved in conceptual and detailed design of several long span bridges and major offshore structures.

SUMMARY

The paper concerns arrangements for limitation of deformations for long span suspension bridges. Reference is made among others to the simple establishment of a horizontal fixation of the main cables at mid span through the stiffening girder and to the possibilities for utilization of hydraulic devices, which can easily be adapted to different tasks for stabilization and damping of cable and girder systems.

RÉSUMÉ

L'article traite des mesures à envisager pour la limitation des déformations des ponts suspendus de longue portée. Entre autres il est fait référence à l'établissement simple d'une fixation horizontale des câbles principaux de la travée principale au tablier rigide et aux possibilités d'utiliser des dispositifs hydrauliques, qui peuvent facilement être adaptés aux différents besoins de stabilisation et d'amortissement des systèmes de câbles ou de tablier.

ZUSAMMENFASSUNG

Der Artikel beschreibt Massnahmen zur Deformationsbegrenzung bei weitgespannten Hängebrücken. Es wird u.a. auf die einfache Etablierung einer horizontalen Stabilisierung der Tragkabel im Hauptfach durch den Versteifungsträger hingewiesen, sowie auf die Möglichkeit, hydraulische Anordnungen, welche sich gut verschiedenen Aufgaben anpassen, für Stabilisierung und Dämpfung der Kabel- und Trägersysteme zu verwenden.



1. INTRODUCTION

During recent years the effort to realize fixed connections across wide and deep waterways has been intensified (Honshu-Shikoku, Store Bælt, Messine Strait, Gibraltar etc.) and the projects comprises suspension bridges with free spans between 1500 and 3000 m for both road- and railway traffic. Free spans of 3 to 4 kilometers are considered to be realistic with present day technology and construction practice.

Earth anchored bridges are characterized by the so-called "deflection effect", by which the system is stabilized for increasing permanent loads, and in this respect deviates considerably from other statical bridge systems. For increasing span lengths and permanent loads the deflection effect gives an additional stiffness, which makes suspension bridge systems especially adequate to carry heavy loads including heavy railway traffic. However, long span suspension bridges are - regardless of increased stiffness through increased cable tension - characterized by considerable deflections, which for bridges with heavy railway traffic requires special precautions in order to fulfil the restrictive demands to the rail profile and the deformations.

In connection with feasibility studies for long span suspension bridges for e.g. the Store Bælt and Gibraltar crossings, the possibilities of increasing the structural stiffness globally and locally have been analysed systematically, partly by modifications of cables and girder, by which unacceptable deformations - often due to asymmetric loads - are suppressed systematically.

Essential aspects in the studies were that bending moments in the bridge girder from variable loads are relatively small due to the dominating stiffness of the suspension cables and so the girder consequently has a great unused capacity to carry longitudinal loads; furthermore present day hydraulic systems are very reliable and they can advantageously be used in bridges either as passive or active elements for load carrying or damping purposes.

2. CABLE ARRANGEMENT

The suspension system and the free spans are normally arranged due to topographical and navigational reasons and eventually geotechnical conditions. The main or the navigational span dominates the bridge structure and the position of the free span can normally be varied only within close limits. It is often possible, however, especially for the side spans, to improve the global system stiffness by suitable modifications of the cable system.

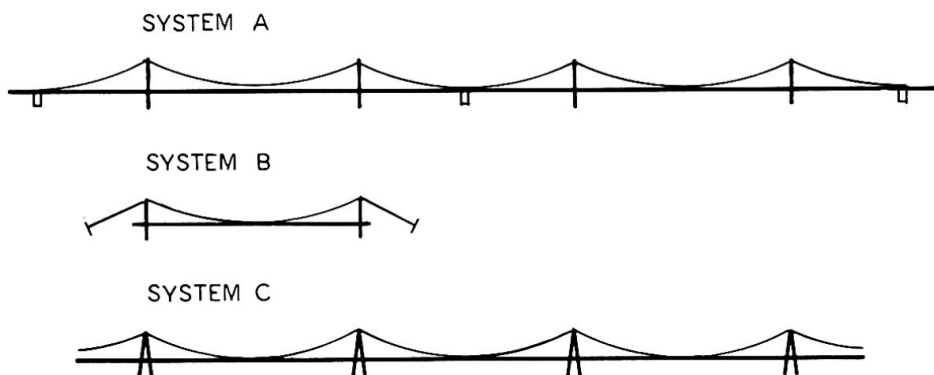


Fig. 1: Suspension Systems.

In conventional three span suspension bridges with flexible pylons, cf. figure 1.A a great deal of the flexibility in the main span is due to cable deformations in the side spans. Shortening of the side spans or the use of straight cables to the anchorages cf. figure 1. System B will imply a significant reduction of the deformations in the main span.

Optimal conditions are achieved in the untraditional single span suspension system, where unbalanced horizontal forces from variable loads are carried by stiff pylons obtained by a triangular configuration in the longitudinal direction. Fig. 1. System C shows a multispan suspension system made of single span systems in mutual balance for permanent loads.

This system will for long distances over deep water and made with very long spans, be attractive in comparison with series of three span bridges - e.g. the Bisan Seto and San Francisco-Oakland bridge - shown in figure 1. System A., because anchorages in deep water are costly and implies increased navigational risks. The multispan system is one of the preferred solutions in the Gibraltar crossing studies presented in another paper at the IABSE Congress in Helsinki 1988 (1).

The required transfer of unbalanced cable forces from traffic at top of pylons means that the ratio between traffic load and dead weight should be low in order to obtain a suitable economic pylon structure. As increased span width decreases the mentioned loading ratio considerable this system will be favourable for very long spans - in particular for rail traffic as the weight and length of a train are constant regardless of the span length.

In figure 2 an example of the total loads on the pylon are given for various spans of a road bridge. The increasing stabilization for increasing span lengths is clear. In addition to the sag ratio of L/8 an extremely low sag ratio of L/12, which implies a large progressively increasing cable weight, is shown.

Pylons of this type requires naturally a very large and robust basis. Consideration of ship collision, current and eventually earthquakes, requiring very massive and resistant substructures, normally coincides with the requirements of the triangular pylon structures.

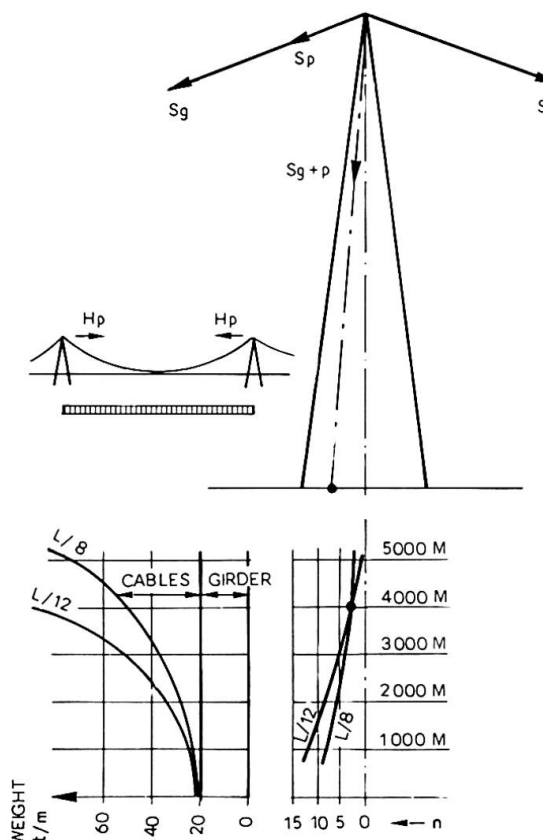


Fig. 2: Resultant forces in pylons for suspension system C and road traffic for cable sag L/8 and L/12.



3. CABLE STABILIZATION

A considerable reduction of the system deformations can be achieved by a fixation of the cables and the girder for relative longitudinal movements at mid-span. The fixation can be established by a clamp locking the cable and the girder centrally, whereby the girder transfers the necessary longitudinal forces for the stabilization to the anchorages or to the rigid pylons as shown in fig. 3 where the force paths are shown for both a three span and a single span suspension system.

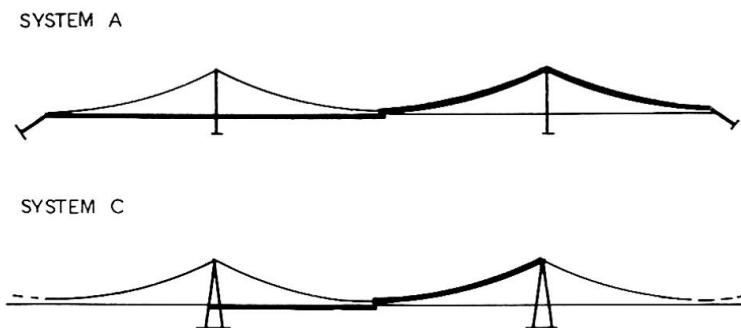


Fig. 3: Stabilization of the cables at midspan by longitudinal fixation.
The force path is shown by a solid line.

The most adequate solution is to utilize only the tensile capacity of the girder, partly because it is larger than the critical compressive load and partly because the tension will tend to have a stabilizing effect on the girder for lateral deflections. The fixation of the girder at the pylons can be made with passive hydraulic cylinders, as assumed above, only capable of transmitting tensile forces. The hydraulic systems allows slow temperature induced movements of the girder while fast movements from traffic and wind are hindered. This alternative statical system arranged to carry traffic loads has no effect for symmetrical loads whereas it is very effective for asymmetric loads, where the effective span width is reduced giving a large reduction of the vertical deflections of the girder near the quarterpoints and close to the pylons and of course also the longitudinal girder movement.

In fig. 4 the effect of the fixation is illustrated for three suspension systems with a free span of 2000 m for roadway and heavy railway traffic. The deformations without and with the girder fixation at the pylons are given. The asymmetric vertical deformations are reduced 20 - 40% and the longitudinal movements are reduced to one quarter of the free longitudinal movements. This reduction is of great importance for the design of the complicated railway expansion joints for large span lengths.

The magnitude of the fixation forces are naturally depending on the intensity of the traffic loads, but will usually correspond reasonably with the tensile capacity of the girder, which is normally available at no cost. The girder forces are reduced by the following:

- the cable fixation is elastic, corresponding to the tensile deformations of the girder and the cable
- the cable stabilization by tensile forces implies that the tensioned part of the girder is in principle free of (or less exposed to) direct traffic loads
- larger traffic loads due to a wider girder etc. are normally balanced by a larger cross sectional area of the girder and consequently a larger tensile capacity
- a central cable fixation allows a larger cable sag and correspondingly the tensile forces in the girder from traffic loads will be reduced.

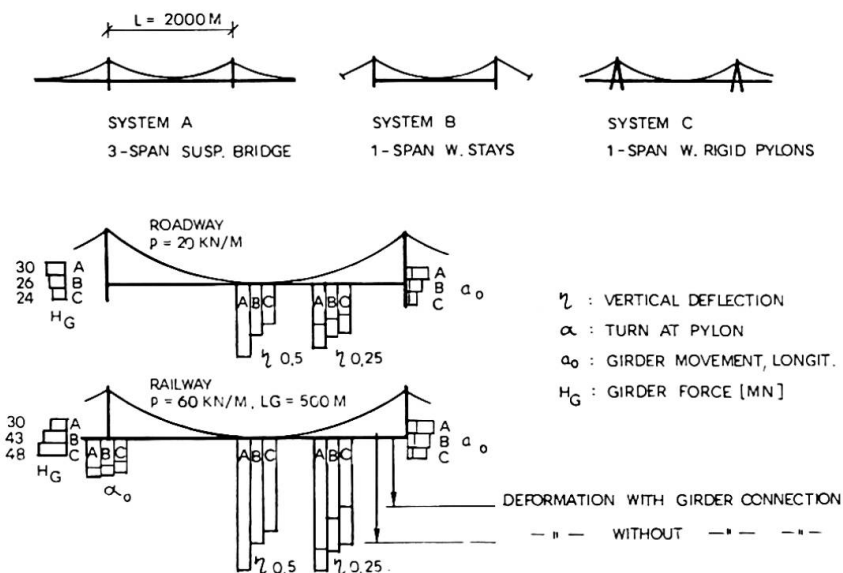


Fig. 4: Effect of cable fixation at midspan by use of the bridge girder.

4. GIRDER CONFIGURATION

The bridge girder itself can also reduce the deformations, although for slender girders the effect is local. This can be achieved either by an active stabilization described in section 5 or by an appropriate girder configuration at the ends of the suspended spans. In figure 5 is shown the transition between the main spans and the approach spans for the Store Bælt project proposals for combined roadway and railway bridges for a suspension and a cable stayed bridge respectively (2). By the extension of the girder beyond the suspended span the requirements of maximum angular discontinuities in the rails have been fulfilled in both the vertical and horizontal direction. Consequently a simplification of the otherwise complicated expansion joints was possible.

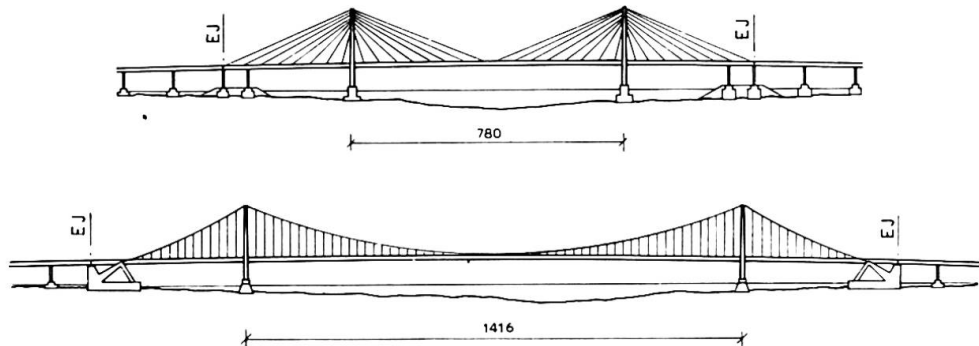


Fig. 5: Girder arrangement and expansion joint position (EJ) for suspension and cable-stayed project proposals for Store Bælt for combined road and railway traffic.

5. GIRDER STABILIZATION

A problematic item for suspension bridges is the structural design of the girder crossing at the pylons: The elastic suspension of the girder in the adjoining spans are terminated by rigid supports at the pylons, which amplifies the angular discontinuity and in addition to girder movements, large vertical and horizontal forces are transferred to the pylons, due to traffic and wind loads.



Some medium suspension bridges are made with continuous girders through three spans, without expansion joints between the anchorages. The continuous girder at the pylons reduces the deformations close to the pylons considerably and thus increases the traffic comfort due to the elimination of the angular discontinuities at expansion joints.

Structural systems with very long spans requires expansion joints at the pylons to accomodate the temperature deformations and in multi span systems e.g. as shown in system C in figure 1, this is the only place to arrange expansion joints. However, by use of hydraulic systems it is possible to arrange support and fixation systems for the bridge girder, which within wide limits can be arranged to fulfil the requirements to continuity and expansion capability. In figure 6 is shown an arrangement for a three span suspension bridge with the following features:

- Expansion joint movements in longitudinal direction without constraints for slow temperature induced movements and fixation for faster movements from traffic loads. Further a damping effect.
- Torsional fixation of the bridge girder, by a hydraulic device, that allows free vertical movements (3). The girder is elastically suspended in hangers made with a suitable low modulus of elasticity.
- The transfer of bending moments is assured by use of pairs of hydraulic cylinders crosswise connected corresponding to the arrangement for the fixation for torsional movements.
- In horizontal direction the girder may be simply supported or as shown partially fixed at the pylon. The transfer of bending moments can alternatively be arranged in the same manner as for the vertical bending moments.

The arrangement can of course be made simpler - according to the needs - by elimination of components and a change of the corresponding functions. The hydraulic systems are all made with passive hydraulics i.e. the forces will only occur as a resistance to movements of the bridge girder. Further some of the hydraulic systems may work actively in connection with special operational situations or generally when the monitoring system has registered exceedance of allowable movements. Finally the hydraulic systems will contribute, actively or passively, to the damping of girder oscillations.

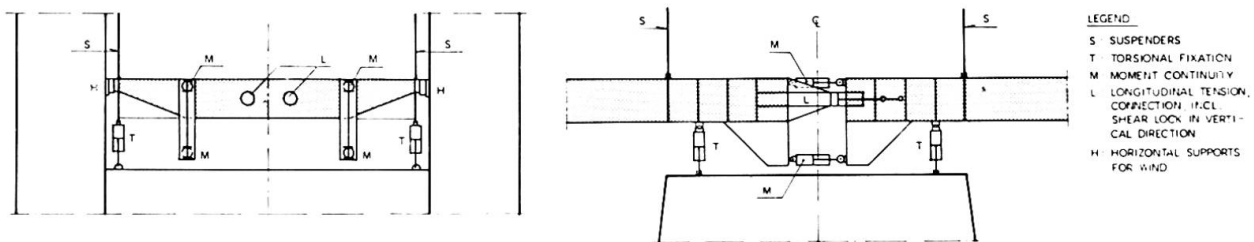


Fig. 6: Hydraulic systems for movement control.

6. REFERENCES

- (1) "Long span Bridge Study for the Gibraltar Strait Crossing". IABSE Congress, Helsinki, 1988.
- (2) "Great Belt Bridge - Tender Projects". 11th IABSE Congress, Vienna, 1980.
- (3) "Torsional Fixation of Girders in Cable Suspended Bridges". 12th IABSE congress, Vancouver, Sept. 3-7th, 1984.

Radical Deck Designs for Ultra-Long Span Suspension Bridges

Nouvelle forme de tabliers pour les ponts suspendus à grandes portée

Brückenträger für Hängebrücken ausserordentlicher Spannweite

Roy RICHARDSON

Consult. Eng.

Kingston-upon-Thames, England

Roy Richardson is an aeronautical engineer with forty years experience in industry, government service and private practice. For more than a decade, he has applied his knowledge of fluid and structural forces to the study of civil engineering structures such as chimney stacks, off-shore platforms and bridges.

SUMMARY

A review of the aerodynamic problems encountered in the design of bridge decks is given, together with solutions adopted in the past and proposed for the future. When the separate problems of aerodynamic stability of the deck and protection of the traffic from high winds are considered together, a new form of deck emerges. The traffic would be completely enclosed in two pear-shaped tubes and the deck would be aerodynamically stable up to the highest wind speeds.

RÉSUMÉ

Un résumé est donné des problèmes aérodynamiques rencontrés dans la forme des tabliers, avec les solutions adoptées autrefois et proposées pour le futur. Lorsque les problèmes de la stabilité du tablier et la protection du trafic vis-à-vis de forts vents sont considérés ensemble, une forme nouvelle des tabliers se présente. Le trafic serait complètement enfermé en deux tuyaux en forme de poire et le tablier serait stable aérodynamiquement lors des vents les plus violents.

ZUSAMMENFASSUNG

Dieser Beitrag gibt eine Uebersicht der aerodynamischen Probleme beim Entwurf von Brückenträgern, mit ausgeführten Lösungen und Vorschlägen für die Zukunft. Aus der Kombination der Windstabilität und des Schutzes des Verkehrs vor starken Winden ergibt sich eine neue Trägerform. Der Verkehr wird in zwei birnenförmige Rohre gelegt und der resultierende Brückenträger bleibt auch bei höchsten Windgeschwindigkeiten stabil.



1. INTRODUCTION

The history of long span bridge design has been a series of quantum leaps, when spans have roughly doubled, followed by long periods of evolution. The last such leap occurred in the early 1930s with the George Washington and Golden Gate bridges. Since then, the longest single span has increased by only 10%

There are natural limits to the unsupported spans of different types of bridge. These limits have been increased in recent years, by the development of stronger and lighter structural materials to support the weight of the traffic. On very long spans however, the static weight-carrying capacity is not the only problem. Wind effects become a crucial feature to be considered in the structural design and the aerodynamic shape of the deck

2. AERODYNAMIC STABILITY AND RESPONSE

There are various types of aerodynamic instability of the deck which must be avoided up to the highest wind speeds. Coupled bending-torsion flutter occurs when the two frequencies coincide. Static divergence is a non-oscillatory instability which occurs when the aerodynamic forces have reduced the torsional frequency to zero. Galloping and stall-flutter are instabilities in pure bending and pure torsion respectively.

Unlike the true instabilities, resonant responses of the deck are rarely destructive, although they can cause discomfort and reduce the fatigue life of the bridge. Such responses occur when the frequency of the vortices shed in the wake of the deck coincides with that of one of the structural modes at low or moderate wind speeds.

Whilst undesirable resonant responses can be suppressed by minor aerodynamic modification or tuned dampers, the avoidance of aerodynamic instability dominates the design of ultra-long spans. Various structural and aerodynamic solution to the stability problem have been either proposed or adopted in the past [1].

2.1 Torsional stiffness

Raising the torsional frequency of the deck, by using either a truss or a fully enclosed torsion box, has been standard practice on long spans for many years. Its purpose is to separate the bending and torsion frequencies sufficiently to ensure that coupled flutter cannot occur up to the highest wind speeds. On potentially unstable deck sections, it also raises the critical stall-flutter speed.

Nevertheless, the additional structural weight of the deck increases the dead-load on the cables, so that purely structural solutions become uneconomic on ultra-long spans.

2.2 Perforated decks

Small slots between the carriageways of conventional truss decks have been used to increase the aerodynamic stability for many years. The reason for this phenomenon was not understood until research was undertaken for the first truly perforated deck (with multiple slots) proposed for the crossing of the Messina Straits.

The slots have two effects. They reduce the destabilising aerodynamic pitching moment in inclined winds and increase the aerodynamic damping in the torsion mode. The first of these effects ensures that the torsional frequency remains reasonably constant up to much higher wind speeds so that it does not coincide with that of bending. The damping effect delays the onset of coupled flutter and eliminates the possibility of stall-flutter.

2.3 Twin decks

The author's twin-deck proposal (Fig.1) used both aerodynamic and structural inertial forces to ensure aerodynamic stability. A large open gap between two rigidly connected carriageways provides the aerodynamic advantages of a deck with multiple perforations to an even greater degree. In addition, the moment of inertia of the combined decks reduces the torsional frequency (but not the torsional stiffness) to a value below that of bending. Thus coupled bending-torsion flutter cannot occur and the only aerodynamic instability is static divergence. Since the torsional stiffness is provided by the widely spaced cables, no torsion box is needed, although the stiff transverse beams increase the dead-load to some extent.

3. PROTECTION OF TRAFFIC FROM WINDS

There has been increasing interest shown by bridge owners in the problem of protecting the traffic from adverse weather conditions, so that the bridge can remain open at all times. Unfortunately some of the proposed solutions create aerodynamic problems for the bridge structure itself.

3.1 Wind barriers

Slatted fences, erected at the deck extremities, can be designed to give considerable protection to the traffic in high winds. However, such barriers can reduce the aerodynamic damping in the torsion mode and cause stall-flutter.

3.2. Enclosed decks

A partially-enclosed deck was proposed for the Tsing-Ma crossing in Hong Kong to protect emergency vehicles from typhoon winds. Large gaps in its upper and lower surfaces however, ensured that it remained aerodynamically stable.

The deck of the Eurobridge proposal for the Channel Link was totally enclosed in a very deep oval tube, completely protecting the traffic from wind, rain and snow. The high torsional stiffness and the aerodynamic shape of the deck eliminated any likelihood of torsional oscillations. Nevertheless the aerodynamic drag would have been high, and both galloping instability and resonant vortex-shedding responses would have presented potentially serious problems for the bending modes.

In an unpublished proposal, the author suggested that a truly elliptic tubular deck, approximately 30% thick, would fulfil the requirements for an enclosed deck (Fig.2). It would completely protect the traffic and have both low aerodynamic drag and high torsional stiffness. Wind tunnel experiments on a section model of such a deck have largely confirmed the predictions. No reference to the report is given in this paper, since the details of the results are confidential to the companies who sponsored the test program.

4. THE DOUBLE PEAR-SHAPED DECK

When the concepts of the twin bridge and the enclosed elliptic deck are merged a totally new form of bridge deck results (Fig.3). Two separate pear-shaped tubes carry the road traffic internally. They are cantilevered on each side of a large central gap by deep transverse beams at intervals along the span. If required, open railway tracks may be carried within the transverse beams, partially protected from the wind by the road traffic tubes.

4.1 Aerodynamic stability

In winds from either direction, the windward deck has a large radius of curvature at its trailing edge and thus generates little aerodynamic lift. In



contrast, the leeward deck behaves like a thick aerofoil section with a moderately sharp trailing edge. These facts can be used to tailor the combined "tandem biplane" section to give little or no midchord pitching moment in inclined winds. The torsional frequency would thus remain sensibly constant up to the highest wind speeds, so that neither coupled flutter nor static divergence could occur.

4.2 Traffic lanes

High-sided commercial vehicles would be carried in the deepest sections of the decks nearest to the centre. Lighter traffic would travel on raised carriageways inside the shallower deck extremities. Further separation of the two types of road traffic would be provided by locating the emergency lanes between them.

4.3 Structure

High torsional stiffness would no longer be needed to prevent wind-induced instabilities. Nevertheless, asymmetric traffic patterns on opposite carriageways could produce unacceptable rotations of the deck unless some torsional stiffness is provided. Such rotations would, however, be minimised by the proximity of the heavy road vehicles and the rail traffic to the centre of the deck. A single central tower, between the two carriageways at each pier, would then support the suspension cables. Any additional torsional stiffness needed could then be provided by a box or truss surrounding each of the deep traffic tubes.

5. ACKNOWLEDGEMENT

The ideas for new bridge decks, proposed by the author in this paper, have been developed whilst acting as a consultant to British Maritime Technology Ltd.

REFERENCES

1. RICHARDSON J. R. The Influence of Aerodynamic Stability on the Design of Bridges. 12th Congress of IABSE, Vancouver BC, September, 1984.



Fig.1 Twin deck

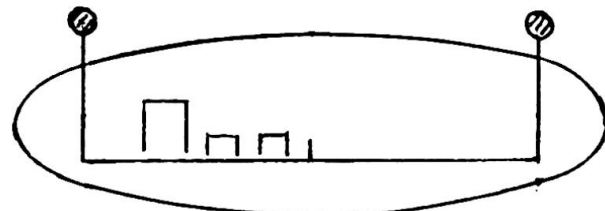


Fig.2 Elliptic deck

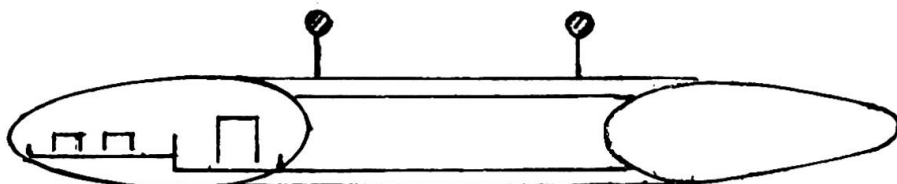


Fig.3 Double pear-shaped deck

Behaviour of Long Span Suspension Bridge Construction

Comportement des ponts suspendus de grande portée lors de la construction

Verhalten weitgespannter Hängebrücken während des Baues

Fabio BRANCALEONI

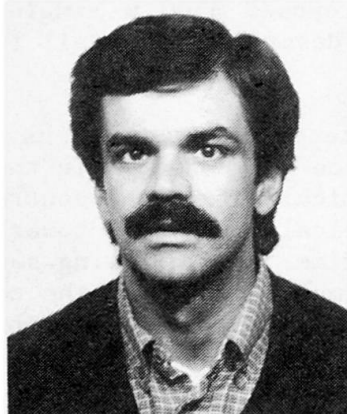
Assoc. Prof.
University "La Sapienza"
Rome, Italy



Fabio Brancaleoni, born 1949, received his civil engineering degree at the University of Rome, where he also had his academic career, but for a year spent at UMIST in UK. Fabio Brancaleoni authored numerous papers in the fields of Structural Mechanics and Dynamics, with several applications devoted to suspension bridges.

Federico CHELI

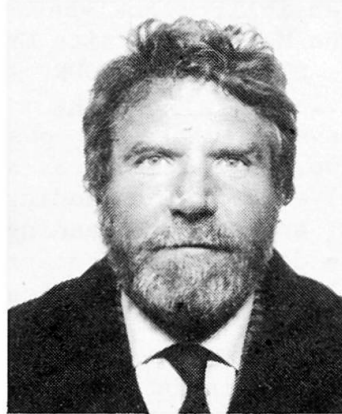
Researcher
Politecnico di Milano
Milan, Italy



Federico Cheli, born 1956, received his Mechanical Engineering Degree at the Politecnico di Milano in 1981, where he is presently researcher at the Dipartimento di Meccanica. His work is concerned with Structural Vibrations, Rotor-Dynamics and Railway Vehicle Dynamics.

Giorgio DIANA

Professor
Politecnico di Milano
Milan, Italy



Giorgio Diana, born 1936, received his Mechanical Engineering Degree at Politecnico di Milano in 1961 and became Professor of Applied Mechanics in 1971. He now holds the course "Vibration of Machines" at Politecnico di Milano. Giorgio Diana authored many papers in the fields of Fluidoelasticity, Rotor-Dynamics and Vibration Problems in Mechanical Engineering.

SUMMARY

Suspension bridge elements can undergo during construction displacements and stresses comparable with those experienced in the service stages, as a consequence both of erection procedures and of environmental effects. The case study of a single span bridge for the crossing of the Messina Straits is presented. Erection simulations are shown for different possible sequences, discussing the structural behaviour, with special attention to aerodynamic stability.

RÉSUMÉ

Pendant la construction, les éléments des ponts suspendus peuvent être sujets à des déplacements et contraintes comparables à ceux rencontrés pendant l'exploitation, soit à cause des procédures de construction, soit des actions locales. On présente ici le cas d'un pont à une travée sur le Détrroit de Messine. On montre les simulations de construction dans différentes séquences possibles, en analysant le comportement de la structure, en particulier la stabilité aérodynamique.

ZUSAMMENFASSUNG

Während des Baues können die Elemente der Hängebrücken Verformungen und Belastungen erfahren, ähnlich denjenigen im Gebrauchszustand, dieser Beitrag behandelt die Hängebrücke für die Meerenge von Messina, und die Bauvorgänge für verschiedene mögliche Folgen, mit speziellem Gewicht auf dem strukturellen Verhalten und der aerodynamischen Stabilität.



1. INTRODUCTION

Different structural safety aspects arise during suspension bridges erection stages, both due to construction procedures and to environmental actions. Attention is focused on the deck erection phase, during which the suspension cables and hence the deck undergo considerable displacements, often comparable or greater than those experienced in service, with the associated stresses in the girders. Hangers slackening phenomena can occur, with consequent overstresses in both deck and hangers in the zones involved. Furthermore, it is known that the danger of classic flutter type aerodynamic instability is considerably increased, due to the closeness of the flexural and torsional mode periods, as put into evidence by the damages suffered for the second Firth of Forth Bridge and by the attention given to prevention measures for the Humber Bridge [10,12,13]. A synthesis of the researches carried out on this topic within the feasibility analyses for a proposed 3300 m single span suspension bridge for the Messina Straits Crossing, described in detail in [7], is herein reported.

2. STATIC BEHAVIOUR

2.1 General remarks

Several different possible erection sequences have been analyzed: the first two, to be viewed as a reference and standard in the field, are:

- a) erection proceeding symmetrically from the centre span,
- b) erection proceeding symmetrically from the towers

To decrease the construction time, the following sequence was also studied:

- c) erection symmetrical and simultaneous from the towers and the centre span
- A final alternative considered arised by the possible use of a single high performance crane vessel in place of a number of traditional devices. Such cranes have a large lifting capacity but a low motion speed and must hence be used continuously on a same advancement front. This produced the need to analyze a number of unsymmetrical sequences, among which the following is presented:

- d) erection proceeding asymmetrically from the centre span, but for two 200 m segments at the towers erected independently from the shore approach. Maximum asymmetry considered was 600 m.

2.2 Modeling and analysis procedure

The numerical model adopted is based on a non linear elastic finite element discretization, with the use of non linear beam, straight cable and curved cable elements. Effects of large displacements and of the addition of structural parts in sequence are taken into account via a modified iterative direct stiffness Newton-Raphson approach in which, once the solution of a set of non linear equations corresponding to a given stage is reached, a separately defined substructure is added through a node connection definition and the solution procedure restarted. The new substructure can be initially prestressed and can be connected to the existing part in any geometric position.

2.3 Displacements and stress response

Exemplificative cables and deck shapes are reported in fig. 1, with respect to the reference state at construction completion. A synthesis of the displacements response is given in fig. 3, where the centre span vertical displacement evolution during construction is shown for the four sequences.

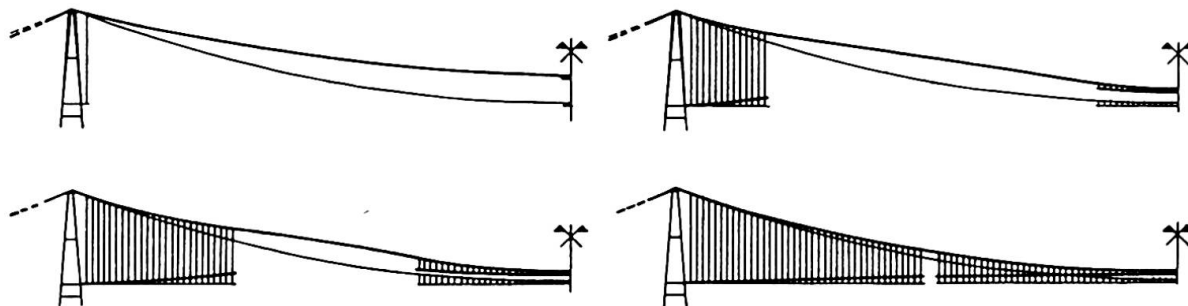


Fig. 1 - Displacements of cables and deck in different erection stages

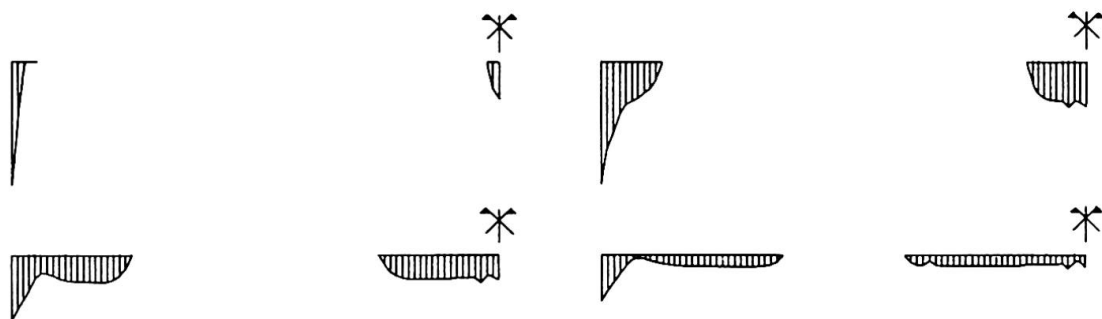


Fig. 2 - Deck bending moment distributions in different erection stages

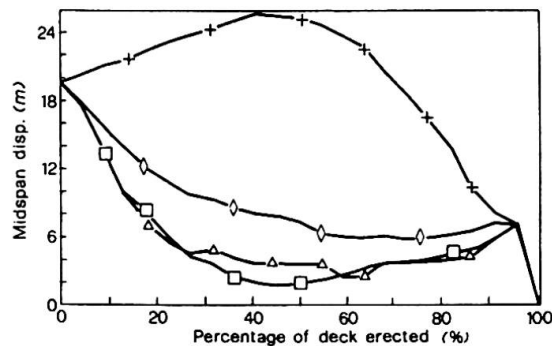


Fig. 3 - Midspan displ. evolution,
□ sequence a), + sequence b),
◊ sequence c), △ sequence d)

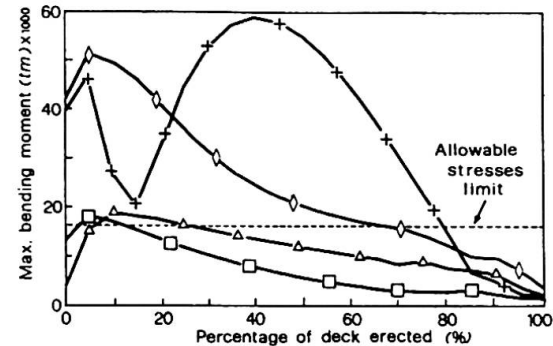


Fig. 4 - Max. deck bending moment
□ sequence a), + sequence b),
◊ sequence c), △ sequence d)

As to generalized stresses, fig. 2 shows four sample bending moments distributions, while fig. 4 reports the evolution of the maximum bending moment in deck, in the hypothesis of complete connection during construction. Cusps in graphs correspond to changes in the zones in which the moment occurs. As it can be seen, all the sequences present, in different measure, parts in which the limit allowable stress minimum moment is transpassed, indicating the need for a more flexible partial connection even on such a large span.

3. AERODYNAMIC STABILITY

3.1 General remarks

This field has received a wide attention in the last twenty years: fig. 5 summarizes the literature results available for different bridges of span from 700 to 1410 m, showing the relative evolution of the critical instability windspeed versus percentage of deck erected [10,12,13,14].

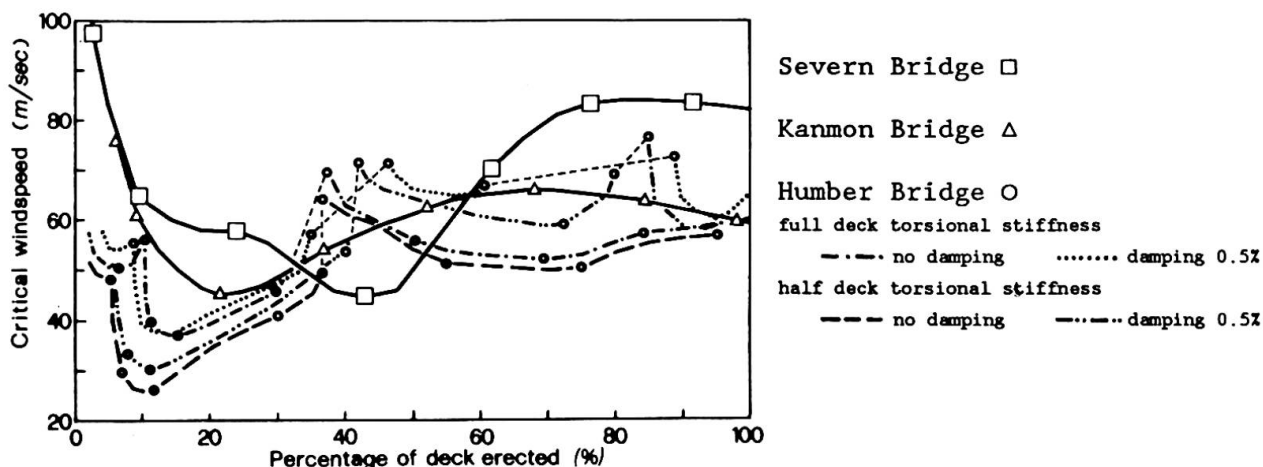


Fig. 5 - Critical windspeed versus percentage of deck erected



The minimum critical speed is typically associated to the early erection stages, in which the deck geometric stiffness contribution and translational-rotational inertial properties are negligible with respect to those of the suspension cables and hence the natural frequencies of modes subjected to possible coupling in the dynamic instability are closer than at structure completion. The subsequent evolution of structural dynamic properties causes a frequency spacing and a mode shapes modification; the former aspect implies higher critical speeds, the second changes in the mode coupling. Consequently different modes are involved in the instability, which becomes even impossible in certain stages [1,2,3,4,10]. To be noted that for the Humber Bridge, whose critical speed reached a minimum around 25 m/sec, measures were taken to prevent instability during erection [10,12]. In the following the problem is analyzed for the proposed bridge, with reference to construction sequence c).

3.2 Arrangement of the proposed deck

The proposed deck, fig. 6, was conceived to be aerodynamically neutral and "transparent". This target was obtained through a careful study of the air flow around and through the deck: highway and railway box girders A are spaced with grids B, so decreasing the pressure difference between the upper and the lower part and hence the aerodynamic lift. The longitudinal external girders C are for feasibility purposes wing-shaped, with inclination determined by wind tunnel tests, so as to act as stabilizers. To make the bridge aerodynamic behaviour independent of the road traffic presence, a lateral aerodynamically transparent curved grid protection D was adopted.

3.3 Procedures adopted for instability windspeed determination

The bridge structured was modeled via a spatial finite element approach [5,6,7]. The corresponding discrete non linear equations of motion are:

$$\underline{\underline{M}}_p \underline{\underline{X}}_p + \underline{\underline{R}}_p \underline{\underline{X}}_p + \underline{\underline{K}}_p \underline{\underline{X}}_p = \underline{\underline{F}}_{aer}(U(t,s), \underline{\underline{X}}_p, \dot{\underline{\underline{X}}}_p, \ddot{\underline{\underline{X}}}_p) \quad (1)$$

with $\underline{\underline{M}}_p$, $\underline{\underline{R}}_p$, $\underline{\underline{K}}_p$ mass, damping and stiffness matrices; $\underline{\underline{F}}_{aer}$ are the external generalized wind forces, defined according to the steady state theory [1,3,4,9]. The force components per unit length are given as, see fig. 7:

$$\begin{aligned} F_y &= 1/2 \rho V^2 B (C_d(\alpha) \cos\psi + C_l(\alpha) \sin\psi) \\ F_x &= 1/2 \rho V^2 B (C_d(\alpha) \cos\psi - C_l(\alpha) \sin\psi) \\ M_r &= 1/2 \rho V^2 B^2 C_m(\alpha) \end{aligned} \quad (2)$$

$$\text{with } \tan\psi = x/V + \theta b_1/V, \quad \alpha = \theta - \psi \quad (3)$$

The aerodynamic coefficients are determined through static experimental wind tunnel tests on deck sectional models, while b_1 is determined through oscillatory tests, also in wind tunnel. Once defined a wind space-time history $U(s,t)$, the bridge response could be obtained via direct integration in time of eq.s (1) [6,8,10,11], but this procedure is too time-consuming for a systematic research. If a constant windspeed $U=\bar{U}$ is assumed and eq.s (1) are linearized in the neighborhood of the static equilibrium configuration [8], they become:

$$(\underline{\underline{M}}_p + \underline{\underline{M}}_a) \underline{\underline{X}}_p + (\underline{\underline{R}}_p + \underline{\underline{R}}_a) \underline{\underline{X}}_p + (\underline{\underline{K}}_p + \underline{\underline{K}}_a) \underline{\underline{X}}_p = 0 \quad (4)$$

where $\underline{\underline{M}}_a$, $\underline{\underline{R}}_a$, $\underline{\underline{K}}_a$ account for the linearized terms of the aerodynamic forces. The instability type and critical speed can then be evaluated analyzing the real part of the eigenvalues of eq.s (4), for variable U . Numerical problems make preferable the use of eigenvalues-vectors calculated for the structure alone, i.e. without the said aerodynamic terms, see [6]. A third alternative considered is the so called forced method [4]: fig. 8 shows a comparison between results obtained by the different approaches: the instability threshold is determined with good agreement, while the total (structural + aerodynamic) damping factor evolution presents considerable differences, see [6] for a discussion of the problem.

3.4 Validation of the theory with a two d.o.f. sectional model

A preliminary investigation was devoted to a validation of the theoretical results via experimental tests on a sectional model. The deck, in the configuration described, is extremely stable: the flutter speed of the physical model was higher than the maximum obtainable in the wind tunnel (60 m/sec). To allow comparisons the critical speed was reduced closing the central grids, obtaining the aerodynamic drag, lift and moment coefficients (C_d , C_l , C_m) versus deck rotation shown in fig. 9, while those of the deck with open grids are reported in fig. 10. In the tunnel tests the experimental critical speed of the model with closed grids was 38 m/sec, while the analytical threshold was calculated as 36 m/sec.

3.5 Synthesis of results for the full bridge

Proceeding to the behaviour of the full bridge, fig. 11a shows the first symmetric and antisymmetric flexural and torsional natural modes of the bridge with 30% of the deck erected, while fig. 11b shows the same modes when the deck is erected at 80%. In fig. 12 the variations of the first natural flexural and torsional frequencies as a function of the percentage of the erected deck are reported. The minimum ratio between the periods of the analogous flexural and torsional modes are 1.32 for the antisymmetric modes and 1.23 for the symmetric one when the deck is entirely assembled; the same ratios reduce to 1.06 and 1.16 when the deck is erected at 20%. Fig. 13 shows the trend of the critical speed versus the percentage of deck erected. The curve has, of course, a vertical asymptote at 0%; a first minimum takes place at 40%: for this erection stage the flexural and torsional coupled have shapes characterized by an antinode at midspan; a second minimum is found at 65%: in this zone the flexural and torsional modes coupled are characterized by a node at midspan. In the intermediate zones, where the mode shape correspondence is lower, the critical speed is higher, but the variations are generally lower than those discussed for smaller bridges, despite of the frequencies closeness, due to the lesser influence of the deck inertial properties with respect to those of the suspension cables. The critical speed at deck completion was found to be 130 m/sec.

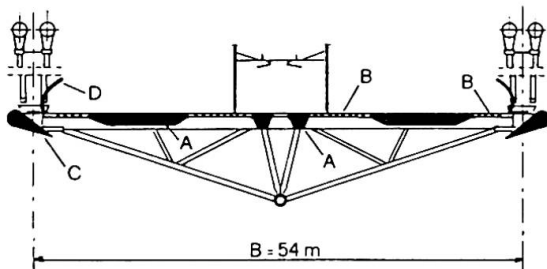


Fig. 6 - Deck cross section

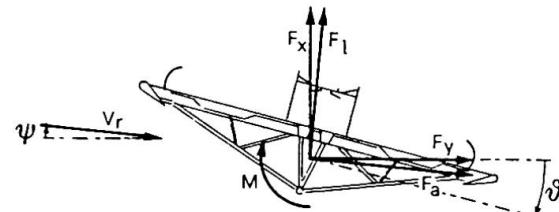


Fig. 7 - Aerodynamic forces

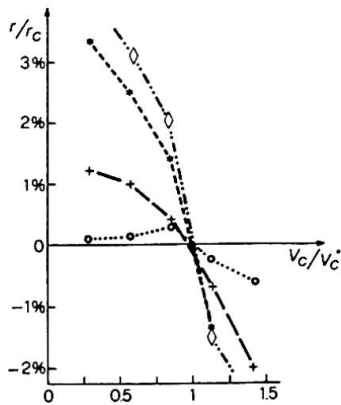


Fig. 8 - Critical speed analysis, different methods

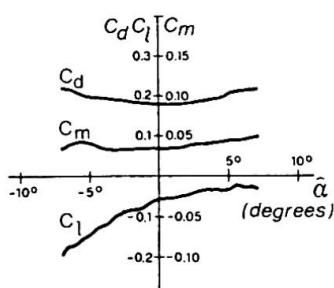


Fig. 9 - Aerodynamic coeff. with open grids

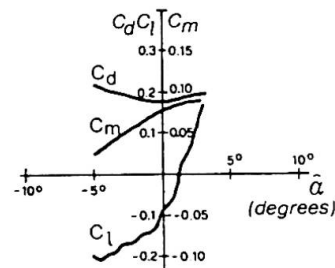


Fig. 10 - Aerodynamic coeff. with closed grid

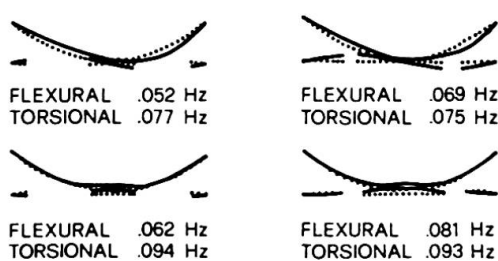


Fig. 11 - Mode shapes for deck erected at a) 30%, b) 80%

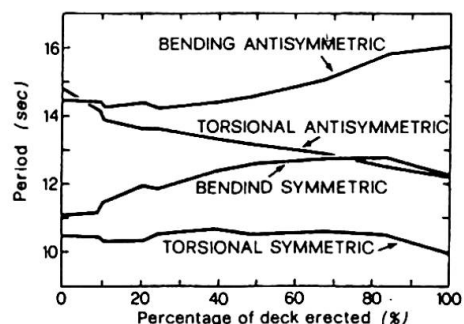


Fig. 12 - Natural frequencies evolution during the erection

4. CONCLUSION

Several aspects connected to suspension bridge structural behaviour in erection have been discussed. Considerable importance has been shown to have dynamic instability phenomena due to wind action, for the prevention of which it is believed to have a paramount influence a sound aerodynamic design of the bridge deck.

5. REFERENCES

- [1] DAVENPORT A.G., The Action of the Wind on Suspension Bridges, Proc. of In. Symp. on Suspension Bridges. Lab. Nac. de Engenh. Civil, Lisboa 1966.
- [2] DAVENPORT A.G., The Experimental Determination of the Response of Bridges to Natural Wind. Proc. of II Usa-Japan Research Seminar on Wind effects on Structures, Univ. of Tokyo, 1976.
- [3] IRWIN H.P., Wind Tunnel and Analytical Investigations of the Response of Lion's Gate Bridge to a Turbulent Wind. N.R.C., Canada, LTR-LA 210, 1977.
- [4] DIANA G., FALCO M., GASPERETTO M., On the Flutter Instability of a Suspension Bridge Using the Finite Element Method. paper n.77-DET-140, Proc. A.S.M.E. Conf., Chicago, 1977.
- [5] CURAMI A., FALCO M., The Dynamic Behaviour of a Large Suspension Bridge - Part II: Dynamic Response to Turbulent Wind. Costr. Metalliche n.2, 1982.
- [6] DIANA G., FALCO M., GASPERETTO M., CURAMI A., PIZZIGONI B., CHELI F., Wind Effects on the Dynamic Behaviour of a Suspension Bridge. Report, Dipartimento di Meccanica, Politecnico di Milano, 1986.
- [7] BRANCALEONI F., CASTELLANI A., D'ASDIA P., FINZI L., SANPAOLESI L., Alternative Solutions to Control the Deck Deformability in a Long Span Suspension Bridge. Proc. IABSE Congress, Helsinki, 1988.
- [8] DIANA G., MASSA E., PIZZIGONI B., A Forced Vibration Method to Calculate the Oil Film Instability Threshold of Rotor-Foundation Systems. IFTOMM Int. Conf. on "Rotordynamics Problems in Power Plants", Rome, 1982.
- [9] SCALAN R.H., TOMKO J.J., Air Foil and Bridge Deck Flutter Derivatives. ASCE J. of Eng. Mech. Div., V. 97, 1971.
- [10] BRANCALEONI F., BROTTON D.M., Analysis and Prevention of Suspension Bridge Flutter in Construction. Earth. Eng. Struct. Dyn., 9, 489-500, 1981.
- [11] BRANCALEONI F., BROTTON D.M., The Rôle of Time Integration in Suspension Bridge Dynamics. Int. J. Num. Methods in Eng., Vol. 20, 715-732, 1984.
- [12] NMI Reports on the Aerodynamic Stability of the Humber Bridge in Erection Conditions, NMI 89/0353 and NMI 89/0361, 1977.
- [13] YAMAGUCHI T. et al., Aerodynamic Stability of Suspension Bridges under Erection. Proc. Conf. Wind Effects on Build. and Struct., Tokyo, 1971.
- [14] WALSHE D.E., A Resume of the Aerodynamic Investigations for the Fort Road and the Severn Bridges. J. English Inst. Civil Eng., 7001, 87-108, 1965.

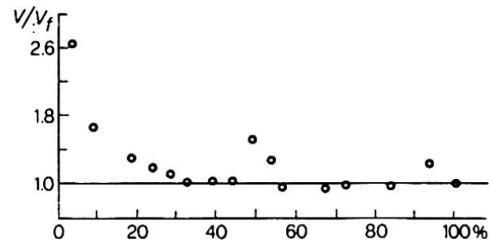


Fig. 13 - Trend of critical speed evolution during the erection

Considerations for Wind Effects on a 1,990 m – main span Suspension Bridge

Effet du vent sur la portée principale (1990 m) d'un pont suspendu

Windeinflüsse bei einer Hängebrücke von 1990 m Spannweite

Masamitsu OHASHI

Director,
Honshu-Shikoku Bridge Auth.
Tokyo, Japan

Isao OKAUCHI

Professor,
Chuo University
Tokyo, Japan

Nobuyuki NARITA

Vice Director General,
Ministry of Construction;
Tsukuba, Japan

Toshio MIYATA

Professor,
Yokohama Nat. Univ.
Yokohama, Japan

Naruhito SHIRAISHI

Professor,
Kyoto University
Kyoto, Japan

SUMMARY

The paper presents some design considerations for wind effects on a very long span suspension bridge, the Akashi Kaikyo (Straits) Bridge, with a total length of 3,910 m. Included here are primarily the studies of comparison of various deck configurations such as truss and box stiffening constructions and their variations to combat the flutter instability in relation to the whole bridge design.

RÉSUMÉ

L'article présente quelques considérations faites au stade du projet sur les effets du vent sur un très long pont suspendu, le pont sur le détroit de Akashi Kaikyo avec une longueur totale de 3910 m. Les études et comparaisons de différents types de tablier de même que les constructions en treillis ou en caissons et leurs réactions aux instabilités dues à l'oscillation du pont sont considérées.

ZUSAMMENFASSUNG

Dieser Beitrag behandelt die Bemessungsüberlegungen betreffend der Windeinflüsse bei einer Hängebrücke grosser Spannweite, der Akashi Kaiko Brücke mit einer Gesamtlänge von 3910 m. Es werden hier vor allem die Studien der verschiedenen Brückenträger und Versteifungskonstruktionen zur Verhinderung von Wind-Instabilität behandelt.



1. INTRODUCTION

Construction of the Akashi Kaikyo Bridge which will cross the Akashi Straits with a shore-to-shore distance of about 4 km, has been a matter of many years' standing within the Honshu-Shikoku Bridge Project in Japan. The official go-ahead came in 1986, but actual construction works commenced in the spring of 1988. Comparisons among various design proposals and construction methods were made, based on such conditions as topography and geology of the sea bottom, tidal current speed, the navigational lanes, etc., as well as the considerations on the difficulty, term and cost of construction. They led to the choice of a three-span, two-hinged suspension bridge with a total length of 3,910 m (a main span of 1,960 m and side spans of 960 m), which would be the longest span length in the world. Its extremely flexible features would require, in particular, careful procedures and considerations for specified limit states, which represent aerodynamically static and dynamic effects and stability of the superstructure as well as satisfactory earthquake resistance of the substructure. From the very beginning of the project, numerous investigations have been carried out on these problems. The paper presents outlines of some considerations for wind effects, in particular, a competition among deck configurations of typical proposals to combat the flutter instability.

2. SUMMARY OF CONSIDERATIONS FOR WIND EFFECTS

In order to determine the bridge scheme and construction method, the Honshu-Shikoku Bridge Authority has been conducting various surveys and studies on structural designs. Initially, the Akashi Kaikyo Bridge was planned in the form of a combined highway-railroad bridge with a double deck trussed construction. Afterwards, however, owing to a change in social circumstances, the policy was altered to the construction of a highway bridge with six lanes. The final plan of the span construction is as shown in Fig.1.

In the meantime, in the early stage of design and investigation, the proposal of (1) trussed deck constructions was emphasized on the basis of former experiences in the Honshu-Shikoku bridges, while (2) shallow closed box decks, aiming at lower wind load and lighter dead load and (3) non-stiffened deck construction with open slots, feasible for higher stability were proposed to make various comparisons. Those cross sections are No. 11-17 in Figs.2 and 3. The aerodynamic stability was generally studied through sectional model wind tunnel tests in a smooth flow. It was found at this stage that few trussed constructions could satisfy the requirements for flutter stability.

Referring to such results at early stage, the design considerations for wind effects began in earnest in 1982, as the time was getting ripe for the execution of the bridge construction. At this stage of the investigation, all the problems due to a very long span ever experienced were reconsidered, particularly the effects of turbulent wind and the wind environment of the Akashi Straits, while the study on suppression of flutter and vortex excitation were also continued. These works have been conducted through field data analyses, wind tunnel tests and numerical analyses. As far as the proposals were concerned, several box decks and variations were compared to search for better deck constructions with respect to flutter stability than trussed decks, which were also studied to get more rational design proposals under the wind load. The examples are the cases of No. 21, 22 and 71, and from No. 23 through No. 62 in Figs.2 and 3. It was concluded up to the present that two cases could fulfil the prescribed flutter stability requirements and were to be investigated in more detail. Those were a conventional truss deck and a closed box deck combination of two different heights.

As for the preliminary design procedures for wind effects on the Akashi Kaikyo Bridge, the design code established in 1976 was to be temporarily applied, while some alteration would be expected in a short time. According to the present code, primary provisions are as follows; (1) reference wind speed of 43 m/sec (wind speed of 150 year return period, 10 min. average and at 10 m height above sea level) is provided for the site of the Akashi Straits. (2) Design wind loads are calculated by equivalent wind speed of about 74 m/sec after a correction of peak gust response effect. (3) Critical wind speed of flutter must be higher than 78 m/sec in wind incidence between 3 and -3 degrees.

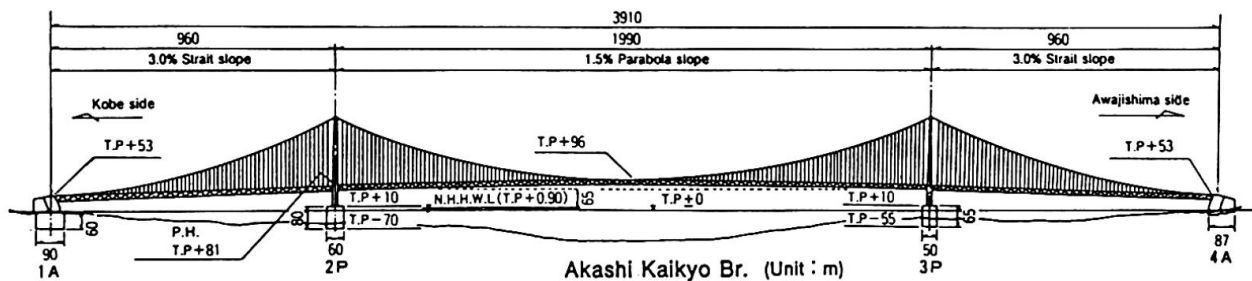
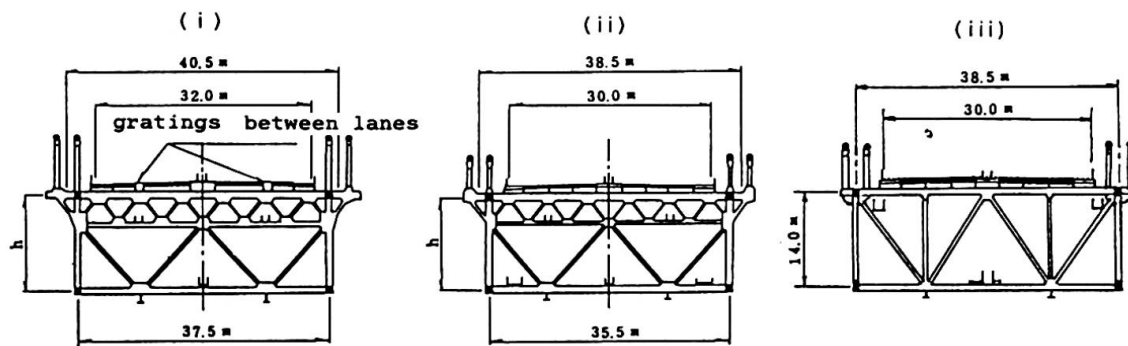


Fig.1 General View

Fig.2 Dimensions and Cross Sections of Typical Proposal of Truss Deck

series number	1 1	1 2	1 3	2 1	2 2	7 1
cross section	(i)		(ii)		(iii)	
span length l (m)	1,000+2,000+1,000			950+2,000+950		960+1,960+960
sag ratio f / l	1/9.5			1/8.5		1/9.5
deck height h (m)	1 4	1 2	8	1 4	1 2	1 4
dead load (t/m/Br)	deck w _s	26.7	26.2	25.3	27.5	26.8
	cables w _c	18.7	18.7	17.8	16.0	15.8
	total	45.4	44.9	43.1	43.5	42.6
torsional frequency f _T (Hz)	0.148	0.136	0.113	0.152	0.136	0.137
tor. rigidity of deck GJ × 10 ⁸ (t·m ²)	1.98	1.53	0.73	1.51	0.83	1.00
flutter stability by wind tunnel test	OK	OK	NO	OK	NO	under test





3. CONSIDERATIONS ON TRUSS DECKS

Geometry of primary members of the truss deck bridge are to be determined by wind loads. The trussed construction is generally quite rational in structural mechanics, which leads to frequent adoption as a traditional stiffening deck of a suspension bridge. Among the Honshu-Shikoku bridges, trussed decks produced good results for the Innoshima, Ohnaruto, Shimotsui and South- and North-Bisanseeto bridges. As for the Akashi Kaikyo Bridge, truss decks were proposed from the beginning of design competitions (Fig.2). Wind tunnel tests led to some stable cross section designs against flutter instability. These cases provided few problems in vortex excitation, gust responses, statical instability, etc. as well.

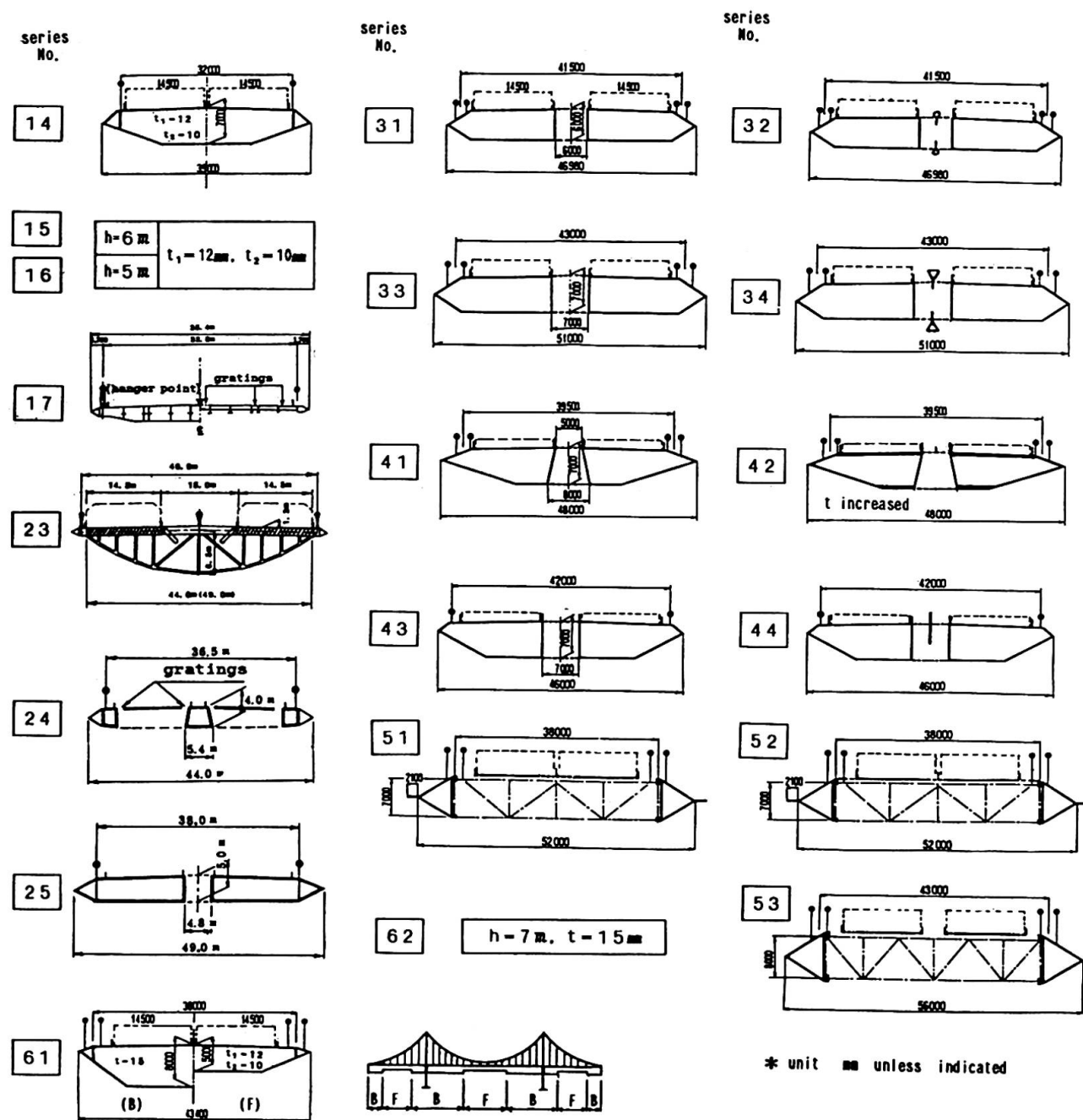


Fig.3 Cross Sections of Typical Proposals of Box Deck and Variation

It has been recognized that the truss construction was generally unfavourable in a higher drag wind load as well as a heavier dead load. In case of the Akashi Kaikyo Bridge, the greater lateral deflection of the deck reached more than 30 m at span center under the design wind load. However, this effect on the sub-structure design could not be a major design factor, because another severe seismic loads predominated over in the determination of the pier dimensions. Therefore, present attention for the truss decks is to seek after the more practical, economical and stable improvement of structural designs implementing less drag wind loads.

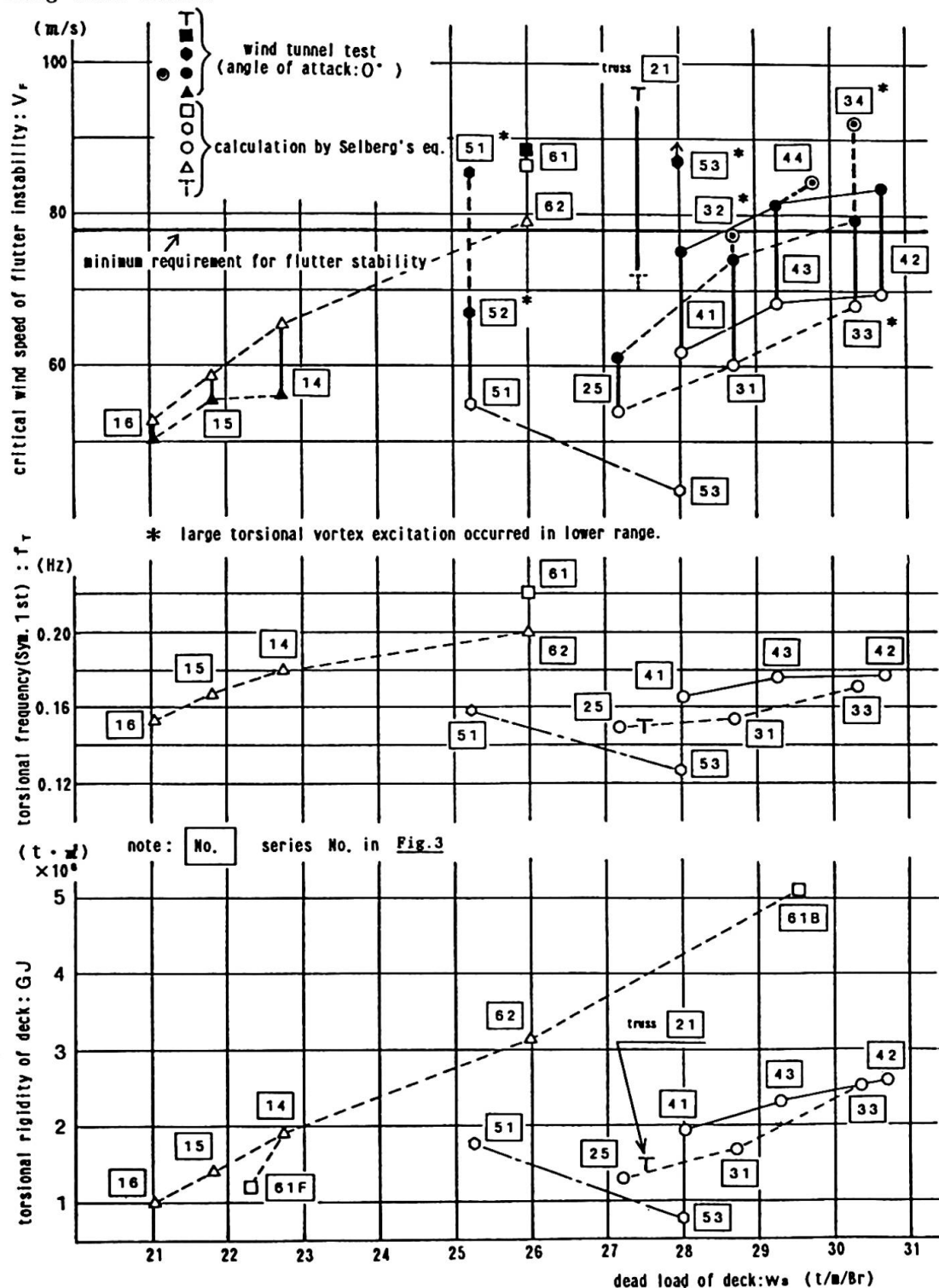


Fig. 4 Flutter Stability Competition of Typical Deck Proposal



4. CONSIDERATIONS ON BOX DECKS AND VARIATIONS

It was appreciated that the closed shallow box deck would have the advantage of a relatively favourable stability, a lower drag wind load, a lighter dead load, etc. According to the conventional design of the box deck, geometry of primary members can be usually determined by only minimum thickness of metal requirement for maintaining rigidity and corrosion preservation, because the wind and live loads leave a considerable stress margin. When a closed shallow box deck for the case of 2,000 m main span is designed, owing to the minimum thickness requirement, the onset wind speed of flutter is considerably lower than the required level because of fairly low torsional natural frequency. A calculation shows that range of the mainspan length for the required level of flutter stability to be satisfied is less than only 1,700 m according to the Japanese code.

In order to overcome this weak point for box decks, two alternative means to raise critical flutter speed were considered; (1) a structural approach to provide greater torsional stiffness by increasing metal use or by optimizing deck allocation, or (2) an aerodynamic approach to improve flutter properties by providing a couple of open slots between deck surfaces or by combining a sort of stabilizer. Typical proposals of box decks and variations are as shown in Fig.3. Referring to the results of wind tunnel tests vs. dead load of deck construction, which are indicated in Fig.4, it was concluded at present that the most economic and stable deck configuration might be a combination of two closed box decks of different heights. Further investigations are still in progress.

5. CONCLUDING REMARKS

An outline of the considerations and investigations for wind effects on the Akashi Kaikyo Bridge made so far are described in this paper. The present conclusions are as follows; (1) the design for wind effects on a very long-span suspension bridge with 2,000 m main span could be carried out by an extension of the conventional design method. (2) Some deck configurations of truss satisfied the required level of flutter stability. In conjunction with the substructure design, the dead and wind loads were not necessarily definite design factors since the seismic loads might predominate. (3) As for the box decks, some means had to be found whereby the critical flutter speed could be raised to the required level without onsets of vortex excitation. The structural approach to provide greater torsional stiffness by arranging an appropriate steel increase in the bridge axis was quite effective, compared with aerodynamic alteration of the deck configurations to improve flutter properties, for instance, by providing a couple of open slots between deck surfaces. (4) Other aerodynamic effects such as vortex excitation, gust response and statical instability are also important factors, among which the effects of gust response have an appropriate contribution in the wind loads, fatigue design, etc.

REFERENCES

1. Honshu-Shikoku Bridge Authority, Wind Effects Design Code (1976), March 1976.
2. MIYATA T., OKAUCHI I., SHIRAISHI N., NARITA N. and NARAHIRA T., Preliminary Design Considerations for Wind Effects on A Very Long-span Suspension Bridge, Proc. 7th Int. Conf. Wind Engineering (Aachen, West Germany), July 1987.

Rohrleitungshängebrücken

Suspension Pipeline Bridges

Ponts suspendus pour conduites

W. M. FRIDKIN

Kand, d.t. Wiss.
Melnikow-Inst.
Moskau, UdSSR

Wladimir Fridkin, geboren 1938. Studium Institut für Verkehrswesen in Moskau. Spezialisierung als Ingenieur für Brückenbau. Tätigkeit bei der Untersuchung der Rechenverfahren weitgespannter Metallkonstruktionen.

M. M. KRAWZOW

Ingenieur
Melnikow-Inst.
Moskau, UdSSR

Michail Krawzow, geboren 1935. Studium Institut für Verkehrswesen in Moskau. Spezialisierung als Ingenieur für Brückenbau. Tätigkeit bei der Projektierung und Untersuchung von Metallkonstruktionen, insbesondere von Brücken.

ZUSAMMENFASSUNG

Es werden Wechselbeziehungen zwischen der Konstruktionsform und dynamischen Parametern – Perioden und Formen freier Schwingungen – von Rohrleitungshängebrücken mit einer Dreieckgitteraufhängung und Windgurten bei Stützweiten von 660 m bis 950 m bei veränderlicher Seilfachwerkform und Ausführung des Verbandes zwischen Windgurten und dem Versteifungsträger gegeben.

SUMMARY

In the report the interrelation between the structural form and dynamic response – periods and modes of natural vibration – of suspension pipeline bridges with a triangular lattice of suspenders and wind chords for spans from 660 m to 950 m while varying the lattice form and the type of bracing between the wind chords and the stiffening truss is described.

RÉSUMÉ

L'article étudie les relations entre la forme structurale et le comportement dynamique – période et mode de vibration naturelle – de ponts suspendus pour conduites. Ces ponts d'une portée de 660 m à 950 m ont des suspentes en forme de treillis triangulaire et des membrures de contreventement dont les formes, le type et le comportement varient.



1. EINLEITUNG

Es wurden konstruktive Formen einfeldriger Rohrleitungshängebrücken (1)-(4) untersucht, die die Weiterentwicklung eines vorgespannten Systems mit geneigten Hängern sind. Das System (1), bei dem geneigte Hänger unmittelbar am gitterförmigen Versteifungsträger befestigt sind, wurde in der UDSSR für die grösseren Brückenspannweiten über den Amudarja (660m) und den Dnjepr (720m) erfolgreich verwendet.

Es wurden rechnerisch die Perioden und Formen freier Schwingungen ebener und räumlicher einfeldriger Brückensysteme bestimmt, wobei die Verbandausführung zwischen Windgurten und dem Versteifungsträger berücksichtigt wurde. Für bestehende Brücken sind theoretische Periodenwerte geringer freier Schwingungen mit Versuchsergebnissen dieser Bauwerke verglichen.

Die Untersuchungsergebnisse erlaubten, Reaktionen der Konstruktionen auf äussere dynamische Einwirkungen wie Wind, Erdbeben und andere Faktoren genau zu bewerten und das Bauproblem aerodynamisch stabiler, weitgespannter Rohrleitungshängebrücken mit rationellen Parametern für die dynamischen Eigenschaften zu lösen.

2. THEORETISCHE VORAUSSETZUNGEN DER UNTERSUCHUNG

Die untersuchten Hängesysteme gehören zur Klasse weitgespannter Systeme einer erhöhten Steifigkeit. Die Besonderheit der theoretischen Analyse besteht in der Berücksichtigung der Längskräfte, die in Stäben wirken.

Die Perioden und Formen freier Schwingungen wurden an diskreten Stabmodellen theoretisch untersucht. Die Perioden und Formen wurden mit Hilfe der Methode der Finiten Elemente auf der Grundlage standardisierter Methoden dynamischer Berechnung für linear-deformierte Stabsysteme bestimmt. Die Besonderheit dynamischer Berechnungen besteht in der Linearisierung geringer freier Schwingungen unter Berücksichtigung, im dynamischen Gleichgewicht, der Drehwinkel der Sehnen zweigelenkiger Stäbe, die die Seilelemente einer Hängebrücke modellieren.

Für die ER-Deformationsberechnung bei der Bestimmung der Nachgiebigkeitsmatrixelemente wurde die Methode zusätzlicher Steifigkeitsparameter verwendet (5).

Diese Verwendung kam auf die Einführung in die Bezugsdaten zusätzlicher Verbände hinaus - bei schwimmenden Einspannungen in allen Kabel- und Windgurtknoten - und auf die Bestimmung für Stäbe fiktiver Biegesteifigkeiten.

3. DIE BESONDERHEITEN DER KONSTRUKTIONSSCHEMAS UNTERSUCHTER HAENGEBRUECKEN

Die geneigten Hänger werden in der Konstruktion der 720m Rohrleitungshängebrücke nach dem Schema (1) (Abb. 1), im weiteren gekennzeichnet als C1, unmittelbar am Aussteifungsbinder befestigt. Die Hängebrücke nach dem Schema C2 hat vorgespannte Seiluntergurte, die Befestigungsknoten geneigter Hänger an Quertraversen verbinden, auf welchen die Rohrleitungen (oder der Versteifungsträger) lagern. Dieses System (2) sichert eine gute Montierbarkeit der Rohre und des Versteifungsträgers durch Längsverschieben und führt zu einer 10%-Stahleinsparung gegenüber dem Schema C1.

Die charakteristische Eigenschaft der konstruktiven Formen C1 und C2 besteht in der längs-unbeweglichen Befestigung des zweigurtigen vorgespannten Windsystems gegenüber dem Versteifungsträger oder dem biegsamen Untergurt im Brückenmittelfeld.

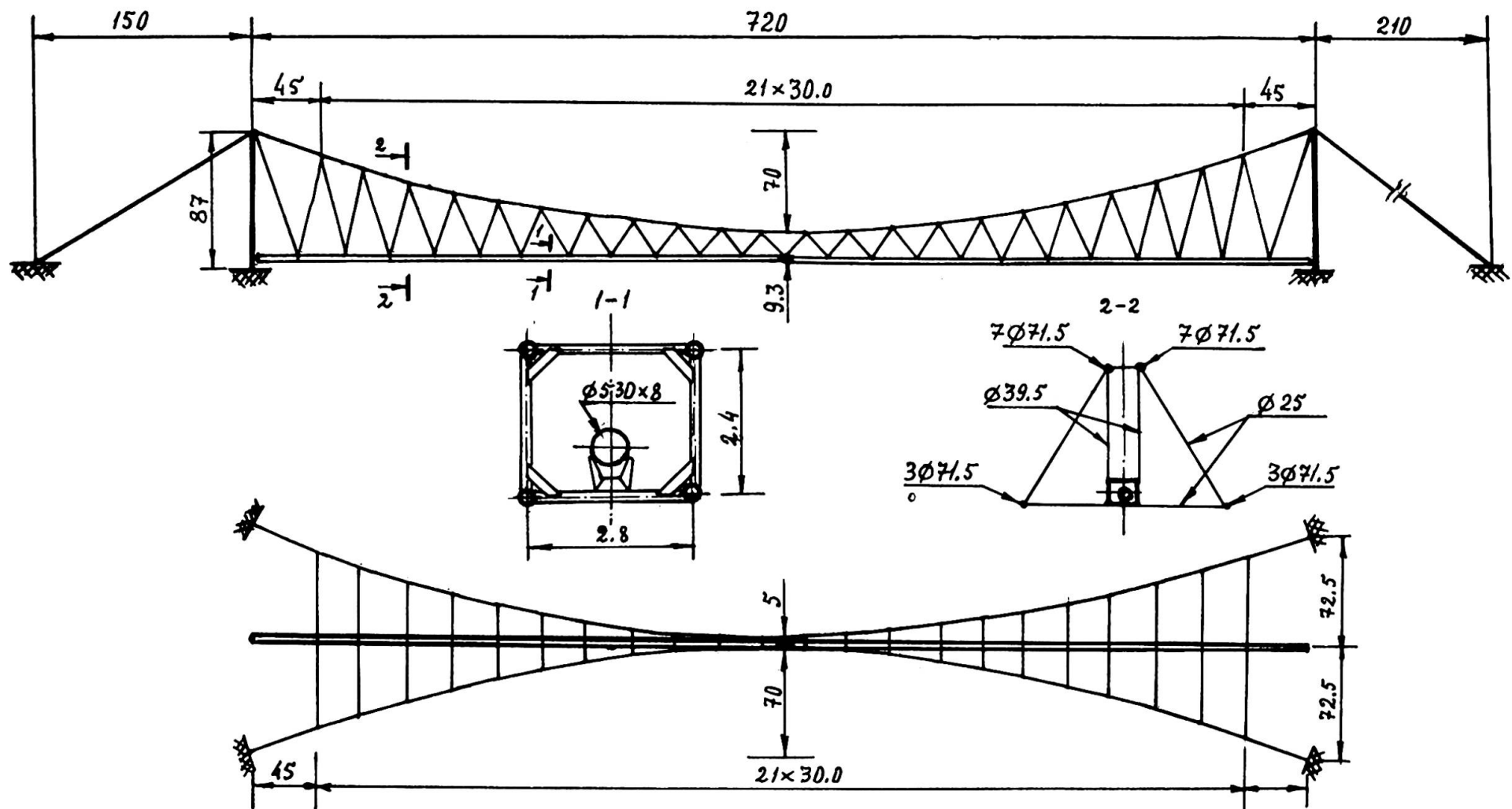


Abb. I. Rohrleitungshängebrücke mit einer Stützweite von 720 m (Schema CI)



Diese Befestigung vermindert die Durchbiegungen einer Hängebrücke infolge der Vertikalbelastungen und beeinflusst spektrale Kennwerte freier Schwingungen merklich, indem das Spektrum zur Seite höherer Frequenzen verschoben wird (3). Das Schema CI wurde bei Stützweiten von 660 m, 720 m und 950 m, das Schema C2 - bei Stützweite von 950 m untersucht.

Zur Erhöhung der Torsionssteifigkeit wurde eine Konstruktion mit entlang der Brückenlänge abwechselnder Spannseilbefestigung des Windsystems an Ober- und Untergurten des Versteifungsträger vorgeschlagen (4). Diese Lösung wurde bei Varianten des Schemas CI - bei CI.I - verwendet.

Bei der Windeinwirkung quer zur Brücke wird die Innenkräftesymmetrie im Windverband gestört, und bei der ungenügenden Vorspannung verringert sich auch die Längssteifigkeit des Windgurtes, der mit seiner Wölbung dem Windstrom gegenüber liegt merklich. Eine Zahlenanalyse des Schemas CI mit der Stützweite 950 m hat gezeigt, dass die obenerwähnte Erscheinung vernachlässigt werden kann, wenn das rechnerische Niveau der zu kontrollierenden Vorspannungskräfte im Windverband unter Berücksichtigung einer ungünstigen Temperaturwirkung und einer Spannungsrelaxation angenommen wird.

Der Tragsicherheitsnachweis der Windgurte führt kaum zu einer Erhöhung der Seilmassen, da die Grenzzustandmethode erlaubt, für Seilelemente der Windsysteme von Rohrleitungshängebrücken erhöhte rechnerische Grenzwerte anzunehmen (6).

Die Unterschiede bei den Längen und Neigungswinkeln der Hauptkabelabspannungen und die unsymmetrische Anordnung der Ankerfundamente des Windsystems, welche durch Uferprofil und geologische Besonderheiten der Gründung bestimmt wird, stören die Formsymmetrie freier Schwingungen und geben ihnen einen räumlichen Charakter, der zur Entwicklung aerodynamischer Instabilität beiträgt. In vielen Fällen kann aber eine günstige Formverteilung freier Schwingungen erreicht werden, und zwar in Vertikal- und Biege-torsionsschwingungen im Grundriss und unter komplizierten Bedingungen der Windsystemverankerung durch das Verschieben des Befestigungsknotens der Windgurte am Versteifungsträger vom Brückenmittelfeld her zur Seite eines der Ufer, unter Ausnutzung gekürzter Ablenktraversen (7).

4. DIE MITWIRKUNG VON TRAGKONSTRUKTIONEN UND ROHRLEITUNGEN

Die Wahl rechnerischer Modelle von Rohrleitungshängebrücken berücksichtigte für die Analyse deren freien Schwingungen die Rohrsteifigkeit und wirklichen Verhältnisse der Befestigung der Rohrleitungen im Brückentragwerk sowie das Kompensationsschema der Temperaturverformungen, besonders bei Röhren grossen Durchmessers. Im Fall geringer Schwingungen bei Rohrleitungen, die mit einem flüssigen Produkt gefüllt sind, kann die theoretisch bewegliche Rohrauflagerung nach der Versteifungsträgerlänge und in Kompensatorenbereichen nicht immer realisiert werden. Diese Erscheinung verlangt eine genaue Analyse des wirklichen "dynamischen" Brückensystems mit der Notwendigkeit das rechnerische Modell zu präzisieren. Die Bewertung des Deformationsmoduls der Kabel und Gurte eines Windsystems bei geringen Bauwerksschwingungen, die zum Beispiel während der Versuche erregt werden, ist auch zu analysieren.

Das Verständnis für die Eigenheiten des Verbandverhaltens bei Schwingungen des Systems "Hängebrücken - Rohrleitungen" erlaubt, dissipative Eigenschaften genau zu berücksichtigen und die Effektivität vorgeschlagener Dämpfung der Schwingungen zu bewerten. Nach Versuchsergebnissen mit der 720 m-Brücke CI lagen die logarhythmischen Dekremente für beobachtete Schwingungsformen bei der Amplituden von I/2500 der Brückenstützweite im Intervall von 0.045 - 0.065 (8).

5. DIE ANALYSE FREIER SCHWINGUNGEN BEI ROHRLEITUNGSHAENGEBRUECKEN

Die Ergebnisse theoretischer Berechnungen und die Versuchsergebnisse für Brücken der Schemas CI und C2 mit Stützweiten von 660 m bis 950 m sind in der Tabelle I aufgeführt, wobei Symmetriarten der Schwingungsformen - bis zu 6 Formen - angegeben werden.

Die Berechnungen berücksichtigen bei der Bauwerkssymmetrie bis zu 400 Freiheitsgrade räumlicher Modelle. Die Massen wurden bei den mit dem Produkt gefüllten Rohrleitungen über die ganze Brückenstützweite bestimmt.

Nur das System CI - 660 m wurde nach ebenem Stabsystemschemas - dem vertikalen und horizontalen - berechnet. Der Vergleich der Berechnungs- und Versuchsergebnisse zeigt Periodenwerte vertikaler Schwingungen (beim Reihenwechseln der Formsymmetrie) und einen etwas grösseren Fehler für Biege-Torsionsschwingungen im Grundriss, was durch eine Näherungsberechnung des vollen Brückenschubes im Verhalten des zweigurtigen Windsystems erklärt werden kann.

Im System CI - 720 m, berechnet mit einem räumlichen Modell, ist eine gute Ueber-einstimmung zwischen Berechnungs- und Versuchsergebnissen zu einigen Hauptformen vertikaler und biege-torsionsfreier Schwingungen erreicht.

Die untersuchten Systeme und deren Spannweiten	Arten freier Schwingungen	Schwingungsperioden und Formen: symmetrische und schrägsymmetrische					
		I	2	3	4	5	6
<u>CI - 660m</u> Berechnung Versuche	vertikale	3.38	<u>3.27</u>				
	biege-torsion	4.83	<u>4.01</u>	3.64			
	vertikale	3.36	<u>3.23</u>				
	biege-torsion	5.5	<u>3.8</u>				
<u>CI - 720m</u> Berechnung: beim Fehlen des Windverbandes	vertikale	4.49	<u>3.55</u>	2.36	<u>1.78</u>	1.29	<u>1.13</u>
	biege-torsion	15.38	<u>9.98</u>	7.32	<u>4.80</u>	4.33	<u>3.74</u>
	vertikale	4.38	<u>3.69</u>	2.44	<u>2.16</u>	1.43	<u>1.31</u>
	biege-torsion	6.12	<u>5.89</u>	4.06	<u>3.68</u>	3.16	<u>3.11</u>
beim Fehlen des Verbandes im Mittelfeld; vollmontierte Konstruktion (Versuche)	vertikale	<u>3.71</u>	<u>3.69</u>	2.44	<u>1.82</u>	1.43	<u>1.15</u>
	biege-torsion	<u>6.10</u>	<u>4.13</u>	4.03	<u>3.17</u>	<u>3.00</u>	<u>2.97</u>
	vertikale	<u>3.41</u>	<u>3.34</u>				
	biege-torsion	6.20		3.92	<u>3.10</u>		2.92
<u>CI - 950 m</u> Berechnung	vertikale	<u>5.87</u>	<u>5.28</u>	3.95	<u>3.11</u>	2.38	<u>2.00</u>
	biege-torsion	<u>7.95</u>	<u>5.96</u>	<u>5.28</u>	<u>4.27</u>	3.85	<u>3.83</u>
<u>C2 - 950 m</u> Berechnung	vertikale	4.87	<u>4.29</u>	3.38	<u>2.62</u>	2.30	<u>2.15</u>
	biege-torsion	7.31	<u>5.04</u>	4.95	<u>4.52</u>	4.03	<u>3.99</u>

Tabelle I Die Perioden und Formen freier Schwingungen der Hängebrücke



Eine weitere Erhöhung der Berechnungsgenauigkeit kann nur beim Vorhandensein präzisierter Deformationsmodulwerte für konkrete Seilpartien erreicht werden. Man kann grosse (bis 15 Sekunden) Periodenwerte der Biege- Torsionsschwingungen im Montagestadium beim Fehlen eines Windsystems feststellen. Bei diesen Perioden sind Hängebrücken zur Pulsationskomponente der Querwindeinwirkungen sehr empfindlich, wobei letztere nach empirischen Spektren (von Dawenport oder Van der Hoven (9)) bestimmt wird.

Das System C2 ist frei von diesem Mangel. Die Windgurte in diesem System werden vor dem Verschieben des Versteifungsträgers gespannt und die Perioden der Biege-Torsionsschwingungen übersteigen die 8 Sekunden nicht, sogar für die 950 m-Stützweite.

Die Längsbefestigung der Windgurte am Versteifungsträger (C1) oder unteren Seilgurte (C2) trägt zur Periodenverringerung der Vertikal- und Biege-Torsionsschwingungen nach schrägsymmetrischen Formen bei, wobei die Erhöhung der Bauwerksstabilität zum Biege-Torsionsflattern gesichert wird. Der Vergleich des durch die Bau- und Betriebserfahrung bestätigten Systems C1 und des neuen Systems C2 bei der Stützweite von 950 m zeigt im ganzen die Konkurrenzfähigkeit dieses neuen Systems. Man muss auch auf den Vorteil des modifizierten Systems C1.I gegenüber C1 hinweisen bezüglich Torsionsformen freier Schwingungen. Bei der 950 m-Brücke C1.I wurden Perioden freier Torsionsschwingungen in Formen, die mit der Biegung des Versteifungsträgers im Grundriss nicht verbunden sind, geringer: symmetrische - von 1.75 s nach 0.79 s, schrägsymmetrische - von 1.71 s nach 0.76 s, was auch zur Erhöhung aerodynamischer Stabilität beiträgt.

6. ZUSAMMENFASSUNG

Die angeführten Angaben zeigen, dass dynamische Kennwerte geringer freier Schwingungen weitgespannter Rohrleitungshängebrücken in grossem Masse von konstruktiven Lösungen abhängen, und dass sie sich mit der Länge der Brückenstützweite gesetzmässig ändern. Sie können mit vorhandenen Rechenmitteln berechnet werden, wobei das räumliche Systemverhalten, seine Vorspannung und die geometrische Nichtlinearität der Verformungsgesetze zu berücksichtigen sind.

LITERATURVERZEICHNIS

1. A. s. SSSR N 391218. Büll. "Otkritija. isobretenija" N 31/73.
2. A. s. SSSR N 1081263. Büll. "Otkritija, isobretenija" N II/84.
3. SLONIM E.JA. Wlijanie prednaprjashennoj 2-chpojasnoj horisontalnoj fermi na usilija i deformazii wertikalnoj reshettschatoj wantowoj fermi. R.s.ZINIS, ser. 7,bip. 4(45), s. 15-19.
4. A. s. SSSR N 1048024. Büll. "Otkritija, isobretenija" N 38/83.
5. FRIDKIN W.M. O postroenii algoritmow rastscheta wisjatschich i wantowich kombinirowannich konstrukcij s utschetom geometritscheskoy nelinenosti. Trudi ZNIIPSK, M., 1980, s.114-122.
6. KRAWZOW M.M., FRIDKIN W.M. i.dr. Rekomendazii po rastschetu protschnosti stalnich kanatow, primenjaemich w stroitelnich metallokonstrukcijach. ZNIIPSK, M., 1982, s.24.
7. A. s. SSSR N 1096327. Büll. "Otkritija, isobretenija" N 21/84.
8. SCHLOWSKIJ E.I. i dr; Naturnie ispitaniya wisjatschego truboprovodnogo mosta tscheres Dnjepr proletom 720m. Trudi ZNIIPSK, 1980, s.81-88.
9. KAZAKEWITSCH M.I. Aerodinamika mostow. "Transport", M., 1987, s. 17-24.

New Damper for Tower of Long-Span Suspension Bridge

Nouveau système amortisseur pour la pile d'un pont suspendu de grande portée

Schwingungsdämpfer für die Türme einer grossen Hängebrücke

Yozo FUJINO

Assoc. Prof.
University of Tokyo
Tokyo, Japan

Manabu ITO

Professor
University of Tokyo
Tokyo, Japan

Benito PACHECO

Assist. Prof.
University of Tokyo
Tokyo, Japan

Yozo Fujino, born in 1949, graduated from the University of Tokyo and received his Ph.D. from the University of Waterloo in 1976. His research interests are structural dynamics and structural reliability.

Manabu Ito graduated in 1953 and received his Dr.Eng. degree from the University of Tokyo. He has been engaged in teaching and research on bridge engineering and structural dynamics at the same university.

Benito Pacheco, 28, obtained his B.S. from the University of the Philippines and Dr.Eng. from the University of Tokyo. He is into structural dynamics.

SUMMARY

A new damper, relying on the motion of shallow water in a rigid cylinder, is studied through free vibration tests of a single-degree-of-freedom model of bridge tower with a natural period of 2 sec. For a large damping effect at small amplitude of tower vibration, it is necessary to tune the sloshing period of the liquid to the natural period of the tower; hence the name Tuned Liquid Damper. Breaking of surface waves, while highly dependent on vibration amplitude, is the main mechanism of energy dissipation. There seems to be an optimal TLD size for a given frequency and amplitude of vibration.

RÉSUMÉ

Un nouveau système amortisseur, basé sur le mouvement de l'eau dans un cylindre rigide est étudié au moyen d'essais de vibrations libres dans un modèle à un degré de liberté pour une pile de pont présentant une période naturelle de deux secondes. Afin d'obtenir un important effet d'amortissement pour une faible amplitude de vibrations de la pile, il est nécessaire d'ajuster la période de liquéfaction du liquide à la période naturelle de la pile; d'où le nom d'"amortisseur liquide accordé". Le brisement de la surface des vagues dépend directement de l'amplitude de vibrations, et est le mécanisme principal de dissipation de l'énergie. Il semble exister un "amortissement liquide accordé" pour chaque fréquence et amplitude de vibration.

ZUSAMMENFASSUNG

Ein neuartiger Schwingungsdämpfer, basierend auf der Schwappbewegung von Wasser in einem steifen Zylinder, wird mit Versuchen an einem Modell für einen Brückenturm von 2 Sekunden Grundschwingungszeit studiert. Für eine hohe Dämpfungswirkung bei kleiner Schwingungsamplitude muss die Schwappperiode des Wassers auf diejenige des Turmes abgestimmt werden; daher die Bezeichnung: abgestimmter Flüssigkeitsdämpfer. Das Brechen der Oberflächenwellen ist stark von der Schwingungsamplitude abhängig und bildet die Hauptursache der Energiedissipation. Es scheint für jede Kombination von Frequenz und Amplitude eine andere optimale Dämpfergrösse zu resultieren.



1. INTRODUCTION

With the increase of span length, the wind-induced vibrations of the towers of cable-suspended bridges tend to become a subject of discussion, not only at the free-standing erection stage but also after the completion of the bridge, particularly in case of cable-stayed bridges where the constraint of stay cables on the lateral bending of the tower is unexpectedly small. To increase the structural damping is an efficient way to suppress such vibrations.

This contribution discusses a new kind of mechanical damper, herein named Tuned Liquid Damper (TLD) [Fig. 1] relying on motion of shallow liquid inside a rigid container for absorbing and dissipating structural vibration energy. Liquid dampers have been in use in space satellites and marine vessels. Modi and Sato [1, 2] were among the first to suggest their application to ground structures including towers and buildings. Growing interest in TLD [3-5] is attributable to several potential advantages, including low cost, easy installation even in already existing structures, few maintenance requirements, and adaptability to temporary use. However, adequate modelling and clear explanation of TLD mechanism are lacking despite studies so far indicating its effectiveness. Here are reported some insights and data from an experiment designed to demonstrate the TLD's fundamental mechanism, with emphasis on parameters that immediately relate to practical implementation.

2. EXPERIMENT PROCEDURE

To simulate one mode of a tall flexible bridge tower, a heavy steel platform [Fig. 2] was designed with natural period T_S of 2 sec (or frequency $f_S = 0.5 \text{ hz}$), and mass m_S ranging from 116 to 440 kg. The structure, i.e. platform, was given initial displacement while taking care that the liquid in the TLD was quiescent before the structure was released into free vibration. Both structural displacement and liquid surface height at one side of the TLD were recorded.

Unlike in past experiments that employed small models, large prototype-size cylinders (40 cm and 60 cm diameters) were used here as liquid containers, with a view to using multiple identical TLDs in massive actual towers. With mass ratio, dimension, and vibration frequency thus made equal to those of prototype, it was possible to sidestep some dynamic fluid similarity requirements that would be difficult if not impossible to satisfy simultaneously.

3. RESULTS OF EXPERIMENT

Additional damping $\Delta\delta$ (= logarithmic decrement with TLD attached - structural damping) is shown in Fig. 3 for several cases where $\phi = 40 \text{ cm}$; $m_S = 116 \text{ kg}$; and the liquid is plain water. Figure 4 shows a comparison of TLD for the diameters 40 cm and 60 cm. A = amplitude of structural vibration; h = depth of liquid; $a = \phi/2$ = radius of cylinder; γ = ratio of fundamental sloshing frequency of liquid to frequency of structure; μ = ratio of liquid mass to mass of structure.

3.1 Effect of frequency tuning: Each curve of $\Delta\delta$ versus A in Fig. 3 corresponds to a different liquid depth h and, accordingly, different frequency ratio γ . It should be noted that the liquid in TLD is generally shallow, e.g. the ratio h/a is below 0.1 in most of the cases where additional damping is significant. As Figs. 3 and 4 show, high additional damping $\Delta\delta$ is obtainable when the frequency ratio is about $\gamma = 1.0$, which is the nominal tuning condition for the present system. The additional damping at tuned condition is particularly high when the amplitude A is small. In fact $\Delta\delta$ exhibits strong dependence on A when $\gamma = 1.0$, and has a peak at a certain small amplitude. The peak $\Delta\delta$ just

mentioned corresponds to a liquid mass that is only about 1% of structure. On the other hand, additional damping $\Delta\delta$ is rather low at frequency ratios that are very different from $\gamma = 1.0$, despite large liquid mass ratio.

Figure 4 shows that the condition of tuning seems unnecessary, however, for large amplitude A , where the same moderate additional damping $\Delta\delta$ is obtained almost regardless of frequency ratio γ . This may suggest the use of γ less than 1.0, to make the liquid mass ratio μ accordingly lower. Still, γ should be close to 1.0 if high $\Delta\delta$ is to be obtained specially at small A ; the name Tuned Liquid Damper is on account of this latter requirement.

3.2 Effect of container size: In tuning the natural frequency of liquid to the frequency of structure, it is possible to choose from among different sizes and their corresponding required liquid depths. The question in practice is whether to use one large TLD or multiple smaller ones. Figure 4 can also compare the efficiency of TLD for different diameters. On comparing the respective peaks of $\Delta\delta$ at about $\gamma = 1.0$ and $\mu=1.2\%$, it is seen that the larger TLD gives higher peak $\Delta\delta$. Figure 5 compares one large TLD with five small ones, again showing that the peak $\Delta\delta$ is higher for larger TLD, even as almost equal mass ratios correspond to these peaks. Thus for the present case it is indicated that, for the same mass ratio, the bigger TLD is more effective in producing large $\Delta\delta$.

3.3 Effect of other parameters: As presented in detail in Ref. 5, higher $\Delta\delta$ is produced with: low viscosity of liquid; smooth bottom of container; and adequate gap between liquid and roof of container. Additional damping is practically linearly proportional to liquid mass ratio or number of identical TLDs, provided the frequency ratio is about $\gamma = 1.0$ and the mass ratio is low.

4. DISCUSSIONS

4.1 Liquid motion and additional damping: As Fig. 3 illustrated, the additional damping $\Delta\delta$ due to the TLD depended much on structural vibration amplitude A . In fact the type of liquid motion changed as the amplitude A . It was found that the type of liquid motion consistently corresponding to rather large $\Delta\delta$ (say, $\Delta\delta > 0.03$ in Fig. 3) is that with two waves travelling on half-circles along the wall, as shown in Fig. 6.

Wave height was also measured at a point near the container wall, on a diameter along the direction of structural motion. Figure 7 shows an example wave record and its counterpart structural displacement record, corresponding to curve (3) in Fig. 3. The wave record provided a good estimate, even if the recorded positive peaks included some effect of splashing during the type of liquid motion described in Fig. 6, and even if very low wave troughs could not be recorded at all.

For the case shown in curve (3) in Fig. 3, $\Delta\delta$ had a peak value at around $A = 0.25 \text{ cm}$ and dropped drastically for still smaller amplitude. Inspection of the wave record showed that for $A > 0.25 \text{ cm}$, the wave height H was greater than 1.2 cm which was the depth of liquid h in that TLD. Wave breaking, with the associated turbulence at the wave crest, was to be expected when wave height H reached a value about equal to liquid depth h ; indeed turbulence at the wave crest was observed during the experiment.

The same case also showed, however, that while wave breaking occurred the resulting $\Delta\delta$ would not necessarily be larger or the same at larger amplitude A . This could be understood by recalling that $\Delta\delta$ is proportional to the ratio $\Delta E/E$, where the kinetic energy E in the denominator is proportional to A^2 . The per cycle energy dissipation ΔE in the numerator turned out to be nearly



proportional to A [Fig. 8] rather than A^2 , for the range of amplitudes considered. This indicates that $\Delta\delta$ is attributable to energy dissipation rather than mere absorption by the damper. In other words, $\Delta\delta$ is attributable to dissipation by wave breaking instead of mere transfer of energy into the liquid. Should simplified mechanical modelling of TLD in terms of mass, spring, and damping elements be attempted, the almost linear relation between per cycle energy loss ΔE and amplitude A [Fig. 8] in the amplitude range considered suggests a property of coulomb-type damping instead of viscous.

4.2 Choosing the appropriate size of cylinder: Figures 4 and 5 showed that, for the same liquid mass ratio, the bigger (60 cm) TLD was better since higher $\Delta\delta$ was produced. The advantage of the bigger diameter, for given period of TLD vibration, may be associated with the manner of liquid motion [Fig. 6]: two waves develop along half circles and hit together twice per cycle. Each time that the waves meet, the energy dissipated is proportional to the velocity of the converging waves; this velocity is in turn proportional to the length of the half-circle arc that they traverse every half-cycle.

Energy loss per cycle was plotted versus amplitude A in Fig. 8, for 40 cm and 60 cm TLDs at $\gamma = 1.0$. It showed that, at each amplitude A , the energy loss per cycle in the 60 cm TLD was almost 10 times that in the 40 cm TLD. The mass ratio involved in both cases was $\mu = 1.2\%$; but the actual liquid mass in the 60 cm TLD was 4 times as much. The ΔE per unit liquid mass was almost 2.5 higher in the larger TLD.

Other considerations may rule out the use of very large TLD, however. Figure 9 illustrates that for tuning to given period (or given frequency), there is a wide range of possible cylinder sizes; each size ϕ has its own corresponding required liquid depth h . The necessary relative liquid depth h/ϕ is not constant, however; instead it increases rapidly in the range of large ϕ . Very high h/ϕ in very large TLD would not be very efficient, as some liquid near the bottom would tend to be immobile and ineffective. Limitations on available space for installation would be another practical constraint.

In any case, the deeper liquid would require a higher wave height H , hence a larger structural amplitude A , before energy dissipation by wave breaking can start. For example, the 40 cm TLD required about $A = 0.5$ cm [Fig. 3]; the 60 cm TLD required about $A = 1$ cm. It is indicated that there may be an optimal size of TLD for given structural period (or frequency), amplitude of vibration, and space limitation.

5. SUMMARY

A new kind of mechanical damper, called Tuned Liquid Damper or TLD, which has certain advantages for suppression of vibrations of tower-like structures was investigated experimentally. It is indicated that energy dissipation in TLD is due mainly to wave breaking, which explains various TLD properties.

Within the range of parameters considered in the experiment, the larger TLD is more effective. However, because of changing liquid condition from shallow to deep, for given frequency and amplitude of structure there may be a cylinder diameter that produces optimal amount of additional damping. Limitation of space for installation would be another practical constraint to TLD size. The subject of optimal TLD size still requires further investigation.

ACKNOWLEDGMENTS: The authors are grateful to Dr. M. Isobe of Univ. Of Tokyo; and to Mr. K. Fujii and Mr. T. Sato of Shimizu Co. for their very useful comments.

Likewise they thank Mr. I. Shino, Mr. P. Chaiseri, Mr. P. Warnitchai, and Mr. L.M. Sun of University of Tokyo for their help in the experiment.

REFERENCES

1. MODI, V.J. and WELT, F. 1987. Vibration control using nutation dampers. Proc Intl Conf Flow Induced Vib, Bowness-in-Windermere, England, 369-376
2. SATO, T. 1987. Tuned sloshing damper. Japan J Wind Eng, 32, 67-68
3. MIYATA, T., YAMADA, H., and SAITO, Y. 1987. Feasibility study on damping of wind-induced vibrations of structures by breaking of sloshing water. Japan J Wind Eng, 32, 65-66 (in Japanese)
4. NOJI, T. et al. 1987. Study on a vibration damper system using hydrodynamic force of sloshing (Parts 1,2,3). Proc Conf Arch Inst Japan, 867-872 (in Japanese)
5. FUJINO, Y. PACHECO, B.M., CHAISERI, P., and SUN, L.M. 1988. Fundamental study on tuned liquid damper (TLD) - a new damper for building vibrations. Proc Symp/Work on Serviceability of Bldgs, Ottawa, Ontario, Canada, 14pp

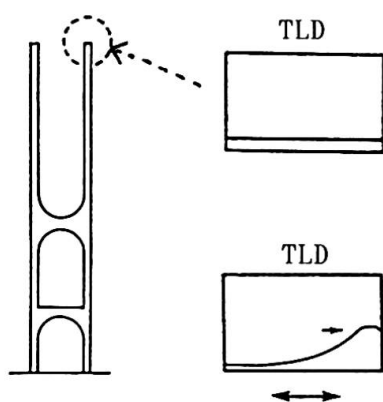


Fig. 1 TLD installed on a bridge tower

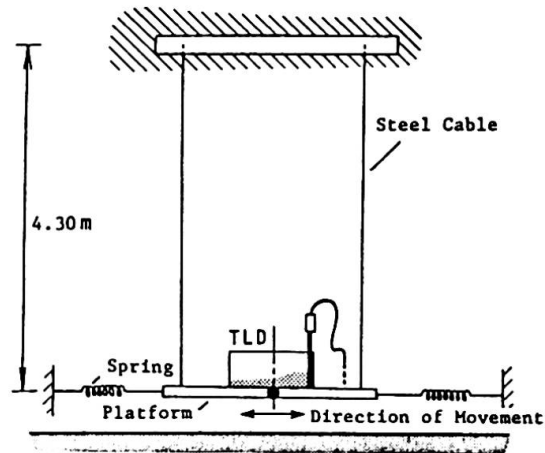


Fig. 2 SDOF structural model with TLD

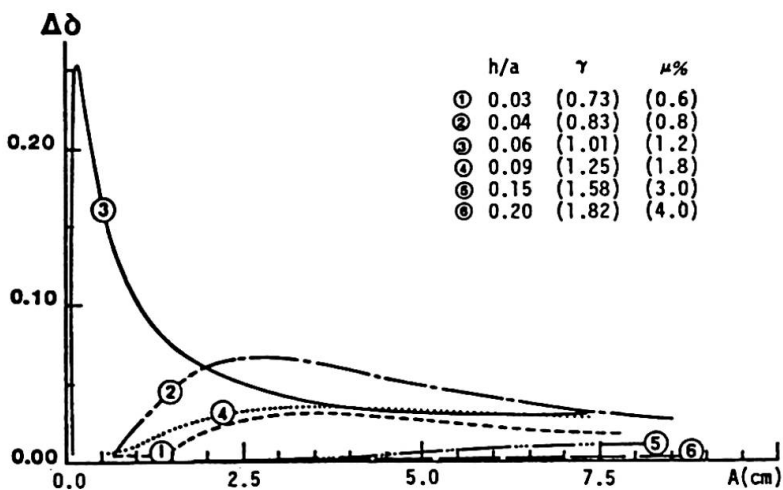


Fig. 3 Additional damping due to TLD

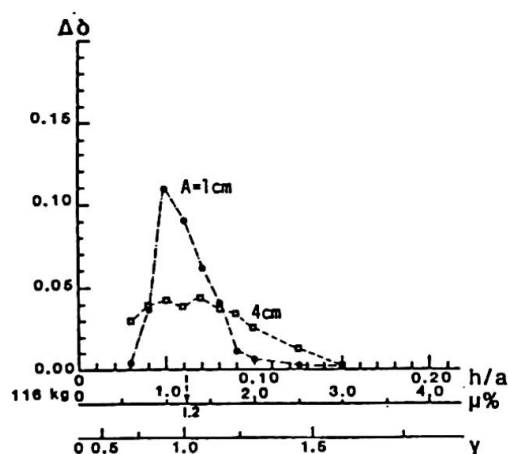
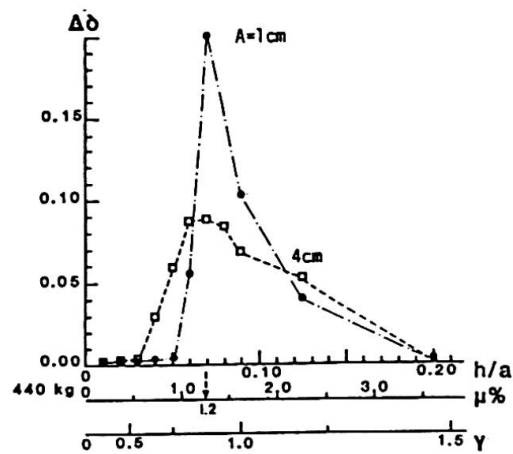
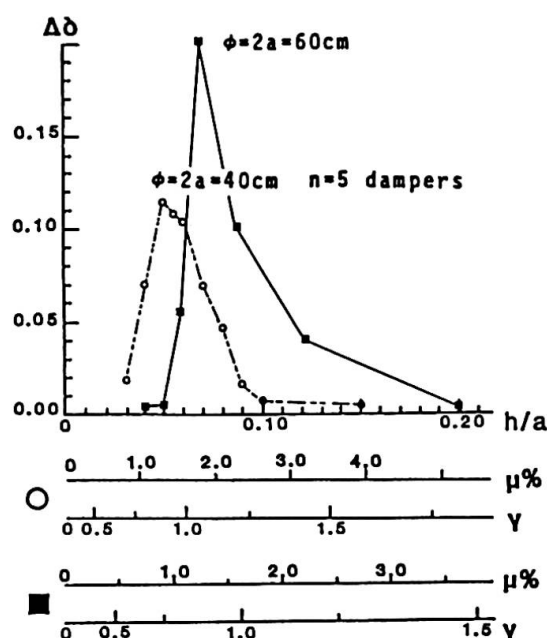
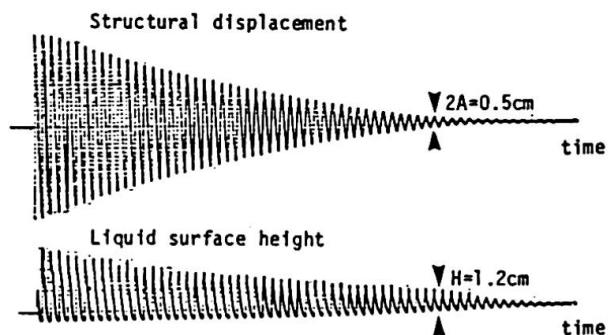
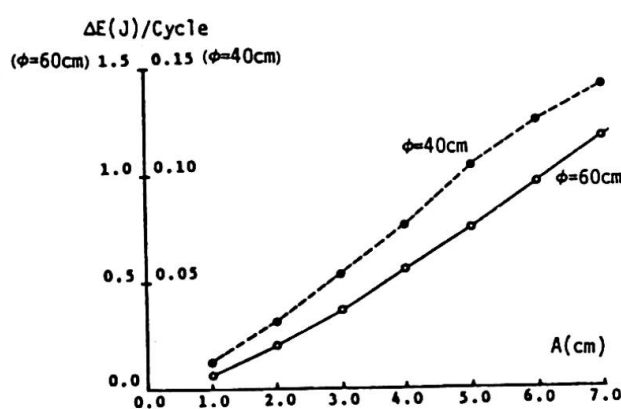
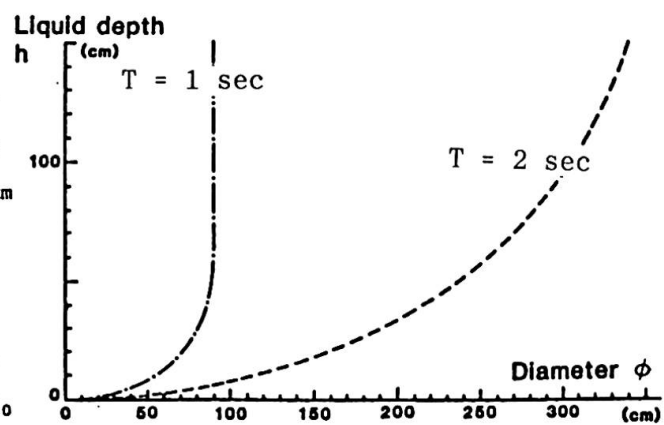
(a) $\phi = 40 \text{ cm}$; $m_S = 116 \text{ kg}$ (b) $\phi = 60 \text{ cm}$; $m_S = 440 \text{ kg}$

Fig. 4 Comparison of TLD for the diameters 40 cm and 60 cm

Fig. 5 Comparison of one large and five small TLDs ($m_S = 440 \text{ kg}$)Fig. 6 Liquid motion when $\Delta\delta$ is largeFig. 7 Time histories for Case (3)
in Fig. 3 ($\gamma = 1.0$; $h = 1.2 \text{ cm}$)Fig. 8 Energy loss per cycle
versus vibration amplitudeFig. 9 Required depth
versus container diameter

Deck Deformability in a Long Span Suspension Bridge

Déformation admissible du tablier d'un grand pont suspendu

Trägerverformungen bei einer grossen Hängebrücke

F. BRANCALEONI

Assoc. Prof.
University of Roma
Roma, Italy

A. CASTELLANI

Prof.
Politechnic of Milano
Milano, Italy

P. D. ASDIA

Assist. Prof.
University of Roma
Roma, Italy

L. FINZI

Professor
Politechnic of Milano
Milano, Italy

L. SANPAOLESI

Professor
University of Pisa
Pisa, Italy

SUMMARY

A 3300 meter, single span suspension bridge has been designed for a stable crossing of the Messina Straits, for both highway and railway use. The reliable running of trains requires stringent limits to the deck deformability, in particular in the transition zone between the suspended and the supported deck. For the same diameter of the main cables, and the same general structural arrangement, two alternative solutions to reduce the deck deformability are discussed; additional cable stays to reduce the vertical displacement in the vicinities of the towers, during the train entrance; and inclined suspenders to increase to longitudinal stiffness and the vertical stiffness with regard to concentrated loads.

RÉSUMÉ

Un pont suspendu d'une longueur de 3300 m et d'une unique portée a été projeté sur le détroit de Messine à l'usage de l'autoroute et du chemin de fer. La viabilité du train pose des limites rigides à la déformabilité de la charpente. Pour le même diamètre des câbles principaux et le même arrangement de la charpente, on prend ici en considération deux solutions alternatives pour réduire la déformation admissible du tablier, des étais supplémentaires pour réduire les déplacements verticaux à proximité des tours et des suspentes inclinées pour augmenter la rigidité longitudinale et verticale pour des poids concentrés.

ZUSAMMENFASSUNG

Es wurde eine Hängebrücke mit einer Spannweite von 3.300 m als Ueberquerung der Meerenge von Messina sowohl für den Strassen – als auch für den Eisenbahnverkehr entworfen. Die Befahrbarkeit mit der Eisenbahn erfordert strenge Grenzwerte für die Verformbarkeit des Brückenkörpers, vor allem in der Uebergangszone zwischen dem aufgehängten und dem gestützten Teil. Bei gleichem Durchmesser des Hauptkabels und bei gleicher allgemeiner Struktur werden zwei alternative Lösungen zur Reduzierung der Verformbarkeit des Brückenkörpers diskutiert: zusätzliche Kabelstange in der Nähe der Tragpfeiler zur Reduzierung der vertikalen Versetzung bei der Zugpassage, schräge Tragkabel zur Erhöhung der Längs- und Vertikalsteifigkeit in Bezug auf konzentrierte Belastung.



1. INTRODUCTION

The suspension bridge under consideration is characterized by the following figures (fig.1):

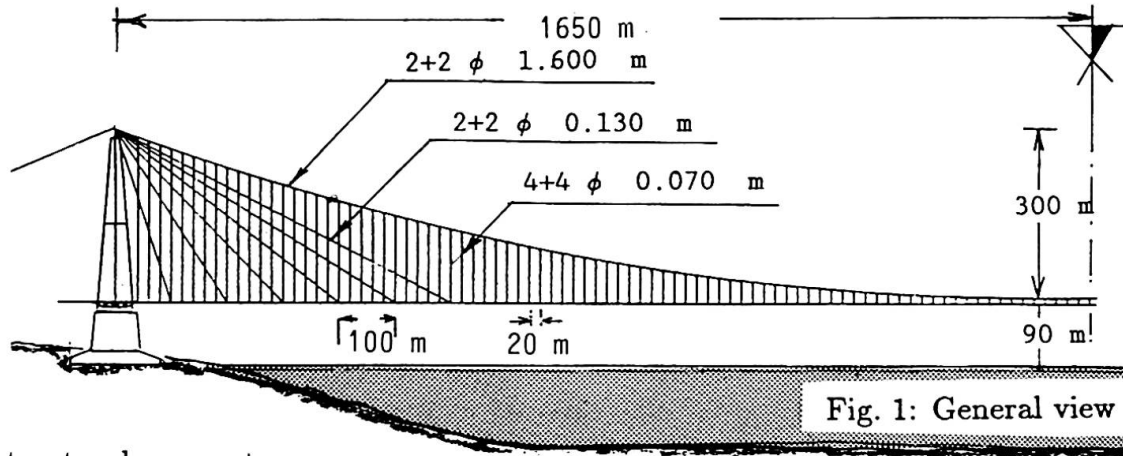


Fig. 1: General view

The main structural parameters are:

Cables:	diameter	1.60 m (n.4)
	length	990+3370+990 m
	weight	50.5 t/m
Deck:	cross section area	1.354 m ²
	moment of inertia	8.835 m ⁴
	dead load	42.70 t/m
Hangers:	diameter	d = 0.070 m (n.8 at 20 m)
Cable stays:	diameter	d = 0.130
Towers:	cross section area	8.64 m ²
	moment of inertia	187.7 m ⁴
	height above mean high water	400 m
	height over the concrete basis	310 m
sag/span ratio = 1/11, height of the towers 400 m (3+3) lateral highway traffic lanes + (1+1) emergency lanes (1+1) central railway tracks + (1+1) service lanes		

Table I

At both ends of the deck damped bumpers have been designed to reduce the longitudinal movements to $\pm .50\text{m}$ that is the displacement due to the possible deck elongation under the yearly thermal excursions. In absence of bumpers, unsymmetrical live loads cause movements of the deck with a given proportion of longitudinal tension and compression, resulting in a null net elongation over the entire length. This holds, as a first approximation, also in presence of damped bumpers. Therefore the above gap amplitude, in any live load combination, is available for the thermal elongation.

In any particular thermal condition, the longitudinal movement of the deck due to live load not covered by the remaining gap amplitude, is absorbed by tension and compression of the deck itself. The thermal and live load being uncoupled, the alternative configurations of the suspension system here considered are to be analysed in both conditions of ends free or one end longitudinally supported.

The two central railway tracks are stiffened by a longitudinal lattice beam, of 10 m height, to guarantee the local runnability requirement. A transition zone at the ends of the bridge is designed to comply with the train runnability specifications.

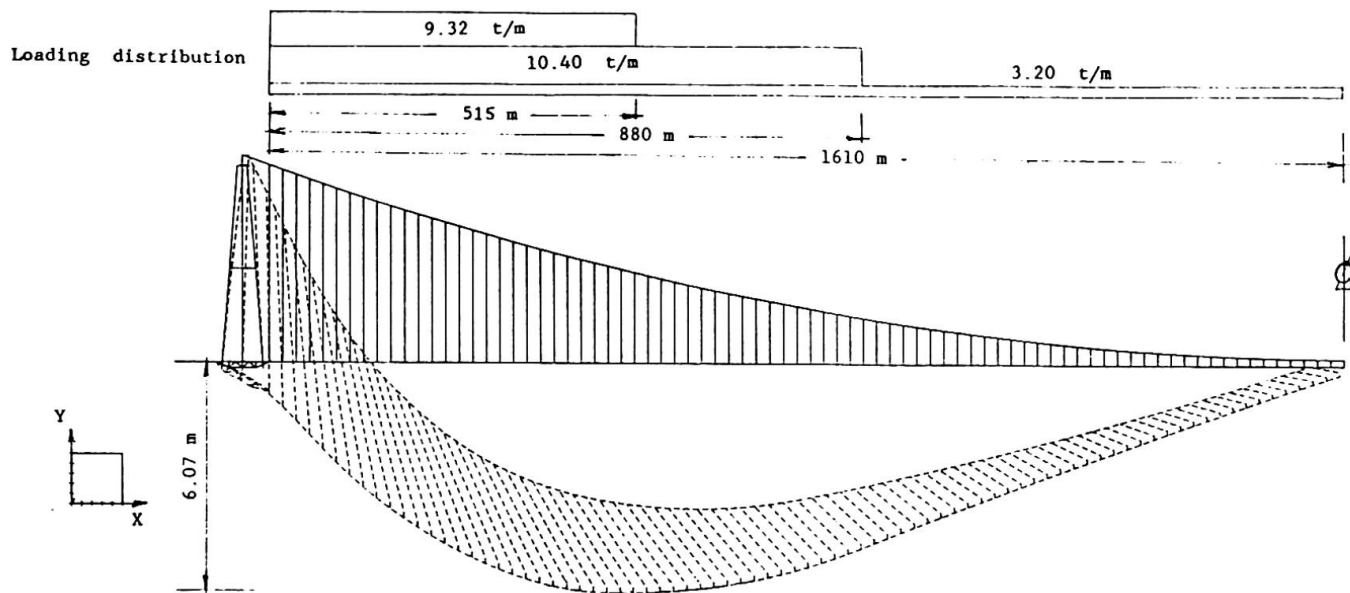


Fig. 2: deck deformed shape without stays

The mathematical analyses have been performed with an ADINA (Automatic Dynamic Incremental Nonlinear Analysis) bidimensional finite element model taking into account geometric nonlinearity with finite displacements.

The towers and the deck have been modeled through beam elements; cables, hangers and fan cable stays have been modeled through truss elements. Hydraulic dashpots at the end of the deck have been simulated through gap elements, which allow longitudinal displacements of $\pm .50$ m.

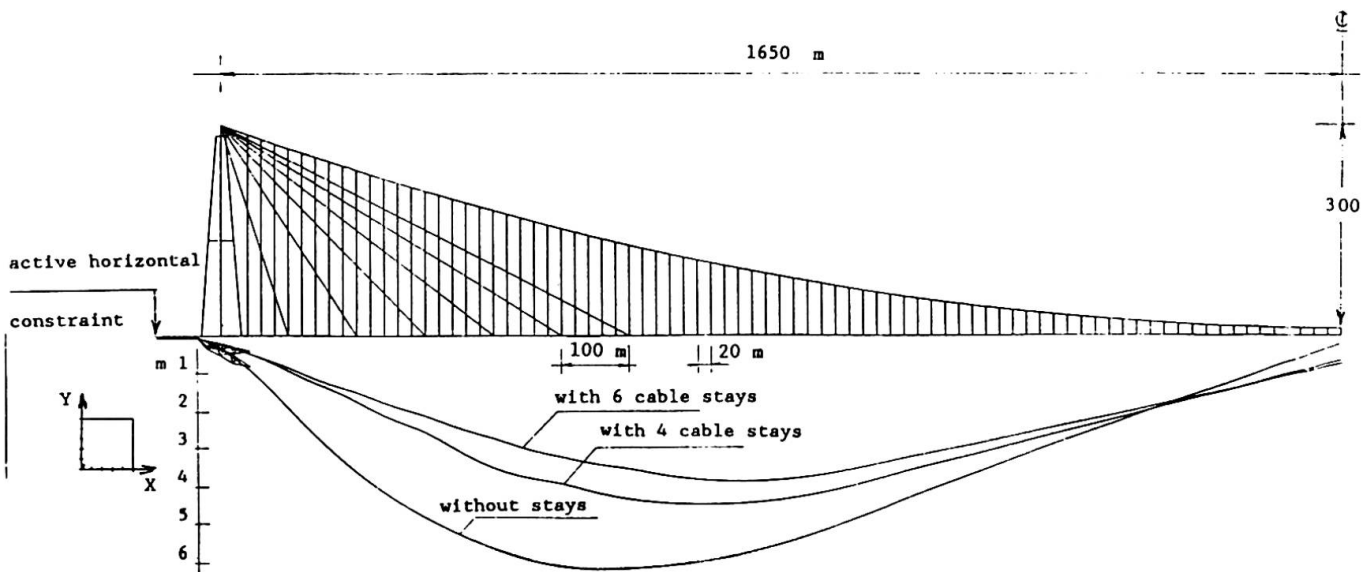


Fig. 3: deck deformed shape for different shapes



2. ADDITIONAL CABLES AT THE TOWERS

Combining the suspension and the cable stayed system has been proposed in several occasions in the design of long span crossings, since its first appearance at the Brooklyn Bridge.

As discussed in ref. (6), the advantage of additional cable stays may be directed towards minimal deck slope - to cope with train runnability requirements - or towards a more general objective, in particular the minimal material requirement. The results here shown refers to the first objective only.

Among the different combinations, the loading condition which governs the runnability is that in fig.2, where three kinds of loads are assumed: 1) a heavy train of 9.32 t/m, and 515 m length; 2) a heavy lorries of 10.4 t/m, and 880 m length; and 3) a car traffic of 3.2 t/m along the entire deck length. Results of the optimization process will be discussed with reference to this loading distribution.

The corresponding diagrams for displacement are shown in fig.2 and 3. Fig.2 shows the bridge deformed shape without stays, when the horizontal constraint is active at the left pier. For the same abscissa, the displacement of the cables is different from that of the deck. The resulting inclination of the hangers provides thus an axial force in the deck.

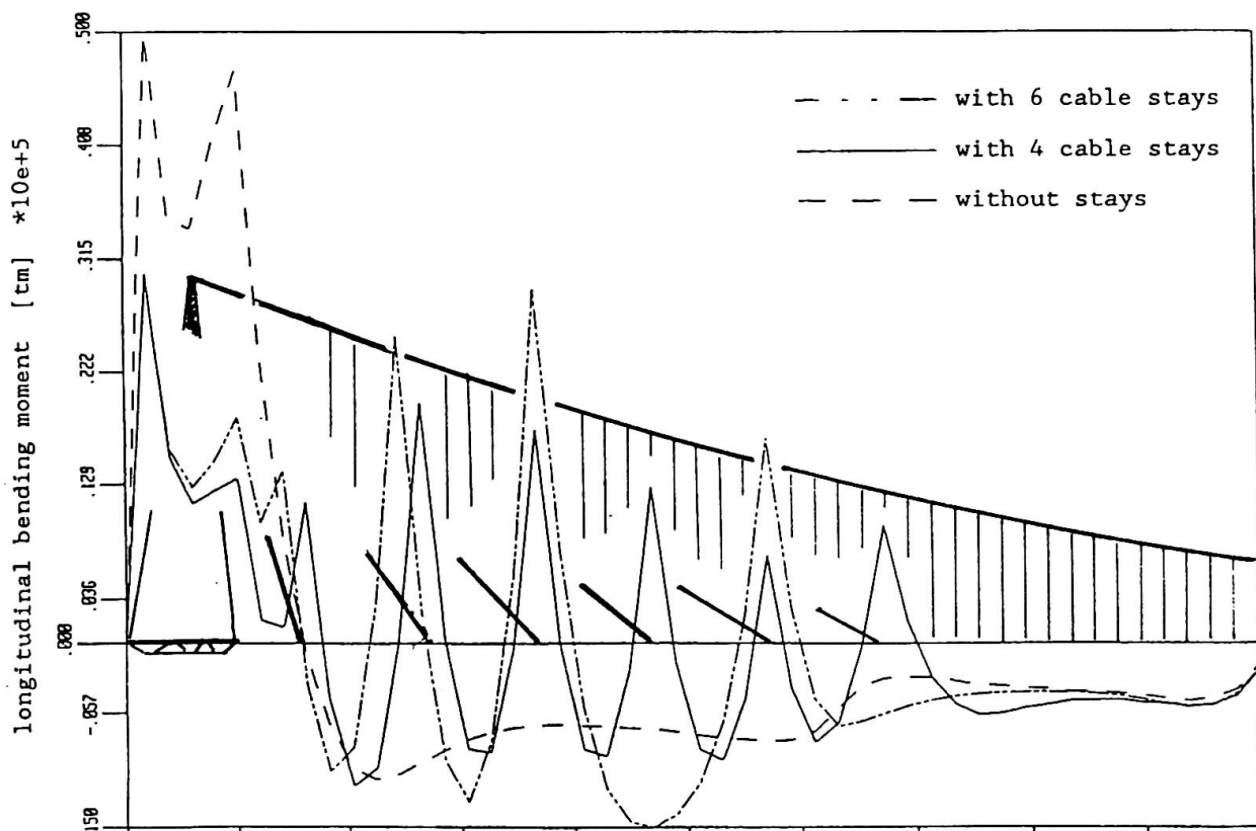


Fig. 4: deck bending moment for different configurations

The effect is enhanced by the cable stays presence which plays a different role according to whether left or right horizontal constraint is active. In general, the middle portion of the deck is in tension, both for the prestressing action provided by the tendons and for the live load transfer. The end portion of the deck, near that constraint which is in force, is in compression. The higher

axial forces are in this portion, and therefore are of the compression type, (see table 2). Vertical displacements and thus the deck slope are only marginally affected by the horizontal constraint.

longit. bond	significant values	without stays deck cables	with 6 cable stays deck cables		
free	ΔX [m]	-1.12	-1.78	-2.10	-1.50
	ΔY [m]	-6.35	-6.23	-5.54	-5.51
	θ [%]	19.72	-----	14.31	-----
	Nmax [t]	-225.		-7108.	
ΔN stays				1476.	
fixed at left edge	ΔX [m]	-0.13	-1.67	-0.13	-0.90
	ΔY [m]	-6.07	-5.96	-4.04	-3.93
	θ [%]	19.03	-----	9.52	-----
	Nmax [t]	3465.		11208.	
ΔN stays				2219.	
fixed at right edge	ΔX [m]	-0.16	-1.67	-0.73	-1.03
	ΔY [m]	-6.08	-5.96	-4.46	-4.28
	θ [%]	19.05	-----	10.87	-----
	Nmax [t]	-3408.		-10211.	
ΔN stays				1917.	
with gap +/-0.50m	ΔX [m]	-0.50	-1.72	-0.50	-1.03
	ΔY [m]	-6.19	-6.07	-4.35	-4.27
	θ [%]	19.31	-----	10.63	-----
	Nmax [t]	1127.		8600.	
ΔN stays				2028.	

Table 2: the four models significant values

The way the hydrolic dashpots are devised, the end constraint condition may be either fixed or sliding, depending on temperature and the involved horizontal displacement. Thus, in practice, any one of the three conditions shown in table 2 is to be accounted for. The introduction of cable stays results therefore in a sensible increase in the axial force in the deck, mainly of a compression type. For a deeper understanding of the problem, however, the change of the bending moment diagram is to be accounted too, contemporary to the axial force. See, for instances, fig.4.

3. INCLINED HANGERS

Inclined hangers provide a limited increase in the deck stiffness, at the expenses of an additional longitudinal displacement. When this is prevented by the end bumpers, an additional normal stress arises in the deck. Table 3 shows the main terms of the comparison between alternative solutions, under the same loading combination previously considered. Here configuration 1 refers to inclined hangers all along the suspended span, and configuration 2 refers to inclined hangers along a central portion of 240 m length. Notice that, among bridge designers, inclined hangers are reported to offer increased damping with reference to vertical hangers, under longitudinal and vertical dynamic excitation. Apparently this assesment is based on a single measure given by reduced scale physical model. In this regards, the present authors believe that, unless similar results are got in a full scale structure, one cannot rely on them. Besides the additional damping could not be other than a measure of internal friction or of alternate bending stresses in the hangers related to the peculiar design of the connection. Some possible disadvantage in terms of fatigue have been reported in the literature.



Table 3. Performances of inclined hangers solutions

longit. boundary		Inclined hangers	
		Configuration 1	Configuration 2
free	ΔX (m)	1.34	1.26
	ΔY (m)	6.38	6.54
	N_{max} (t)	5500	880
fixed at left edge	ΔX	0.76	0.71
	ΔY	5.44	5.52
	N_{max}	17600	13200
fixed at right edge	X	0.92	0.76
	Y	6.14	6.18
	N_{max}	16000	13000

4. REFERENCES

1. Gimsing, N., "Cable Supported Bridges", John Wiley and Sons, 1983.
2. Torii, K., Ikeda K., Nagasaki, T., "A Non-iterative Optimum Design Method for Cable-Stayed Bridges", Proc. of the JSCE, n.368, i-5, April 1986.
3. Sigmundsson R., Hjorth-Hansen E.; "Along-wind Response of Suspension Bridges with Special Reference to Stiffening of Horizontal Cables", Eng. Structures, vol.3, Jan. 1981.
4. Castellani, A., Felotti, P., "Lateral Vibration of Suspension Bridges", ASCE, Journal of the Structural Div., Sept. 1986 n.8.
5. Castellani, A., "Safety Margins of Suspension Bridge under Seismic Conditions", ASCE, Journal of the Structural Div., n.8, July 1987.
6. Finzi, L., Castellani, A., Bascialla, E. "Cable Stays to Comply with Runnability Requirements in Long Span Suspension Bridges", Int. Conf. on Cable Stayed Bridges, Bangkok, 1987.
7. Brancaleoni F., "Verformungen von Haengebruecken unter Eisenbahnlasten", Der Stahlbau, Darmstadt, Feb. 1979.
8. Brancaleoni F., Brotton D.M., "Analysis and Prevention of Suspension Bridge Flutter in Construction", Journal of Earth. Eng. and Struct. Dynamics, N.5, 1981.

Leere Seite
Blank page
Page vide

Leere Seite
Blank page
Page vide